Title
Symbiosis in the Fossil Record: Eocene Nummulites and Pleistocene Reefs of Egypt

Author
Casazza, Lorraine Rebecca

Publication Date
2012

Peer reviewed|Thesis/dissertation

Symbiosis in the Fossil Record: Eocene *Nummulites* and Pleistocene Reefs of Egypt

by
Lorraine Rebecca Casazza

A dissertation in partial satisfaction of the
requirements for the degree of
Doctor of Philosophy
in
Integrative Biology
in the
Graduate Division
of the
University of California, Berkeley

Committee in charge:

Professor Emeritus Jere H. Lipps
Professor Anthony D. Barnosky
Professor Bonnye Lynn Ingram

Spring 2012

Abstract

Symbiosis in the Fossil Record: Eocene *Nummulites* and Pleistocene Reefs of Egypt

by
Lorraine Rebecca Casazza

Doctor of Philosophy in Integrative Biology
University of California, Berkeley
Professor Emeritus Jere H. Lipps, Chair

Symbiosis is an intimate association between two or more different species encompassing a spectrum of interactions from parastism, through commenalism to mutualism. Although it was once thought to be rare and unusual, we now understand symbiosis to be remarkably common and it has emerged as a key factor in evolutionary processes and major evolutionary transitions. Relative to other biological disciplines paleontology has been somewhat limited in its contributions to understanding symbiosis, but the fossil record is uniquely suited to answer some research questions on the topic. The research projects of this dissertation use the fossil record to examine aspects of symbiosis in two types of calcifying, marine organisms: larger foraminifera and hermatypic corals. Geochemical methods can be used to detect ancient symbiosis in the fossils of some calcifying, marine organisms because the presence of photosynthesizing algal symbionts can alter the stable carbon and oxygen isotope signatures of calcium carbonate host shells. Detecting the presence and degree of diagenetic alteration of calcium carbonate tests is critical for the integrity of isotopic studies carried out on them. In order to establish that foraminiferal tests from an exceptionally preserved, rare sample from the Eocene of Egypt are pristine and will yield reliable isotopic results in a study of symbiosis, light microscopy, scanning electron microscopy (SEM), backscatter electron imaging and electron dispersive spectrometry (EDS) are used to detect and identify diagenetic minerals in the foraminifera *N. gizehensis*, *Uvigerina* spp. and *Cibicides* spp. Potential sources of contamination in this Eocene sample include dolomite, gypsum, and more rarely recrystalized test calcite, however all can be detected and avoided for isotopic analyses. Carbon and oxygen isotopic analyses of pristine test material, pure dolomite, and recrystalized calcite were carried out to calculate how much contamination a sample can have and still yield reliable results. General recommendations for establishing the degree of alteration in rare, calcium carbonate samples include an initial investigation using light microscopy, SEM, backscatter electron imaging, and EDS to establish diagenetic patterns in fossil taxa, after which visual inspection with a light microscope may be adequate to distinguish between altered and unaltered individuals. For rare or precious specimens, SEM and EDS yields sufficient qualitative results without carbon-coating so that sample integrity may be preserved. If the condition of the sample permits preliminary isotopic testing, then an allowable percentage of contamination can be calculated to ensure reliable isotopic results. The pristine preservation of these Eocene foraminifera makes them appropriate for stable isotope analysis to detect ancient

symbiosis. It is widely accepted in the literature that extinct species of larger foraminifera hosted algal symbionts, and that the evolution of larger foraminifera has been driven by algal symbiosis. However, there is no definitive evidence for symbiosis in fossil larger foraminifera. The known characteristics of stable isotope chemistry in extant symbiotic rotaliid foraminifera are used to test the hypothesis that the extinct rotaliid, *Nummulites gizehensis*, hosted photosynthesizing endosymbionts. The carbon isotopic signatures of symbiotic rotaliid foraminifera are 3-5‰ lower in $\delta^{13}C$ than calcite in equilibrium with ambient seawater, and exhibit a less well-supported trend of increasing $\delta^{13}C$ values over ontogeny. The micro- and megalospheric *Nummulites gizehensis* tested show a mean negative shift of 3.75‰ relative to contemporary fossil equilibrium calcite as calculated from co-occurring *Uvigerina* spp. and *Cibicides* spp. Seven out of nine microspheric individuals show the expected ontogenetic trend in $\delta^{13}C$ over ontogeny, however all of the megalospheric forms show the opposite trend. Like their larger extant relatives, *Nummulites gizehensis* appear to have hosted photosynthesizing symbionts. Calcifying, symbiotic, marine organisms also provide one of the best case studies for understanding symbiosis in relation to environmental conditions. Reef building corals, taxa known to host photosynthesizing algal symbionts today and also confirmed as an ancient symbiosis, flourish in times of warm, nutrient-poor ocean conditions and all but disappear during periods of cooler, nutrient-rich conditions. Coral reefs are endangered globally, and predicting their response to changing environmental conditions is a priority for researchers and managers. The fossil record of Red Sea fringing reefs provides a unique opportunity to study the history of coral survival and recovery in the context of environmental catastrophe. Coral assemblage data from eight emerged fossil reef terraces on the Egyptian coast are described and used to determine if and how coral assemblages change from Middle to Late Pleistocene and Late Pleistocene to modern reefs. The first Red Sea occurrence of *Favites micropentagona* is reported from the Middle Pleistocene. Coral taxa are constant over the studied time period, as are coral assemblages, despite likely extinctions of coral species over two-thirds of the Red Sea basin during glacial low-stands. A less saline but still hostile southern Red Sea may have acted as a refuge for small communities of salinity-tolerant taxa during these extinction events, and provided the early settlers for subsequent recolonization. If populations of corals can be sustained, even in marginal and geographically limited habitat, they retain the potential to re-establish themselves when warm, nutrient-poor conditions appropriate for coral symbiosis return.

This work is dedicated to those who enabled me:

Jeanette Irwin
Linda J. Casazza
and
Timothy J. Pearson

Thank you.

Table of Contents

List of Figures and Tables

Acknowledgements

A great number of people deserve my gratitude for providing the intellectual, logistical, financial and moral support that was necessary to carry out this research. What follows is only a partial list of those without whom this dissertation could not have happened.

First and foremost, I would like to express the deepest appreciation to my committee chair and mentor, Professor Jere H. Lipps, who provided me with guidance and intellectual freedom in equal measure, and whose legendary scientific acumen and curiosity has served as my greatest inspiration. I would also like to thank my committee members Professor Anthony Barnosky and Professor Lynn Ingram for their time, attention and insights during busy semesters.

Very special thanks are due to Dr. Amin Strougo of Ain Shams University in Cairo. Not only did he provide fossil material for analyses included in this dissertation, he also shared his expertise in biostratigraphy and extensive knowledge of field sites. I am most appreciative of the many fruitful discussions with him about the paleontology and geologic history of Egypt, as well as trips into the field that were both educational and enjoyable. I would also like to thank Dr. Mohamed Boukhary of Ain Shams University for sharing his time and expertise in the morphology and evolution of *Nummulites.*

I am indebted to the museum scientists of the UC Museum of Paleontology; Dr. Diane Irwin for the hours she spent teaching me to make thin sections and curate my material, Drs. Ken Finger and Pat Holroyd for always making time to answer questions about foraminiferal taxonomy, statistics, or Eocene climate. They were an invaluable resource to me. I am thankful to Dr. Mark Goodwin for advising me during curation, and for his good advice regarding cast-making.

This dissertation would not have been possible without the financial support of a Fulbright Fellowship, administered by the U.S. Department of State. I owe my gratitude to the entire staff of the Binational Fulbright Commission in Egypt; their logistical support in-country was vital to the success of my research. In particular I would like to thank Noha El Gindi for her Herculean efforts on my behalf, Hend Rasmy and Ranya Rashad.

Further funding for this research was provided by a Paleontological Society Student Grant from the Paleontological Society, a Loeblich and Tappan Student Research Award from the Cushman Foundation, a GSA Graduate Student Research Grant from the Geological Society of America, and a Dorothy K. Palmer Award from the UC Museum of Paleontology. I am grateful to all of these organizations for their support of my research.

I would like to thank Dr. Moustafa Fouda of the Egyptian Environmental Assessment Agency (EEAA) in Cairo for his cooperation in procuring permissions to carry out work in the field. I would also like to thank Dr. Muhmoud Hanafy and Dr. Ayman Afifi of the EEAA in Hurghada for their cooperation and assistance with logistics in the field.

I am also indebted to the entire staff of the Egyptian Geologic Museum in Cairo for their hard work and cooperation in getting the fossil material of this dissertation to the UC Museum of Paleontology in the U.S. I would especially like to thank Drs. Medhat Said Abdel Ghany, Abdel Latif, the Assistant Director of the Museum, Dr. Ehab El Saddy, and the dedicated team who spent days meticulously reviewing the contents of my boxes.

I am deeply grateful to Hysum Odema for his tremendous efforts as a driver, guide, translator and field assistant, and for his ability to find coffee at any hour of the day. This work could not have happened without him. For help in the field I would also like to thank Timothy Pearson,

Mariam Hamdy, Dr. Michele Weber, Trent Weber, Dr. Scott Fay, and Drs. Salah Soliman and Wael Hesny of the EEAA in Hurghada.

Sincere thanks to Dr. Wenbo Yang of the Laboratory for Environmental and Sedimentary Isotope Geochemistry for his assistance in isotope analyses, and also to Dr. Timothy Teague of the Department of Earth and Planetary Sciences for training and assistance in the SEM lab.

Deep appreciation is also due to the many faculty members, post-docs and fellow graduate students of the Department of Integrative Biology at the University of California, Berkeley, for providing me with the intellectual foundation and theoretical framework upon which this research is built. The seminars of Professors Kevin Padian, Nicole King, and Anthony Barnosky were especially formative, and it is an honor to have participated in them.

I would also like to thank my colleagues, Katie Brakora and Erin Meyer, for providing camaraderie and unflagging moral support. I have relied heavily on them for motivation, advice and assurance throughout the writing process. I am grateful for my friends and family, who have been patient with my workaholic tendencies during the long years of my graduate career. Finally, my husband, Timothy Pearson, deserves special recognition for his continual support of me and my research. Without him by my side from start to finish, I couldn't have done this.

I. Symbiosis in the Fossil Record: An Introduction

Symbiosis is an intimate association between two or more different species. Its specific definition shifts depending on the researcher, with propositions to restrict its usage to mutually beneficial relationships or expand it to include predator-prey interactions. However, the most widely agreed upon meaning encompasses a continuum that ranges from parasitism, in which one species benefits at the expense of another, through commensalism in which one species benefits while the other is neither harmed nor helped, to mutualism, in which both organisms benefit from the association. In nature these designations grade into one another and symbiotic associations may fall anywhere along the spectrum. For example, even symbioses described as mutualistic rarely if ever benefit both participants equally (Paracer and Ahmadjian 2000). Likewise, symbiotic relationships are not static in evolutionary time; many commensal and mutual symbioses probably began as parasitic associations.

Symbioses are further classified by the nature of the association. Where a symbiont dwells within its host determines if it is endosymbiotic (residing within the host's cells) or ectosymbiotic (residing on the host tissue). Symbionts may be passed by the host organism to offspring during reproduction, or they can be re-acquired in each generation. Relationships may be obligate, meaning that one or both species cannot survive outside of the symbiosis, or facultative, in which one or both can live independently but don't. Symbioses also vary in their specificity; symbionts and hosts may be specific to a single species, or they may be able to form associations with multiple species.

Although it was once thought to be rare and unusual, we now understand symbiosis to be remarkably common, occurring in all forms of life (Paracer and Ahmadjian 2000). It has also emerged as a key factor in evolutionary processes and major evolutionary transitions. The Serial Endosymbiosis Theory, championed by Lynn Margulis in the late sixties, lead to decades of research that has affirmed the evolution of the eukaryotic cell as the result of multiple symbioses between prokaryotes. Symbiosis between plants and fungi formed around 400 million years ago enabled plants to colonize land (Newsham et al. 1995, Wang et al. 2010), an evolutionary step that transformed the face of planet earth. Symbiotic associations, particularly with bacteria, are a source of horizontal gene transfer between species. Once considered impossible, horizontal gene transfer has now been documented across the tree of life, and has been implicated in the evolution of flowers, fruits, and storage structures in some insects and fungi (Paracer and Ahmadjian 2000).

As in the case of the eukaryotic cell, symbiosis can be a source of novelty in evolution. Taken to its most dramatic extreme this can mean the evolution of new species through the merging of two unrelated lineages via symbiosis, a process coined symbiogenesis. By providing an alternative mechanism for the generation of variation, symbiosis presents a departure from traditional or neo-Darwinian evolutionary theory, which focuses on mutation as the sole, ultimate source of novelty (Maynard-Smith 1991). Modern evolutionary biologists have been slow to recognize and incorporate symbiosis into a wider conceptual framework, however this has begun to change.

Scientists across many fields of biology have taken up the study of symbiotic interactions in organisms of every form. Molecular and cell biologists and geneticists have largely taken the lead, although in the last two decades ecologists have also begun to examine symbioses in terms of competition, fitness, population dynamics and co-evolution (Paracer and Ahmadjian 2000). Relative to other biological disciplines paleontology has thus far been somewhat limited in its contributions to understanding symbiosis. In part this is due to the types of innovation symbiosis leads to and the nature of fossil material; symbiosis with bacteria, for example, most frequently leads to new metabolic activities that are largely invisible in fossil materials (Maynard-Smith 1991). However, there are some symbiosis research questions uniquely suited for study in the fossil record, such as detecting ancient symbioses, co-evolution between host and symbiont or morphological change driven by symbiosis, the emergence of new species via symbiogenesis, and the history of symbiotic associations in relation to environmental change.

Geochemical detection of symbiosis in fossil material can provide unequivocal confirmation of the minimum duration of symbiotic associations. For example, the presence of photosynthesizing algal symbionts alters the stable carbon and oxygen isotope signatures of calcium carbonate host shells. Using this approach has lead to the confirmation of ancient symbiosis in hermatypic corals (Stanley and Swart 1995) and some extinct planktonic foraminifera (D'Hondt et al. 1994, Houston and Huber 1998, Houston et al. 1999, Norris 1996, Pearson et al. 1993). Morphological data can also be used to confirm ancient symbiosis, for example extraordinary preservation of ancient lichen in amber (Rikkinen 2003). In many other cases morphological features strongly correlated with modern symbioses have been used to infer its existence in ancient forms. These include hyphal extensions (arbuscules) found in early fossil land plants, which function as exchange sites with symbiotic fungi in modern plants (Strullu-Derrien and Strullu 2007), and bioerosional structures on solitary Pliocene corals attributed to commensal polychaetes known from modern taxa (Martinell and Domenech 2009), to mention only a few.

Once ancient symbiosis has been established in taxa, their fossil record may provide an opportunity to study morphological change driven by symbiosis (Maynard-Smith 1991). If both host and symbiont fossilize then there is the potential to study the historical trajectory of co-evolution, which is so often inferred from modern features of symbiotic associations. Of special interest may be the search for symbiogenesis in the fossil record. This might be inferred from first appearances of fossil taxa that also provide geochemical confirmation of symbiosis, especially if likely non-symbiotic ancestors can be identified.

Calcifying, symbiotic, marine organisms provide one of the best case studies for understanding symbiosis in relation to environmental conditions. Reef building corals, larger foraminifera and giant clams, all taxa known to host photosynthesizing algal symbionts today and some confirmed as ancient symbioses, flourish in times of warm, nutrient poor ocean conditions and all but disappear in cooler, nutrient-rich waters (Cowen 1988). This long historical record confirms

modern observations that these symbioses are adaptive under particular environmental regimes, but not others. Research of this kind is of particular interest as the global climate shifts, and the fate of marine fauna is called into question.

The research projects of this dissertation use the fossil record to examine aspects of symbiosis in two types of calcifying, marine organisms: larger foraminifera and hermatypic corals. Chapter two, Investigation of diagenesis in Middle Eocene benthic foraminifera from Egypt, provides an in depth study of the preservation of Eocene aged calcium carbonate foraminiferal tests. This is an important step in ensuring fossil material used in stable isotope testing still preserves the original isotopic signature, and lays the groundwork for Chapter three, Endosymbiosis in the Eocene Nummulite, *Nummulites gizehensis*. This chapter uses a geochemical approach to confirm the presence of photosynthesizing algal symbionts in an extinct larger foraminifera long hypothesized to be symbiotic. *Nummulites* have an excellent fossil record and morphological test features known to support symbiont function in modern day relatives, making them an outstanding candidate for future studies of symbiont-driven morphological change. They are thought to have evolved from small, Oligocene ancestors, and may also be an example of symbiogenesis.

The fourth and final chapter, Pleistocene Reefs of the Egyptian Red Sea, looks at the history of the reef building corals of the Egyptian coast in relation to Pleistocene climate cycles. It provides a much needed taxonomic description of Middle and Late Pleistocene reef terraces of the Egyptian coast, as well as a discussion of faunal response to and recovery from environmental catastrophe. It confirms that coral symbiosis is adaptive only under warm, nutrient-poor conditions, and considers the best way to preserve corals into the future given their history in the Red Sea.

References

Cowen R. 1988. The role of algal symbiosis in reefs through time. Palaios 3: 221-227.
D'Hondt S, Zachos J, Schultz G. 1994. Isotopic signals and photosymbiosis in Late Paleocene planktonic foraminifera. Paleobiology 20: 391-406.
Houston RM, Huber BT. 1998. Evidence of photosymbiosis in fossil taxa? Ontogenetic stable isotope trends in some Late Cretaceous planktonic foraminifera. Marine Micropaleontology 34: 29-46.
Houston RM, Huber BT, Spero HJ. 1999. Size-related isotopic trends in some Maastrichtian planktic foraminifera: methodological comparisons, intraspecific variability, and evidence of photosymbiosis. Marine Micropaleontology 36: 169-188.
Martinell J, Domenech R. 2009. Commensalism in the fossil record: Eunicid polychaete bioerosion on Pliocene solitary corals. Acta Palaeontologica Polonica 54: 143-154.
Maynard-Smith J. 1991. A Darwinian View of Symbiosis in Margulis L, Fester R, eds. Symbiosis as a Source of Evolutionary Innovation, MIT Press.
Newsham KK, Fitter AH, Watkinson AR. 1995. Multifunctionality and biodiversity in arbuscular mycorrhizas. Trends in Ecology & Evolution 10: 407-411.
Norris RD. 1996. Symbiosis as an evolutionary innovation in the radiation of Paleocene planktic foraminifera. Paleobiology 22: 461-480.

Paracer S, Ahmadjian V. 2000. Symbiosis: An Introduction to Biological Associations. New York: Oxford University Press.
Pearson P, Shackleton N, Hall M. 1993. Stable isotope paleoecology of middle Eocene planktonic foraminifera and multi-species isotope stratigraphy, DSDP site 523, South Atlantic. Journal of Foraminiferal Research 23: 123-140.
Rikkinen J. 2003. Calicioid lichens from European Tertiary amber. Mycologia 95: 1032-1036.
Stanley GDJ, Swart PK. 1995. Evolution of the coral-zooxanthellae symbiosis during the Triassic: a geochemical approach. Paleobiology 21.
Strullu-Derrien C, Strullu D-G. 2007. Mycorrhization of fossil and living plants. Comptes Rendus Palevol 6: 483-494.
Wang B, Yeun LH, Xue J-Y, Liu Y, Ane J-M, Qiu Y-L. 2010. Presence of three mycorrhizal genes in the common ancestor of land plants suggests a key role of mycorrhizas in the colonization of land by plants. New Phytologist 186: 514-525.

II. Investigation of Diagenesis in Middle Eocene Benthic Foraminifera From Egypt

Abstract

The oxygen and carbon isotopic signatures of planktonic and benthic foraminiferal tests are routinely used in paleotemperature and climate reconstructions, however diagenetic processes can alter isotopic ratios of original test material. Detecting the presence and degree of diagenetic alteration of foraminiferal tests is critical for the integrity of isotopic studies carried out on them. In order to establish that foraminiferal tests from an exceptionally preserved, rare sample from the Eocene of Egypt are pristine and will yield reliable isotopic results in a future study (see chapter 3), light microscopy, scanning electron microscopy (SEM), backscatter electron imaging and electron dispersive spectrometry (EDS) are used to detect and identify diagenetic minerals in the foraminifera *N. gizehensis*, *Uvigerina* spp. and *Cibicides* spp. Potential sources of contamination in this Eocene sample include dolomite, gypsum, and more rarely recrystalized test calcite, however all can be detected and avoided for isotopic analyses. Carbon and oxygen isotopic analysis of pristine test material, pure dolomite, and recrystalized calcite were carried out to determine how diagenetic materials affect results. Pure dolomite shows a strong positive shift in $\delta^{13}C$ values relative to all foraminiferal taxa, but $\delta^{18}O$ values similar to those of *Uvigerina* spp. and *Cibicides* spp. Recrystalized calcite shows values slightly more positive than source calcite. General recommendations for establishing pristine preservation in rare, calcium carbonate samples include an initial investigation using light microscopy, SEM, backscatter electron imaging, and EDS to establish diagenetic patterns in fossil taxa, after which visual inspection with a light microscope may be adequate to distinguish between altered and unaltered individuals. For rare or precious specimens, SEM and EDS yields sufficient qualitative results without carbon-coating so that sample integrity may be preserved.

Introduction

The carbon ($\delta^{13}C$) and oxygen ($\delta^{18}O$) isotopic signatures of planktonic and benthic foraminiferal tests are routinely used in reconstructing past ocean temperature, salinity and productivity. For accurate quantitative results, however, the original test calcite must be unaltered from the time it was secreted (Pearson et al. 2001). As tests settle and become buried on the sea floor

processes such as dissolution, inorganic overgrowth and recrystallization can alter isotopic ratios (Crowley and Zachos 2000), and these effects are often magnified with increasing geologic age and the depth of burial (Schrag et al. 1995). Detecting the presence and degree of these diagenetic alterations is critical for the integrity of isotopic studies.

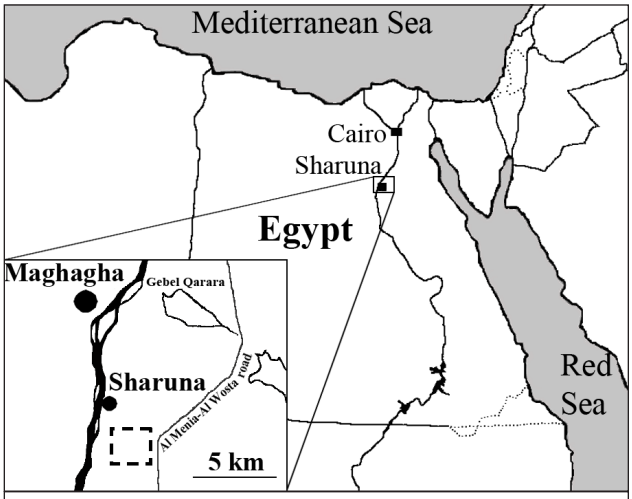

Figure 1. Locality map. Dashed box on inset indicates approximate location of clay pit where samples were collected.

The effect of partial dissolution on isotopic signatures of individual tests is negligible, although in bulk carbonates it can cause slight positive shifts in $\delta^{18}O$ values, but recrystallization and secondary calcite can cause significant changes in isotopic results (Crowley and Zachos 2000). In extreme cases these alterations can be detected with a light microscope or scanning electron microscopy (SEM) and avoided (Crowley and Zachos 2000, Pearson et al. 2001). In other instances, such as recrystallization on a small scale that fails to erase morphological features, diagenetic alterations can be difficult to recognize (Pearson et al. 2001) and impossible to detect under a light microscope (Williams et al. 2007).

This study uses a combination of approaches to investigate the degree and type of diagenetic alteration in three species of benthic foraminifera from the Middle Eocene of Egypt to determine their appropriateness for isotopic analyses in chapter 3 of this dissertation. Light microscopy, SEM, backscatter electron imaging and energy dispersive spectrometry (EDS) are used to detect and identify diagenetic materials. Specifically, the following questions are addressed: 1) is examination with light microscopy adequate to detect diagenetic alteration in specimens, 2) is it necessary to carbon coat specimen to sufficiently detect and identify diagenetic alteration with SEM and EDS, 3) what diagenetic materials are present and what can they tell us about the sample, and 4) how will these diagenetic materials effect carbon and oxygen stable isotope ratios.

The question of carbon coating is relevant due to the rare nature of the sample under examination. Deposits of exceptionally preserved Eocene Nummulites in life position are not common to begin with, and since they were collected in 1987 changes in land use and political environment have made the original field site inaccessible for further collection. Furthermore, the sample is of limited size, and not all specimens appear to have pristine preservation, thus usable material is of limited quantity. Once coated with carbon the samples become unsuitable for isotopic analyses, so determining diagenetic alteration to a high degree of confidence without coating is a priority. Although results will be specific to the Eocene benthic foraminifera examined here, they may still be applicable to other rare, exceptionally preserved samples.

Methods

Bulk samples were collected and washed in 1987 by Dr. Amin Strougo and Dr. Mohamed Boukhary of Ain Shams University, Cairo, from an excavated clay pit located approximately 200 meters west of the Al Menia-Al Wosta road, southeast of Sharuna, Al Minia, Egypt (Figure 1) (pers. comm.).

For this study, megalospheric and microspheric forms of *N. gizehensis* were ground on a horizontal wet diamond grinder to expose equatorial sections, rinsed with deionized water to remove any residue, and dried over night at 60°C.

Sediment from the original bulk sample was sprinkled over a gridded tray, and *Cibicides* spp. and *Uvigerina* spp. were picked using a binocular microscope and fine paint brush, and placed in a micropaleontological slide.

Specimens of microspheric (produced sexually) and megalospheric (produced asexually) *N. gizehensis*, *Uvigerina* spp. and *Cibicides* spp. were visually inspected under a light microscope, and sorted into two groups: 1) tests presumed to be unaltered, which for *Uvigerina* spp. and *Cibicides* spp. meant a white, glassy appearance, and for *N. gizehensis* test interiors that were white, intact and fresh looking, and 2) tests presumed to be altered, i.e. that were discolored, broken, had infilling or other noticeable alteration. Light photographs were taken of presumed unaltered and altered specimens using a Leica M 165 C stereomicroscope with a Nikon Digital Sight DS-Fi1 camera set up. Combine Z, an extended depth of field stacking software, was used to combine multiple images of single *Uvigerina* spp. and *Cibicides* spp. to produce single, focused images.

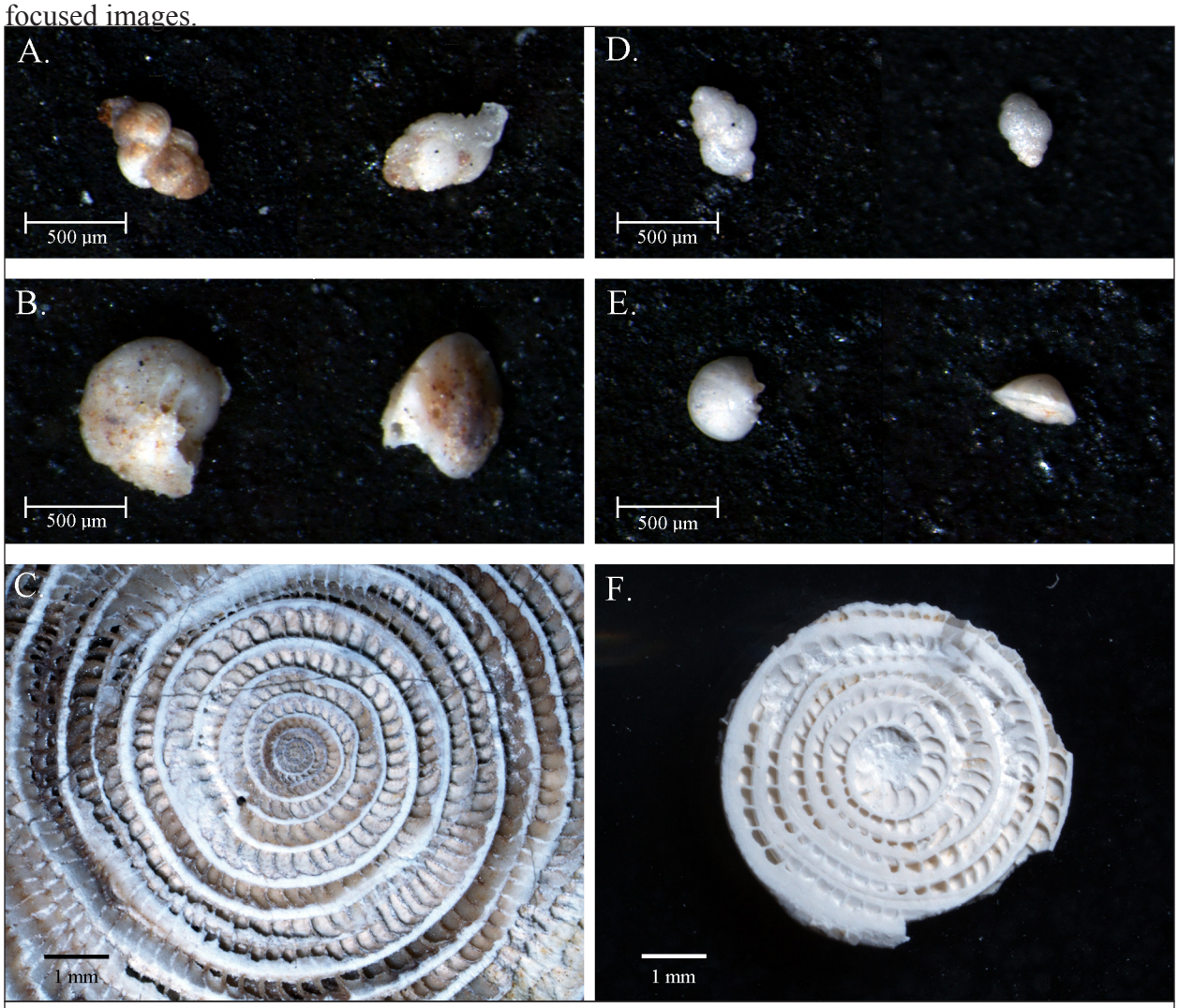

Figure 2. Light photographs of presumed altered and unaltered specimens. A, altered *Uvigerina* sp. B, altered *Cibicides* sp. C, equatorial section of an altered microspheric *N. gizehensis*. D, unaltered *Uvigerina* sp. E, unaltered *Cibicides* sp. F, equatorial section of an unaltered megalospheric *N. gizehensis*.

Examples of each type of specimen were left uncoated and were imaged on a Zeiss Evo MA10 scanning electron microscope in the SEM Laboratory in the department of Earth and Planetary Sciences at the University of California, Berkeley. At the same time backscatter electron imaging (in which the heavier an element is, the lighter it appears on the image) and electron dispersive spectroscopy were carried out. EDAX Genesis Imaging and Mapping software was used to combine the results of x-ray analysis with backscatter images to produce maps showing the location of specific elements on the scanned area of test surfaces. Altered and Unaltered specimens of *Uvigerina* spp. and *N. gizehensis* were then coated in 25 nanometers of carbon and the imaging and mapping procedure was repeated to provide a comparison of results from coated and uncoated specimen.

Element maps and x-ray spectra of whole specimen were used to identify regions of suspected alteration. Spot mode was used to create spectra for those areas of interest, and was used in combination with crystal structure to identify diagenetic minerals. No quantitative analysis of surface composition could be carried out because EDAX software assumes a 2-dimensional polished surface in its calculations and the foraminiferal specimens have highly irregular surface

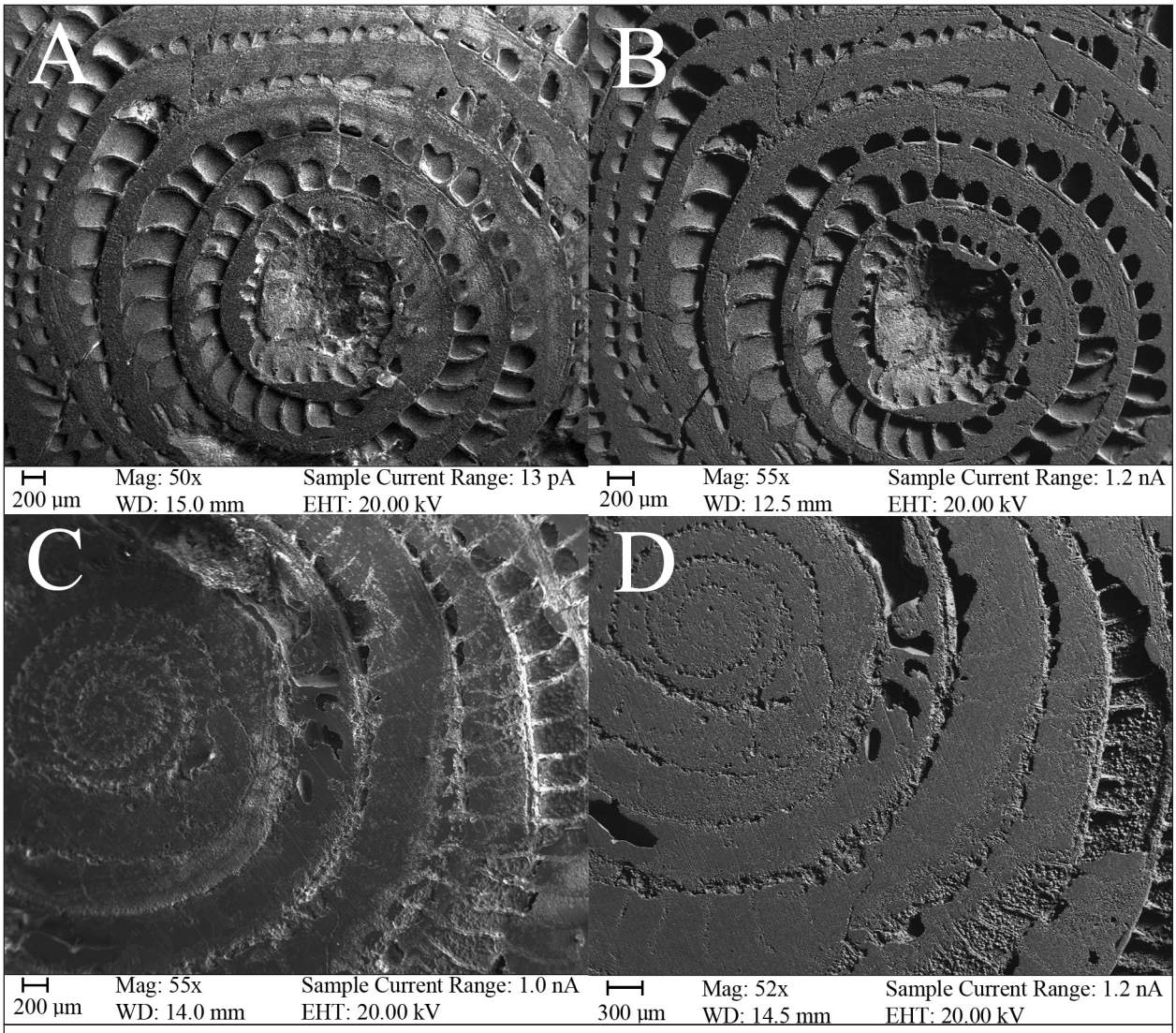

Figure 3. SEM images of altered and unaltered *N. gizehensis* with and without carbon coating. A, carbon coated, unaltered *N. gizehensis*; B, uncoated, unaltered *N. gizehensis*; C, carbon coated, altered *N. gizehensis*; D, uncoated, altered *N. gizehensis*.

topography.

Unaltered test material from megalospheric and microspheric N. gizehensis collected with a scalpel, and bulk samples of Cibicides spp. and Uvigerina spp. were analyzed for their oxygen and carbon isotope ratios. Pure dolomite and recrystalized calcite were also collected from heavily altered *N. gizehensis* for isotopic analysis. Samples containing about 10 to 100 microgram of calcite were used for both carbon and oxygen isotope analyses, which were determined using a GV IsoPrime mass spectrometer with Dual-Inlet and MultiCarb systems in the Laboratory for Environmental and Sedimentary Isotope Geochemistry (LESIG) at Department of Earth and Planetary Science, University of California at Berkeley. Several replicates of one international standard NBS19 and two lab standards were measured along with samples for each run. The overall external analytical precision is +0.04‰ for $\delta^{13}C$ and +0.07‰ for $\delta^{18}O$**.** All values are reported as per mil deviations from the PDB standard in the δ-notation:

$$\delta = \frac{R_{sample} - R_{standard}}{R_{standard}} \text{ x } 1000\,‰ \qquad (1)$$

where R is the ratio of heavier to lighter isotope ($^{18}O/^{16}O$ and $^{13}C/^{12}C$). For a full description of stable isotope foraminifera sample preparation methods see chapter 3.

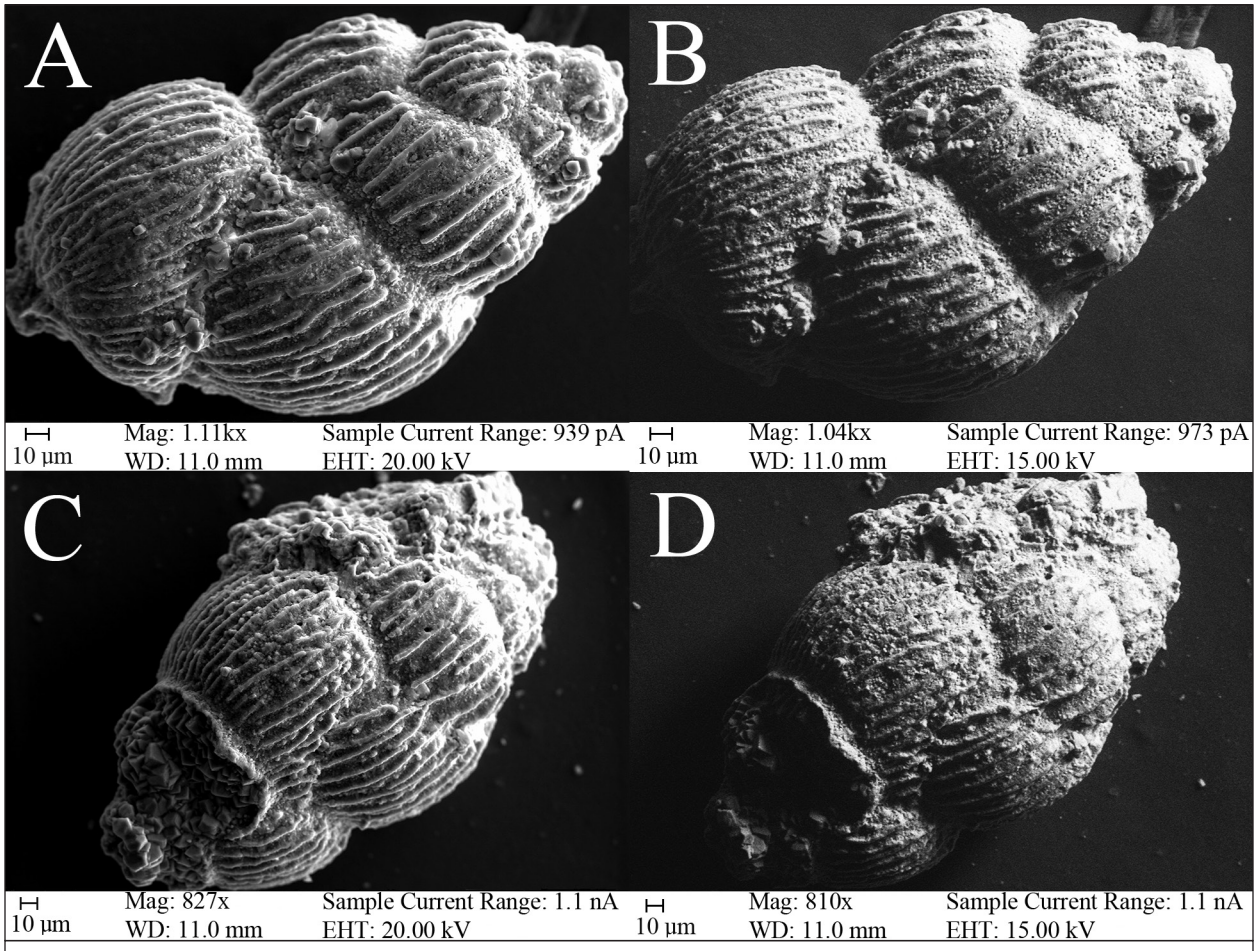

Figure 4. SEM images of altered and unaltered *Uvigerina* sp. A, carbon coated, unaltered *Uvigerina* sp.; B, uncoated, unaltered *Uvigerina* sp.; C, carbon coated, altered *Uvigerina* sp.; D, uncoated, altered *Uvigerina* sp.

Results

Presumed altered compared to presumed unaltered

N. gizehensis, *Uvigerina* sp. and *Cibicides* sp. identified as "altered" and "unaltered" based on visual inspection are pictured as seen under the microscope in Figure 2. Specimens designated "altered" show staining (Figure 2A, B and C) as well as translucent infilling (see second specimen in Figure 2A), secondary crystal growth (Figure 2C), and broken, pitted and worn tests (Figure 2A and B). "Unaltered" specimen are white, without any textures or staining indicative of secondary mineral deposits (Figure 2D, E and F), and in the case of smaller, whole taxa, have

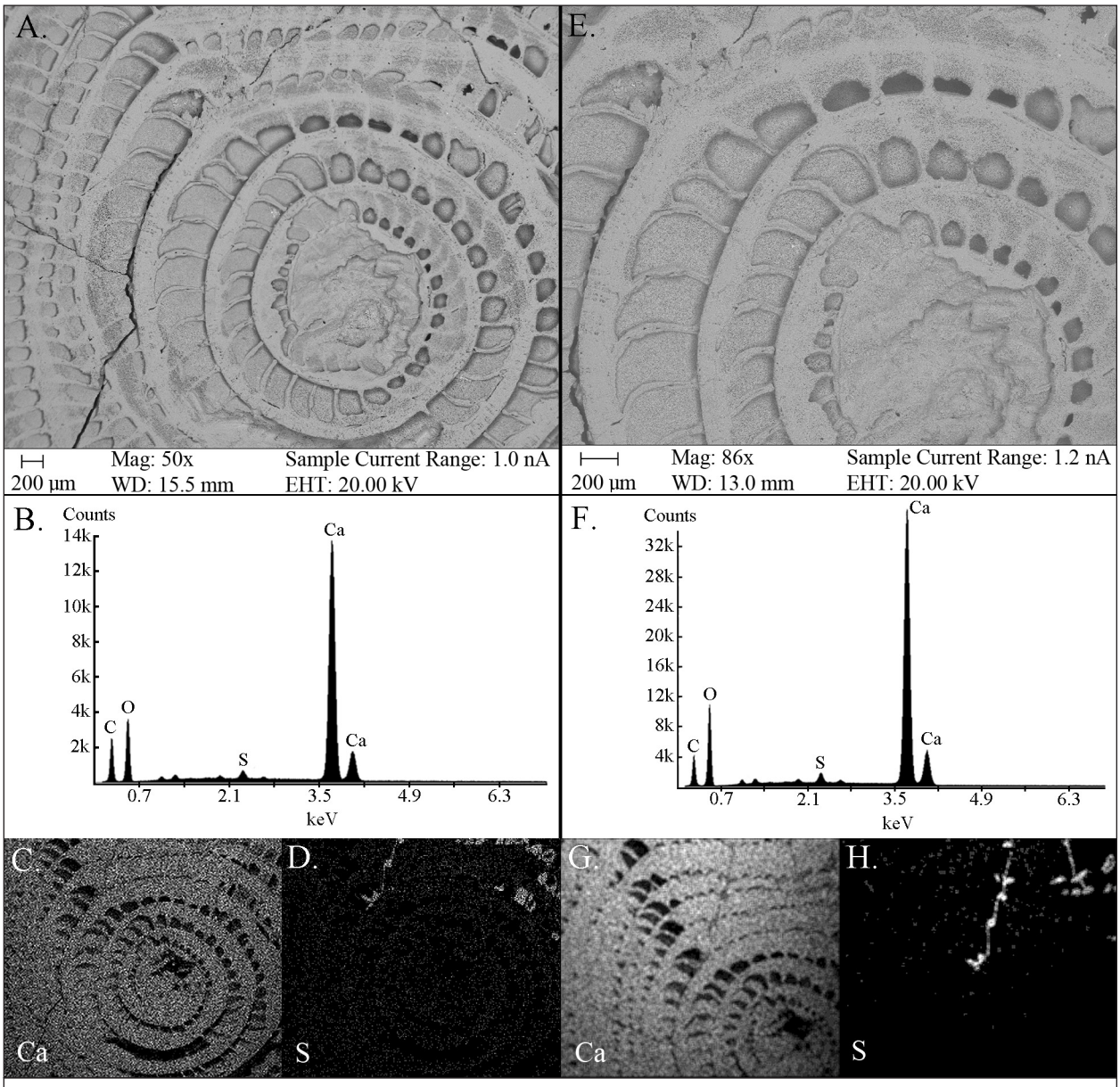

Figure 5. Spectra and element maps for coated and uncoated microspheric *N. gizehensis* presumed to be unaltered. A, backscatter image of carbon coated microspheric *N. gizehensis*. B, x-ray spectrum of the entire *N. gizehensis* surface imaged in A. C, map of calcium distribution over the scanned surface. D, map of sulfur distribution over the scanned surface. E, backscatter image of the same microspheric *N. gizehensis* specimen without carbon coating. F, x-ray spectrum of the entire surface of the uncoated *N. gizehensis*. G, map of calcium distribution over the scanned, uncoated surface. H, map of sulfur distribution over the scanned, uncoated surface.

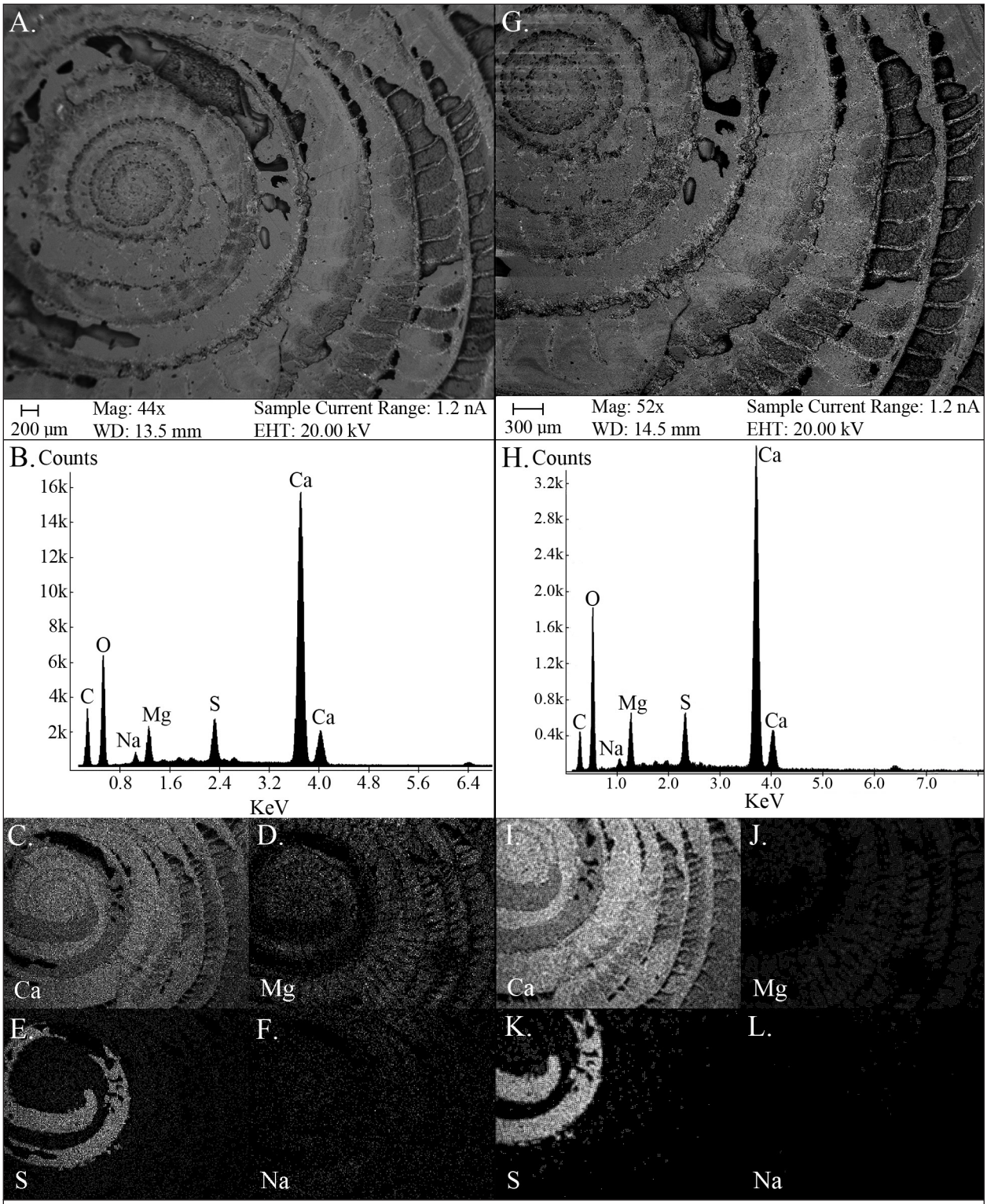

Figure 6. Spectra and element maps for coated and uncoated microspheric *N. gizehensis* presumed to be altered. A, backscatter image of carbon coated microspheric *N. gizehensis*. B, x-ray spectrum of the entire *N. gizehensis* surface imaged in A. C, map of calcium distribution over the scanned surface. D, map of magnesium distribution over the scanned surface. E, map of sulfur distribution over the scanned surface. F, map of sodium distribution over the scanned surface. G, backscatter image of the same microspheric *N. gizehensis* specimen without carbon coating. H, x-ray spectrum of the entire surface of the uncoated *N. gizehensis*. I, map of calcium distribution over the scanned, uncoated surface. J, map of magnesium distribution over the scanned, uncoated surface. K, map of sulfur distribution over the scanned, uncoated surface. L, map of sodium distribution over the scanned, uncoated surface.

tests with a glassy luster (Figure 2D and E).

SEM with EDS and element mapping reveal that specimens presumed to be altered are in fact heavily altered (Figures 6 and 8). Specimens presumed to be unaltered were sometimes found to have secondary mineral deposition not detected during visual inspection, however in these cases the degree of alteration was minor. "Unaltered" *N. gizehensis* were sometimes found to have secondary mineral deposits in pre-existing cracks (Figure 5), and small amounts of secondary crystal growth were found on some "unaltered" smaller taxa (Figure 7).

Carbon-coated compared to uncoated

While carbon coating specimen provided better resolution in SEM imaging, areas of secondary mineral deposition were equally identifiable in SEMs of both carbon coated and un-

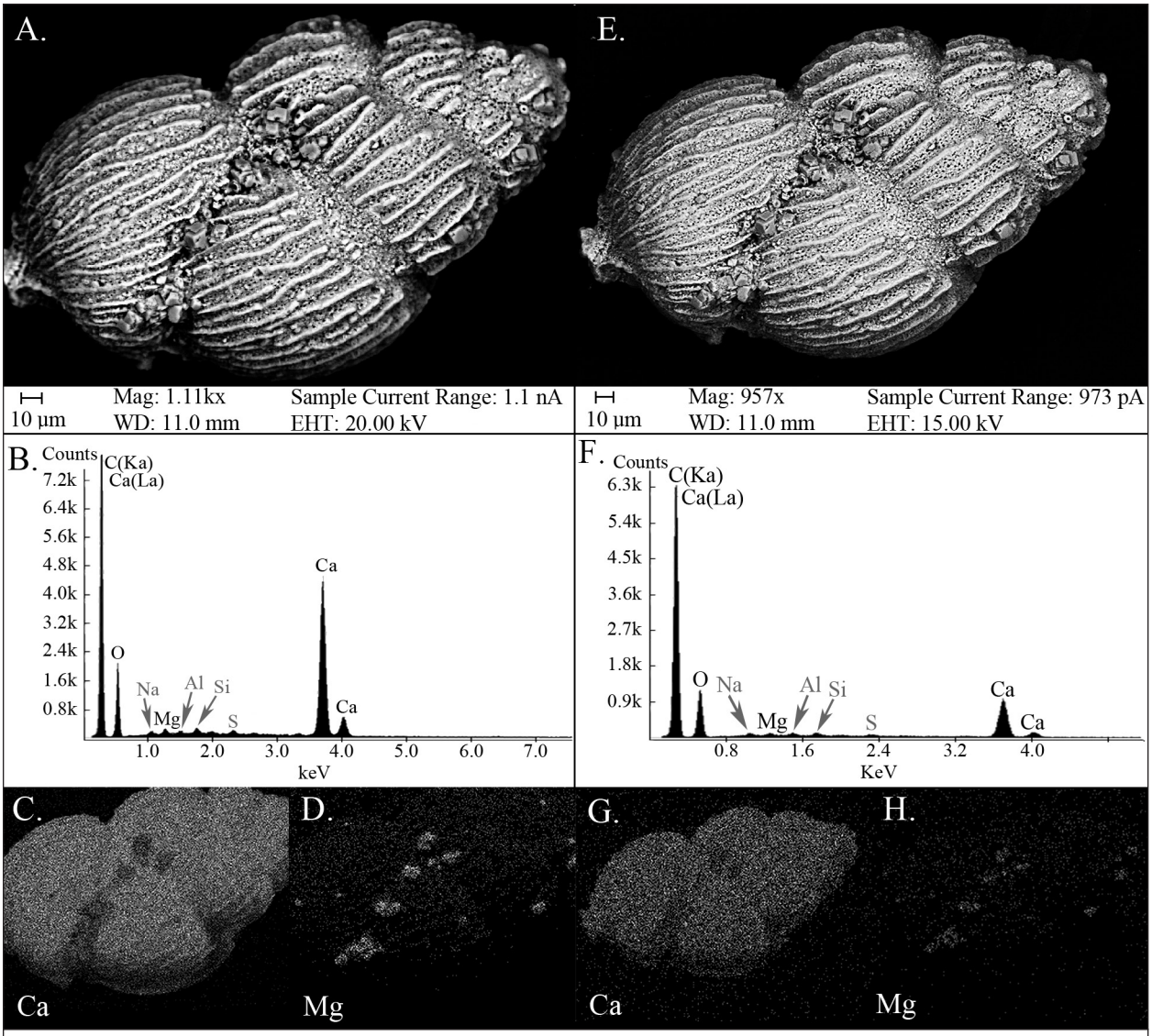

Figure 7. Spectra and element maps for coated and uncoated *Uvigerina* sp. presumed to be unaltered. A, backscatter image of carbon coated *Uvigerina* sp. B, x-ray spectrum of the entire *Uvigerina* sp. surface imaged in A. C, map of calcium distribution over the scanned surface. D, map of magnesium distribution over the scanned surface. E, backscatter image of the same *Uvigerina* sp. specimen without carbon coating. F, x-ray spectrum of the entire surface of the uncoated *Uvigerina* sp. G, map of calcium distribution over the scanned, uncoated surface. H, map of magnesium distribution over the scanned, uncoated surface.

coated *N. gizehensis* and *Uvigerina* sp. In heavily altered *N. gizehensis* infilled chambers could be seen, as well as crystal structures inconsistent with pristine tests (see Figure 3, C and D). A much smaller area of infilling on a presumed unaltered *N. gizehensis* is easy to overlook at the scale used in Figure 3 A and B, however it was visible in both coated and uncoated images at smaller scales. Secondary crystal growth was equally visible on coated and uncoated *Uvigerina* sp., whether the crystal growth was extensive (Figure 4, C and D) or relatively minor (Figure 4, A and B).

EDS preformed on coated and uncoated specimens yielded nearly identical spectra for scans of whole specimens (Compare Figures 5B and 5F, 6B and 6H, 7B and 7F, 8B and 8F). In every case the same elements were detected, however sometimes the relative intensities differed

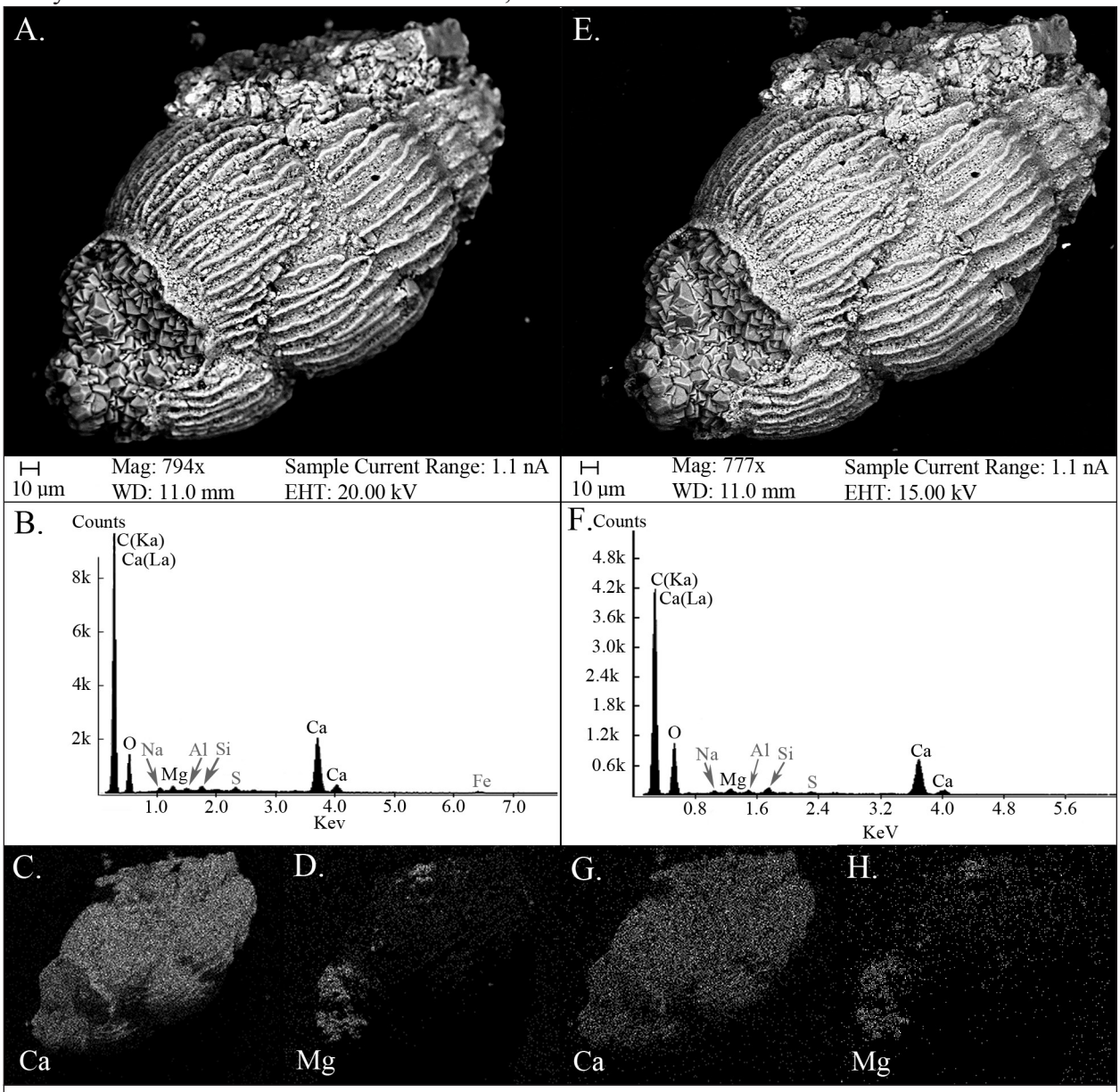

Figure 8. Spectra and element maps for coated and uncoated *Uvigerina* sp. presumed to be altered. A, backscatter image of carbon coated *Uvigerina* sp. B, x-ray spectrum of the entire *Uvigerina* sp. surface imaged in A. C, map of calcium distribution over the scanned surface. D, map of magnesium distribution over the scanned surface. E, backscatter image of the same *Uvigerina* sp. specimen without carbon coating. F, x-ray spectrum of the entire surface of the uncoated *Uvigerina* sp. G, map of calcium distribution over the scanned, uncoated surface. H, map of magnesium distribution over the scanned, uncoated surface.

(compare peaks of Ca relative to other elements in Figure 7, B and F). When element distributions were mapped onto backscatter images, the carbon coated specimens yielded more accurate maps (compare for example Figures 7C and 7G, 7D and 7H, 8C and 8G, 8D and 8H). In some instances the uncoated specimen provided maps with decreased background noise (compare Figures 5D and 5H, 6F and 6L), even though all map images where generated using a net intensity filter, which is designed to remove background spectra so that only peaks are mapped. Despite these slight variations in the map images, both coated and un-coated specimen resulted in maps that adequately described the location and composition of inorganic contamination.

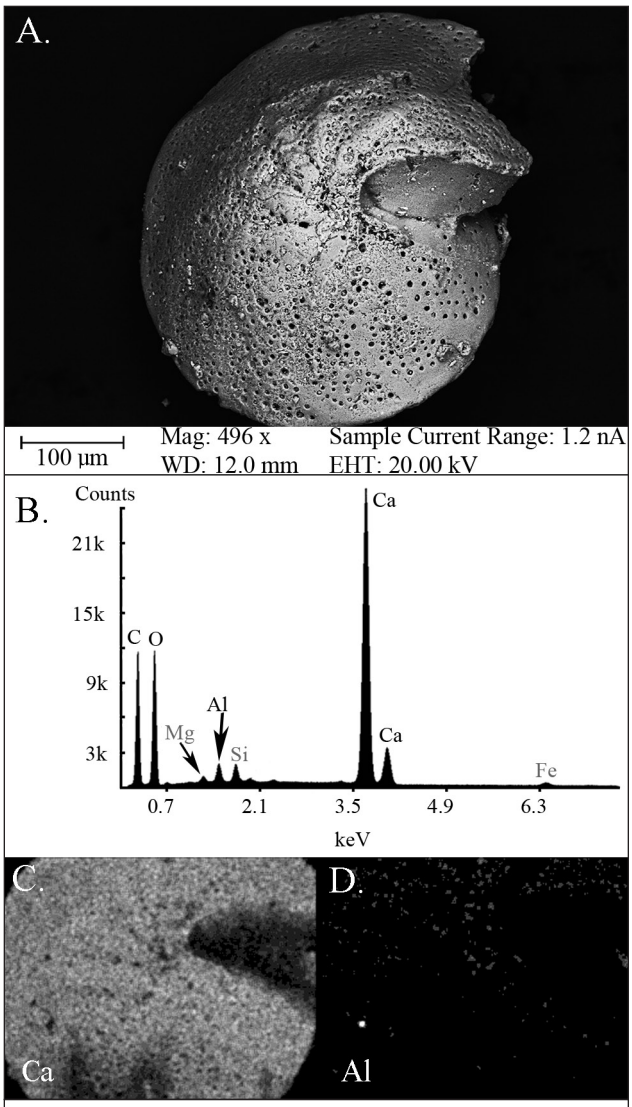

Figure 9. Spectra and element maps for uncoated *Cibicides* sp. presumed to be unaltered. B, x-ray spectrum of the entire surface of the *Cibicides* sp. C, map of calcium distribution over the scanned, uncoated surface. D, map of aluminum distribution over the scanned, uncoated surface.

Identifying diagenetic materials

The crystal structures visible in SEM and backscatter images were used in combination with spectral analyses to identify the different inorganic contamination found on all foraminiferal taxa. Spot analyses performed on rhombohedral crystals found in *N. gizehensis* and both altered and unaltered *Uvigerina* sp. yielded nearly identical spectra (Figure 11); all showed strong peaks for magnesium (Mg) and calcium (Ca). Both the crystal structure and element composition are consistent with secondary dolomite ($CaMg(CO_3)_2$), which is a typical diagenetic mineral of depositional environments. The yellow-brown appearance of these crystals in some specimen (see Figure 2C) is almost certainly a result of iron (Fe) replacing some Mg, which is common in dolomite.

The colorless, monoclinic crystals found in altered and unaltered *N. gizehensis* yielded nearly identical spectra (Figure 12); all showed strong peaks in Ca and sulfur (S). Both the crystal structure and element composition are consistent with gypsum, the most common sulphate mineral, which is also typical of depositional environments and often associated with limestones and clays.

In nearly all the specimen analyzed, small peaks for aluminum (Al), silicon (Si), magnesium (Mg), and sometimes sodium (Na) or iron (Fe) occur, even in cases were no concentrated areas of these elements appear on maps (see Figures 5 - 10). Spot analyses of small, irregularly shaped particles found on nearly all specimens yielded nearly identical spectra (Figure 13); the only differences were in the relative intensities of the elements detected. These foraminifera were

preserved in a clay matrix, and the identified elements are all typical of clay minerals - particularly those found in Egyptian, Eocene, shallow marine clays (Abd-Allah et al. 2009).

Secondary calcite was easy to identify morphologically, but the spectrum for spot analysis of obviously secondary calcite deposits on *Uvigerina* sp. (Figure 14A and B) is indistinguishable from spectra for original test calcite (Figure 16). It is most likely recrystalized test calcite. High resolution images of test surfaces (Figures 14A, 16A and 16B and especially the chamber wall shown in Figure 12B) compared to modern tests known to be uncontaminated (Beavington-Penney and Racey 2004), indicate original test calcite is preserved. Mechanical or chemical weathering of tests is also detectable in images (Figure 14C and D), although it isn't possible to determine whether these alterations occurred before or after burial.

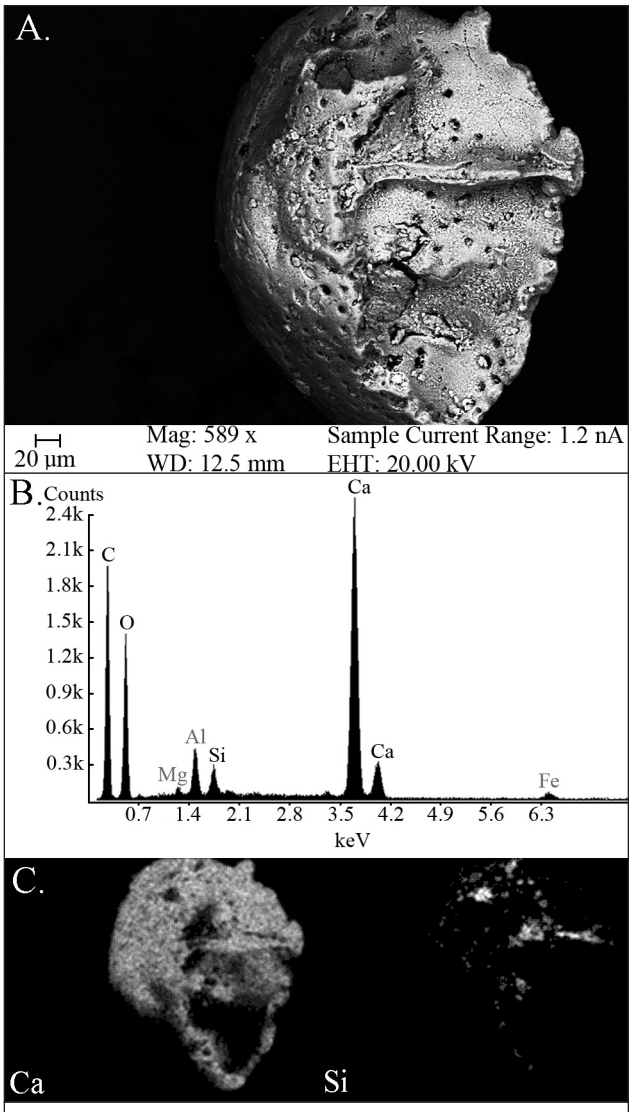

Figure 10. Spectra and element maps for uncoated *Cibicides* sp. presumed to be altered. B, x-ray spectrum of the entire surface of the *Cibicides* sp. C, map of calcium distribution over the scanned, uncoated surface. D, map of silicon distribution over the scanned, uncoated surface.

Stable carbon and oxygen isotopes

Pure dolomite has a positive shift in $\delta^{13}C$ relative to all foraminiferal taxa; +3.2‰ from the average of all *N. gizehensis* values and +1.58‰ from the average of all *Cibicides* spp. and *Uvigerina* spp. values. Its $\delta^{18}O$ is 2.03‰ more negative than the average of all *N. gizehensis* values, but overlaps with $\delta^{18}O$ values of *Cibicides* spp. and *Uvigerina* spp. (see figure 15). The carbon and oxygen isotopic signature of pure dolomite are within the range of calcite that has formed in equilibrium with ambient seawater. This range of values is calculated from adjusted *Cibicides* spp. and *Uvigerina* spp. values (for a complete discussion of methods see chapter 3). This is expected for inorganic calcite precipitating very soon after sample burial.

Recrystalized calcite yields $\delta^{13}C$ and $\delta^{18}O$ values close to those of source calcite, with a positive shift less than 1‰ in both (figure 15).

Discussion

Light microscopy

This study set out to determine 1) whether visual inspection with a light microscope was adequate to detect the presence of diagenetic alteration, 2) whether specimen needed to be carbon

coated to sufficiently detect and identify diagenetic alteration with SEM and EDS, 3) what diagenetic materials are present and what they tell us about the sample, and 4) how will these diagenetic materials effect carbon and oxygen stable isotope ratios.

Visual inspection with a light microscope proved to be better than expected at predicting diagenetic alteration in specimens. This is largely due to the preservational environment, and the type of diagenesis that was most common. The sample was preserved in a clay rich matrix; clay has low permeability, and tests are sealed off from later contact with altering fluids (Pearson et al. 2001). As is the case with tests preserved in such sediments, when smaller taxa were exceptionally preserved they retained the translucent, glassy appearance of modern taxa, and any amount of dissolution or overgrowth was readily identifiable as an absence of "glassiness."

The most common alteration to the tests was infilling and overgrowth with secondary calcite (dolomite). Although dolomite can be colorless, marine sediments from Eocene Egypt are iron-rich (Abd-Allah et al. 2009), and the replacement of Mg with Fe gave the dolomite a yellow-brown hue that was easily detected against the glassy, white of pristine tests.

Visual inspection with light microscopy failed to detect small areas of dolomite overgrowth, especially along test sutures. It also failed to detect small areas of colorless gypsum infilling. For isotopic studies that use multiple smaller taxa to make up a single sample, it's unlikely that very minor amounts of dolomite on one or two individuals will have a significant effect on results. However, in larger taxa such as *N. gizehensis* where sub-sampling is planned, even minor amounts (relative to the whole specimen) of undetected gypsum could have non-negligible effects. In this instance, the use of EDS with element mapping revealed that gypsum

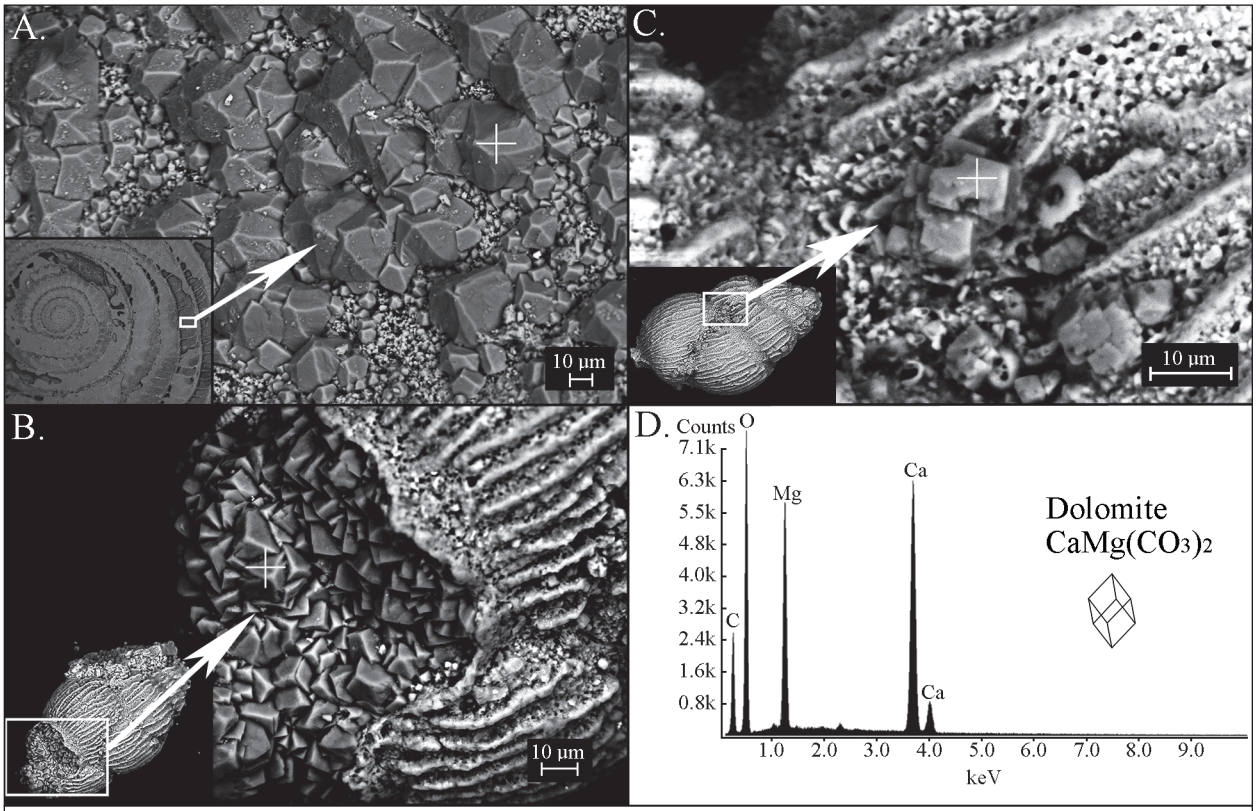

Figure 11. Dolomite in *Uvigerina* sp. and *N. gizehensis*. The white rectangle on the inset pictures show the area pictured in full-size image, and the white cross shows the spot analyzed to produce a localized x-ray spectrum. A, backscatter image of dolomite crystals in altered *N. gizehensis*. B, backscatter image of dolomite crystals in altered *Uvigerina* sp. C, backscatter image of dolomite crystals in unaltered *Uvigerina* sp. D, representative x-ray spectrum of dolomite crystals analyzed on all specimens.

contamination was likely to occur within cracks in the specimen. Once this pattern of contamination was recognized it was simple to avoid sampling near cracks, and to otherwise rely on light microscopy to distinguish between pristine and altered tests.

Carbon coating

Carbon coating is used in scanning electron microscopy (SEM) and electron dispersive spectroscopy (EDS) to prevent charge build-up in samples with low conductivity. This improves image resolution, and in EDS ensures the most accurate quantitative measurements of elements' relative proportions (counts, or intensities). The SEM images here are a demonstration of the better resolution achieved with carbon-coating (see Figures 3 and 4), however coating didn't reveal any diagenetic alterations that were not detectable in lower resolution images of uncoated specimen. If the goal of SEM is to detect diagenesis on rare or precious samples, coating can be skipped in favor of preserving sample integrity.

To quantify the relative proportions of elements in a sample using EDS, the sample must be a flat, polished surface oriented horizontal to the electron beam. Given the irregular topography of whole foraminiferal specimen there was no attempt to quantify element proportions. Rather, the goal was to detect their presence, and use mapping to locate them on the test. For this purpose, carbon-coating didn't provide any significant advantages over uncoated specimen; spectra and element maps were adequate in both cases to locate and identify diagenetic materials (see Figures 5 - 8). If quantitative accuracy is not a priority in EDS, then coating can again be skipped in favor of preserving sample integrity.

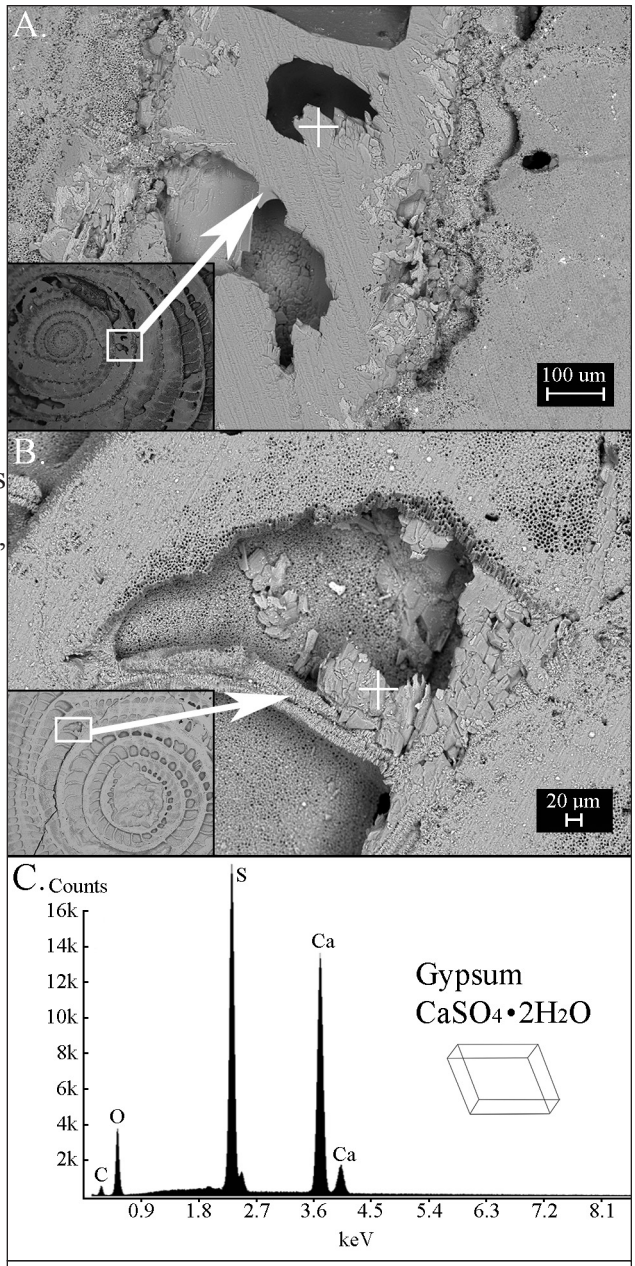

Figure 12. Gypsum in altered and unaltered *N. gizehensis*. The white rectangle on the inset pictures show the area pictured in full-size image, and the white cross shows the spot analyzed to produce a localized x-ray spectrum. A, backscatter image of gypsum in altered *N. gizehensis*. B, backscatter image of gypsum in unaltered *N. gizehensis*. C, representative x-ray spectrum of gypsum crystals analyzed on all specimens.

Diagenesis

The most common diagenetic alterations found on sample taxa were dolomite infilling and overgrowth, and gypsum infilling. Low levels of clay contamination were also seen in nearly

all taxa, and more rarely areas of recrystalized test calcite and dissolution.

The very low levels of aluminum (Al), silicon (Si), magnesium (Mg), sometimes iron (Fe) and rarely sodium (Na) found on nearly all specimen and identified as present in irregularly shaped particles are from the detrital clay in which the specimen were preserved. These are elements typical of clay mineral species in general, and shallow, marine clays of the Egyptian Eocene in particular, which are known to be iron-rich (Abd-Allah et al. 2009). The fine particle size of clay (and absence large grain sizes in the original matrix) indicates this sample was deposited in a low energy environment, such as a sheltered bay. Dolomite and gypsum are both typical post-sedimentary minerals in shallow marine deposits, and common to Middle Eocene limestones of Egypt (Mansour and Holail 2004). The recrystalized test calcite (see Figures 8 and 13A) remains the most difficult to detect with EDS, therefore familiarity with taxa morphology is important in order to recognized structural differences.

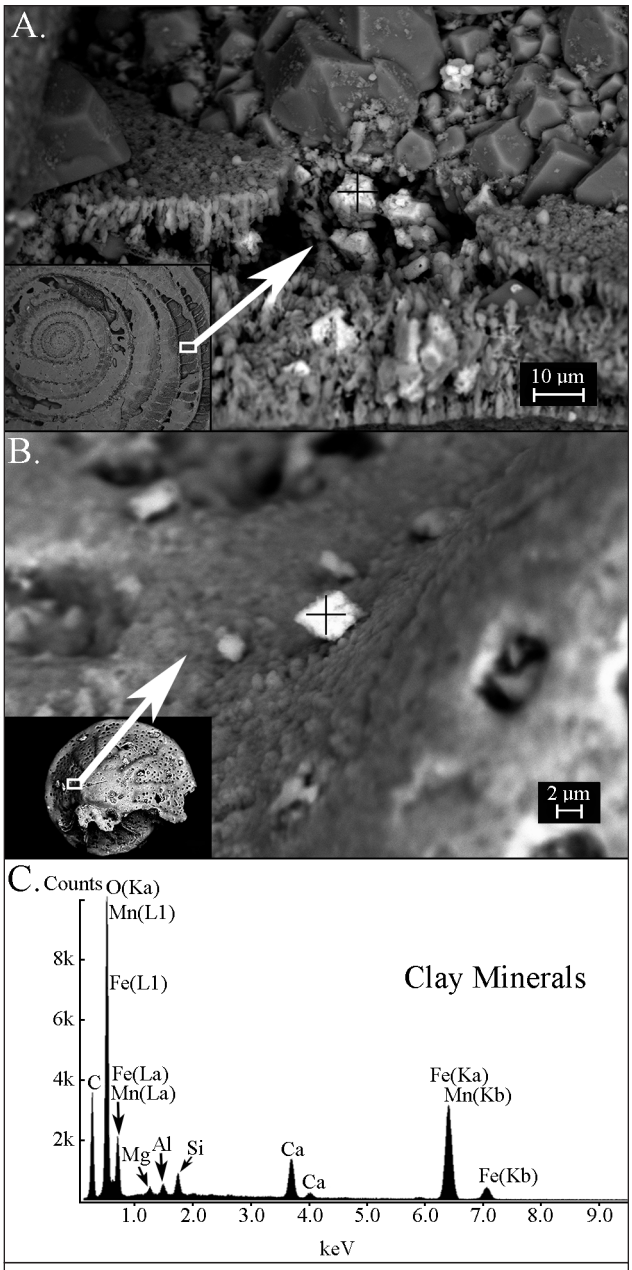

Figure 13. Clay minerals on *Cibicides* sp. and *N. gizehensis*. The white rectangle on the inset pictures show the area pictured in full-size image, and the white cross shows the spot analyzed to produce a localized x-ray spectrum. A, backscatter image of clay particle in chamber of altered *N. gizehensis*. B, backscatter image of clay particle on altered *Cibicides* sp. C, representative x-ray spectrum of clay particles analyzed on all specimens.

Effects on stable isotopes values

Dolomite and recrystalized calcite show positive shifts relative to pristine foraminiferal test calcite in both $\delta^{18}O$ and $\delta^{13}C$. For dolomite, the values found are consistent with calcite inorganically precipitated in equilibrium with ambient sea water. Recrystalized calcite shows values close to those for the source foraminiferal test.

The effects of diagenesis on the stable isotope ratios of biogenic carbonate depend on the difference between the isotopic ratios of the biogenic carbonate and those of the authigenic carbonate (i.e. dolomite or recrystalized calcite), thus it must be determined on a case by case basis. If the delta values are known for both the biogenic carbonate and the authigenic carbonate then it is possible to estimate the point at which samples are too altered to yield reliable results by using the equation of (Blanchet et al. 2012):

$$M = \frac{\delta_{Meas} - \delta_{Biog}}{\delta_{Authi} - \delta_{Biog}} \text{ x } 100 \qquad (2)$$

where M is the mass balanced amount of authigenic calcite added to the sample (in %), δ_{Meas} is the isotopic composition of the contaminated sample, δ_{Biog} is the isotopic composition of the pristine biogenic carbonate, and δ_{Authi} is the isotopic composition of the authigenic carbonate (Blanchet et al. 2012). A conservative cut off for using partially contaminated samples are δ_{Meas} values that are less than or equal to 1 standard deviation from the average δ_{Biog} value. Once δ_{Biog} and δ_{Authi} have been found and δ_{Meas} has been set equal to 1 standard deviation from the δ_{Biog} average, then M can be calculated.

Applying this method to the results shown in Figure 15 indicates that dolomite contamination must be equal to or less than 8% of sample mass to get good results for both oxygen and carbon isotope ratios in *N. gizehensis*, and less than or equal to 7% of sample mass in *Uvigerina* spp. and *Cibicides* spp. However, if one is only interested in the oxygen isotope ratios of *Uvigerina* spp. and *Cibicides* spp., even 100% contamination will yield valid results.

N. gizehensis can contain up to 44% recrystalized calcite and still yield good results for both oxygen and carbon isotope ratios, with 100% contamination still providing oxygen ratios

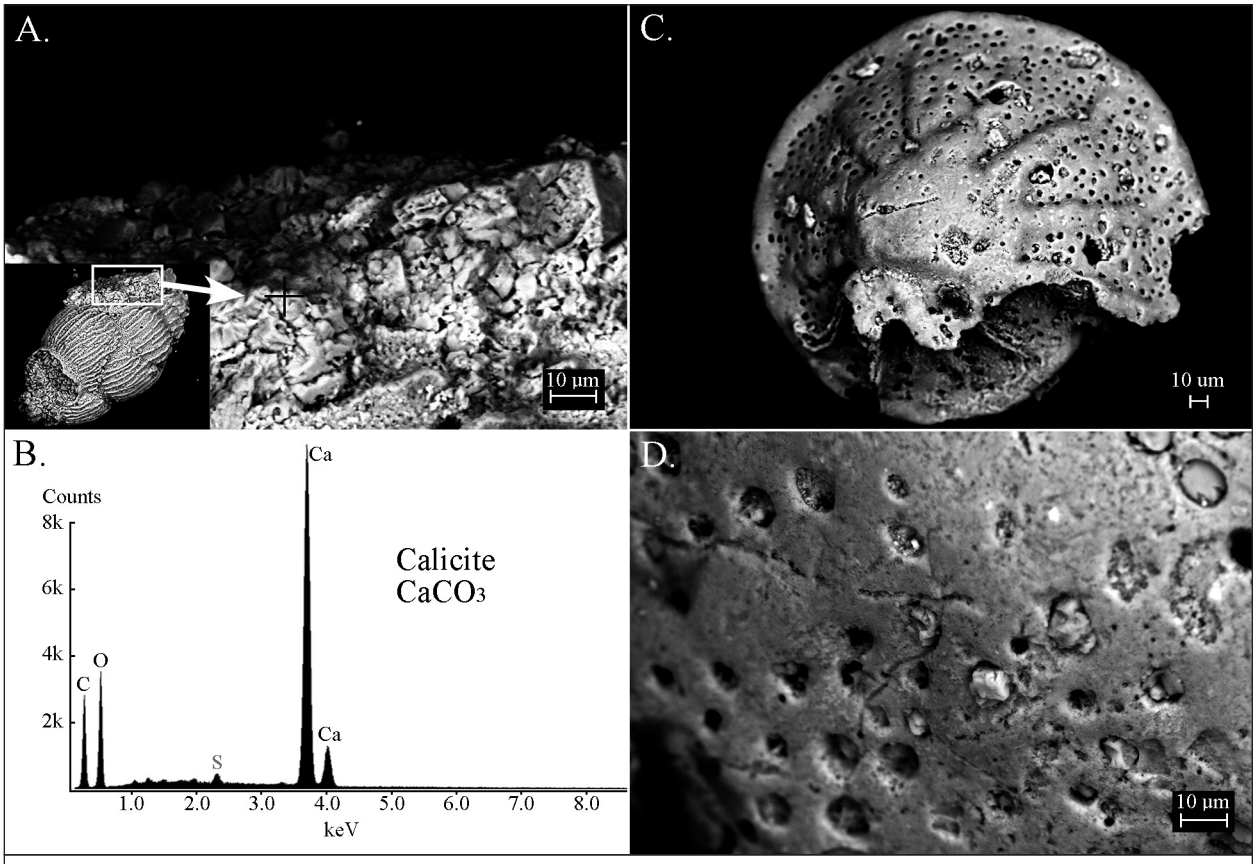

Figure 14. Weathering and secondary calcite in *Uvigerina* sp. and *Cibicides* sp. A, backscatter image of secondary calcite deposit on altered *Uvigerina* sp. The white rectangle on the inset pictures show the area pictured in full-size image, and the black cross shows the spot analyzed to produce a localized x-ray spectrum. B, x-ray spectrum of the secondary calcite shown in A. C, backscatter image of altered *Cibicides* sp. showing chemical or mechanical weathering of test surface, especially around the pores. D, close-up view of another altered *Cibicides* sp. showing weathering of test and clay particles lodged in pores.

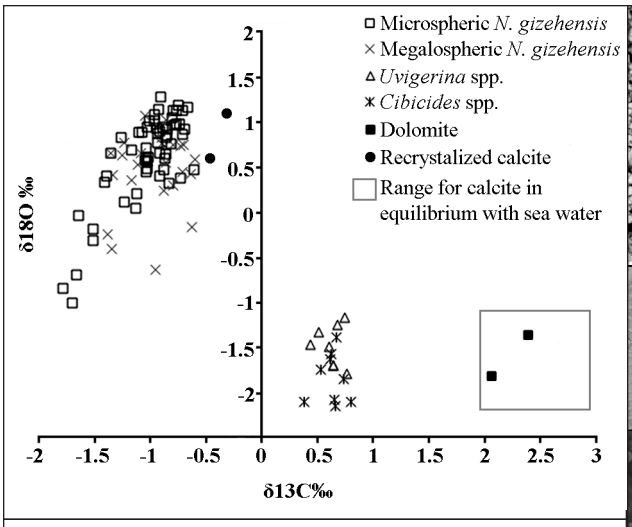

Figure 15. Graph of all δ13C and δ18O including pure dolomite collected from heavily altered *N. gizehensis*, and pristine tests of *Uvigerina* spp., *Cibicides* spp., and sexually and asexually produced *N. gizehensis*. The area within the grey square is the range of δ13C and δ18O values for calcite precipitated in equilibrium with ambient sea water as calculated from adjusted *Uvigerina* spp. and *Cibicides* spp. values (see chapter 3 for full discussion of calculations).

within 1 standard deviation of the pristine biogenic average. For adequate results in *Uvigerina* spp. and *Cibicides* spp., recrystalized calcite must be kept at or below 12% of the sample mass.

These percentages were calculated using only 2 values each for pure dolomite and pure recrystalized calcite, and as such should be relied upon with caution. For more robust results, a larger sample size is suggested. With this in mind, every effort was made to include only 100% uncontaminated biogenic calcite in the later isotopic study.

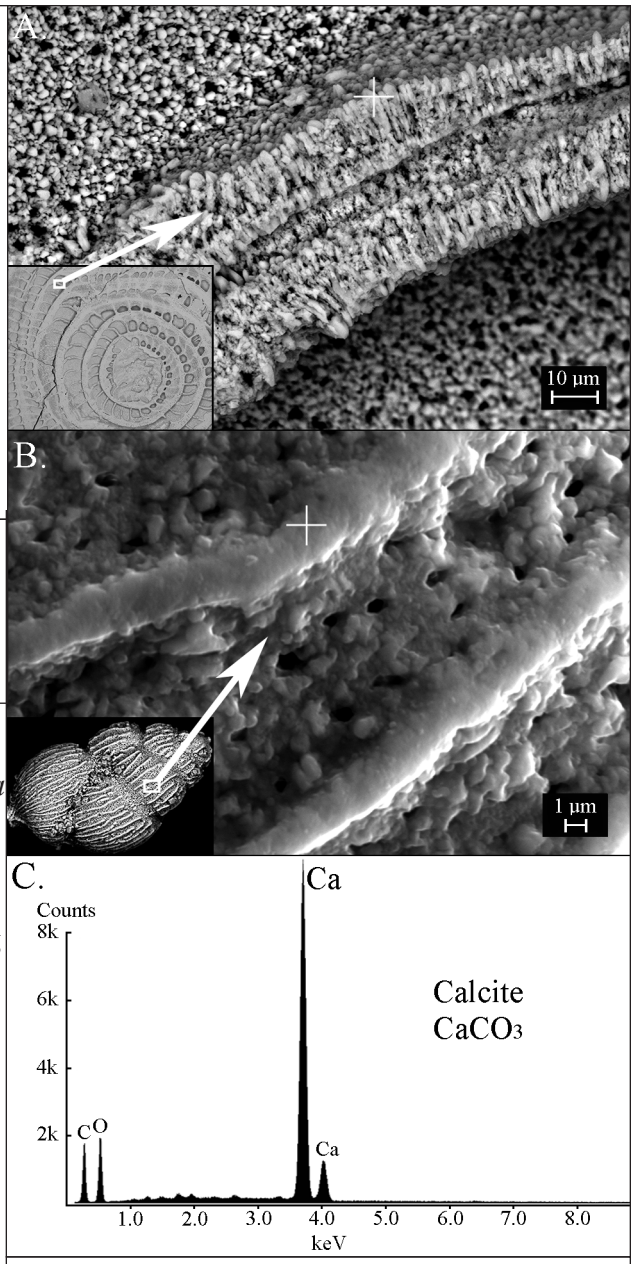

Figure 16. Original calcium carbonate test of *N. gizehensis* and *Uvigerina* sp. The white rectangle on the inset pictures show the area pictured in full-size image, and the white cross shows the spot analyzed to produce a localized x-ray spectrum. A, backscatter image of a chamber wall of unaltered *N. gizehensis*. B, backscatter image of the test surface of unaltered *Uvigerina* sp. C, representative x-ray spectrum of original calcium carbonate tests of analyzed specimen.

Recommendations

The results of this study can be broadly adapted to any study of rare, calcium carbonate samples in which diagenesis is of concern. SEM, backscatter electron imaging and EDS can be used to determine the types of diagenetic material present, and their likely distribution on sample tests, for example along suture lines or within cracks. The same specimens examined using these techniques should also be examined using light microscopy to establish what (if anything) altered material looks like under a basic binocular microscope. If possible, comparison to recent specimens of the same or related taxa should be used to provide an example of pristine test material. In many instances it should be possible to distinguish pristine material from altered

material using only light microscopy, which will make any sub-sampling of material for isotopic analysis more time efficient. For rare or precious specimens, SEM and EDS yield sufficient qualitative results without carbon-coating so that sample integrity may be preserved. If the condition of the sample permits preliminary isotopic testing, then an allowable percentage of contamination can be calculated to ensure reliable isotopic results.

References

Abd-Allah AMA, Dawood YH, Awad SA, Agila WA. 2009. Mineralogical and chemical compositions of shallow marine clays, east of Cairo, Egypt: a geotechnical perception. Journal of King Abdulaziz University - Earth Sciences 20: 141-166.

Beavington-Penney S, Racey A. 2004. Ecology of extant nummulitids and other larger benthic foraminifera: applications in palaeoenvironmental analysis. Earth-Science Reviews 67: 219-265.

Blanchet CL, Kasten S, Vidal L, Poulton SW, Ganeshram R, Thouveny N. 2012. Influence of diagenesis on the stable isotopic composition of biogenic carbonates from the Gulf of Tehuantepec oxygen minimum zone. Geochemistry Geophysics Geosystems 13.

Crowley T, Zachos JC. 2000. Comparison of Zonal Temperature Profiles For Past Warm Time Periods. Pages 50-76 in Huber BT, MacLeod KG, Wing SL, eds. Warm Climates in Earth History. Cambridge: Cambridge University Press.

Mansour AS, Holail HM. 2004. Dolomitization of middle Eocene carbonate rocks, Abu Roash area, Egypt. Carbonates and Evaporites 19: 151-161.

Pearson PN, Ditchfield PW, Singano J, Harcourt-Brown KG, Nicholas CJ, Olsson RK, Shackleton NJ, Hall MA. 2001. Warm tropical sea surface temperatures in the Late Cretaceous and Eocene epochs. Nature 413: 481-487.

Schrag DP, DePaolo DJ, Richter FM. 1995. Reconstructing past sea surface termperatures: correcting for diagenesis of bulk marine carbonate. Geochimica et Cosmochimica Acta 59: 2265-2278.

Williams M, Haywood AM, Vautravers M, Sellwood BW, Hillenbrand C-D, Wilkinson IP, Miller CG. 2007. Relative effect of taphonomy on calcification temperature estimates from fossil planktonic foraminifera. Geobios 40: 861-874.

III. Endosymbiosis in the Eocene Nummulite, *Nummulites gizehensis*

Abstract

It is widely accepted in the literature that extinct species of larger foraminifera hosted algal symbionts, and that the evolution of larger foraminifera has been driven by algal symbiosis. However, there is no definitive evidence for symbiosis in fossil larger foraminifera. This study uses the known characteristics of stable isotope chemistry in extant symbiotic rotaliid foraminifera to test the hypothesis that the extinct rotaliid, *Nummulites gizehensis*, hosted photosynthesizing endosymbionts. The carbon isotopic signatures of symbiotic rotaliid foraminifera are 3-5‰ lower in $\delta^{13}C$ than calcite in equilibrium with ambient seawater, and exhibit a less well-supported trend of increasing $\delta^{13}C$ values over ontogeny. The micro- and megalospheric *Nummulites gizehensis* tested here show a mean negative shift of 3.75‰ relative to contemporary fossil equilibrium calcite as calculated from co-occurring *Uvigerina* spp. and *Cibicides* spp. Seven out of nine microspheric individuals show the expected ontogenetic trend in $\delta^{13}C$ over ontogeny, however all of the megalospheric forms show the opposite trend. Like their larger extant relatives, *Nummulites gizehensis* appear to have hosted photosynthesizing symbionts.

Introduction

"Larger Foraminifera" is an informal, polyphyletic grouping comprising extant and extinct benthic taxa that have calcium carbonate tests, a volume exceeding $3mm^3$ and complex internal morphologies (Hallock 1985, Ross 1974). Extant taxa all belong to the Suborders Miliolina and Rotaliina, and extinct taxa also include Lituolida and Fusulinida. These larger foraminifera have evolved independently multiple times, dominating warm, shallow-water limestones of the Late Oligocene-Early Miocene, Eocene, Cretaceous and Permo-Pennsylvanian (Hallock 1985, Lee et al. 1979, Ross 1974, Tappan and Loeblich 1988). Ross (1974) first proposed that extinct larger foraminifera hosted algal endosymbionts, citing the evolutionary parallels between larger foraminifera and hermatypic corals, their occurrence in oligotrophic paleoenvironments, and complex test morphologies. Since then the ideas that extinct species of larger foraminifera hosted algal symbionts and that evolution of larger foraminifera has been driven by algal symbiosis have become widely accepted (Lee and Hallock 1987).

In the decades since Ross's work, considerable research has been carried out on extant

larger foraminifera and their symbiotic associations that has important implications for the question of endosymbionts in extinct forms. For example, although the associations are flexible, with many foraminiferal species hosting multiple closely-related members of an algal clade (Hallock 1999, Pochon et al. 2004), some degree of host-endosymbiont specificity occurs; rotaliine perforate species host diatom endosymbionts, while imperforate miliolids can host rhodophytes, green algae, or dinoflagellates (Leutenegger 1984). Specialization of this kind requires the evolution of novel characters to allow the recognition and maintenance of symbionts, implying a history of interaction between host and symbiont species. Indeed, phylogenetic analysis of symbiont type in extant Soritid foraminifera found endosymbiosis with algal symbionts to be plesiomorphic for the clade Soritacea (Richardson 2001).

Morphological similarities between extinct taxa and symbiont-bearing extant taxa are often used to infer symbiosis in the extinct forms when the morphological characteristics play a functional role in symbiosis (Cowen 1988). For example, diatom endosymbionts closest to the surface in *Amphistegina lobifera* (family Nummulitidae) fit into cup-like chambers (McEnery and Lee 1981). Similarly, pores on the lateral chamber walls of perforate species *Operculina ammonoides* and *Heterostegina depressa* (family Nummulitidae) function as housing for symbionts and the translucent calcite above creates perfect greenhouse conditions (Hottinger and Dreher 1974). This is consistent with changes in test shape with irradiance, where deeper dwelling individuals increase lateral surface area with a flat growth pattern to increase access to light, and those in shallower waters grow thicker to protect against photo-inhibition (Hottinger and Dreher 1974). Similar test morphology and depth-related growth patterns are found in extinct members of family Nummulitidae, suggesting that they may have also housed photosynthesizing endosymbionts.

Growth experiments have shown that increased light intensity results in increased calcification rates, and conversely without light many symbiont-bearing foraminifera will not grow at all, even if fed (Duguay 1983, Lee et al. 1991). Does this mean endosymbiosis led to large size in their foraminiferal hosts? Although not all foraminifera with endosymbionts are so large and some very large agglutinated foraminifera do not host photosynthetic endosymbionts (Hallock 1985), photosymbionts are hosted in all larger calcareous foraminifera. This pattern of host enlargement is seen in other symbiotic groups such as hermatypic corals and giant clams (Cowen 1988).

Based on Ross's (1974) initial observations and subsequent considerable research on extant symbiotic foraminifera (for review see Lee 2006), the hypothesis that extinct larger foraminifera hosted algal endosymbionts is widely accepted. However, alternative hypotheses are equally feasible in light of available evidence. For example, large cell size may have been selected for because it allows for greater food storage between seasonal periods of productivity in otherwise oligotrophic environments (Hottinger 1982); accompanying test complexity is necessary to increase surface area to volume ratio and strengthen the test (Song et al. 1994). In this scenario symbiotic associations may follow the evolution of larger, more complex morphologies in extinct forms, rather than cause that evolution.

Direct, independent evidence of symbiosis in fossil larger foraminifera is almost entirely absent. Organic, spherical structures were identified as possible symbionts in late Paleozoic fusulinids (Lee and Hallock 1987), but the interpretation is debatable (Beavington-Penney and Racey 2004).Stable isotope trends in the larger foraminifer *Nummulites prestwichianus* from the Middle Eocene Hampshire Basin reveal increasing $\delta^{13}C$ values in *N. prestwichianus* with growth (Brasier

and Green 1993). This trend may be a result of either decreasing calcification rate with age or decreasing photosynthetic activity by symbionts due to test thickening, both of which could result in a decrease in fractionation.

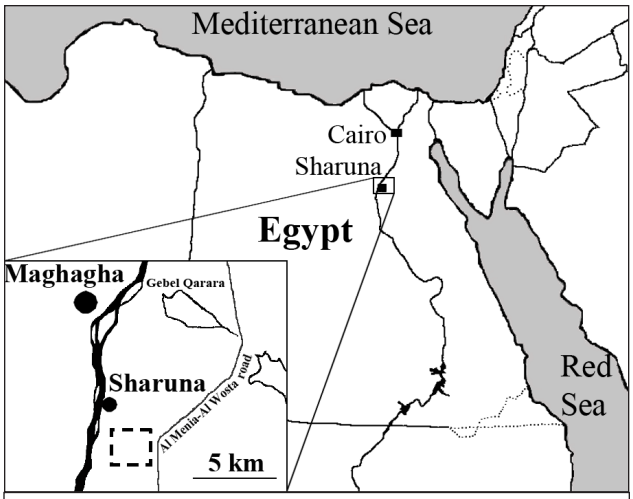

Figure 1. Locality map. Dashed box on inset indicates approximate location of clay pit where samples were collected.

Stable isotope techniques have been used to confirm symbiosis in other calcium carbonate secreting fossil-hosts, however. Known isotopic trends in modern hermatypic corals confirmed symbiosis in Triassic corals (Stanley and Swart 1995), and a number of isotopic studies have been done indicating symbiosis in extinct planktonic foraminifera (D'Hondt et al. 1994, Houston and Huber 1998, Houston et al. 1999, Norris 1996, Pearson P. et al. 1993, Wade et al. 2007). If shifts in stable carbon and oxygen isotopes ratios due to diagenetic alteration, fluctuations in ancient sea-water temperature and ocean productivity can be controlled for, then isotopic analysis may provide the most unequivocal evidence of ancient symbiosis (Cowen 1988).This study uses stable isotope techniques to perform a direct test for the presence of photosynthetic endosymbionts in an extinct Eocene Foraminifer, *Nummulites gizehensis*.

Study design

The Nummulitidae are a family of foraminifera with both extinct and extant members described as "larger." They belong to the sub-order Rotaliida (Loeblich and Tappan 1988), all of whose members secrete bilamellar, hyaline, perforated tests of low Mg calcite. All of the extant symbiotic foraminiferal species belonging to Rotaliida for which $\delta^{13}C$ has been measured relative to calcite in equilibrium with seawater show a negative shift between 3-5 ‰ (Table 5), and in studies where comparisons to equilibrium calcite are not quantified, strong negative shifts that agree with quantified studies are found (Langer 1995). Erez (1978) and others have shown experimentally that the magnitude of this disequilibrium fractionation intensifies with light intensity and photosynthetic rates of symbionts (Langer 1995, Lee et al. 1991, Williams et al. 1981). Furthermore, the shift seen in rotaliids is distinct from the shift seen in symbiotic miliolids or asymbiotic taxa, including asymbiotic rotaliids, that calcify out of equilibrium (Langer 1995, Saraswati 2007, Saraswati et al. 2004, Wefer et al. 1981, Zimmerman et al. 1983). Therefore this distinctive shift should be a reliable indicator of photosynthesizing endosymbionts in fossil rotaliid species. A secondary, less-well supported trend of heavier $\delta^{13}C$ values over ontogeny (Brasier and Green 1993, Wefer et al. 1981) has also been reported, and can be used in conjunction with the signature 3-5 ‰ shift to confirm or reject the presence of photosynthesizing endosymbionts in fossil rotaliids. This project uses the known characteristics of stable isotope chemistry in extant symbiotic rotaliid foraminifera to test the hypothesis that the extinct rotaliid, *Nummulites gizehensis*, hosted photosynthesizing endosymbionts.

If this hypothesis is true, then tests of *N. gizehensis* will show 1) a 3-5 ‰ negative shift in $\delta^{13}C$ relative to contemporary equilibrium calcite, and 2) heavier $\delta^{13}C$ over the ontogeny of the

organism (distance from center of tests). In order to carry out these tests, the following must be known:

1. The mean shift from equilibrium calcite in extant symbiotic rotaliids
2. Ontogenetic sequence of $\delta^{13}C$ in *N. gizehensis*
3. The mean shift from equilibrium calcite in *N. gizehensis*
    A. $\delta^{13}C$ in original test material of *N. gizehensis*
    B. $\delta^{13}C$ of contemporary "fossil" equilibrium calcite
        1. $\delta^{13}C$ of HCO_3 in contemporary fossil seawater
        2. Temperature of contemporary fossil seawater
            a.$\delta^{18}O$ of calcite precipitated in equilibrium with contemporary fossil seawater
            b. $\delta^{18}O$ of contemporary fossil seawater

The mean shift seen in extant symbiotic rotaliids has been calculated from previously published data sets, and $\delta^{13}C$ in *N. gizehensis* tests have been measured directly. In order to calculate the $\delta^{13}C$ of contemporary fossil equilibrium calcite, asymbiotic taxa of co-occurring fossil foraminifera were used as proxies for $\delta^{13}C$ of HCO_3 in fossil seawater and $\delta^{18}O$ of calcite precipitated in equilibrium with fossil seawater. The $\delta^{18}O$ of fossil seawater is an estimate chosen in order to make calculated seawater temperatures comparable to other temperature reconstructions for the middle Eocene. The details and full rationale of each step follow.

Methods

Sample collection and dating

A bulk sample was collected and washed in 1987 by Dr. Amin Strougo and Dr. Mohamed Boukhary of Ain Shams University, Cairo, from an excavated clay pit located approximately 200 meters west of the Al Menia-Al Wosta road, southeast of Sharuna, Al Minia, Egypt (figure 1) (pers. comm.). It comes from a relatively thin (40 cm) nummulite bank from the middle horizon of the Lutetian aged (middle Eocene) Midawara Formation, a succession of marine shelf facies of alternating shale, marl, and glauconitic sandstones and siltstones (Strougo 2008).

The sample is dated to MK4 of the recently revised local Mokattamian Stage (Strougo 2008). Based on larger and planktonic foraminifera, calcareous nannoplankton and macroinvertebrate data, Strougo (2008) correlates MK4 with the early middle Eocene E11 (*Morozovella lehneri* Zone) of the tropical to subtropical planktonic foraminifera zones (Berggren William A. and Pearson 2005, 2006, Wade et al. 2011), and the late NP15/NP16 of calcareous nannoplankton zones (Berggren W. A. et al. 1995). E11 is dated as 42.3-40.5 Mya according to Cande and Kent (1995) and 41.1-39.8 Mya according to Luterbacher et al. (2004). In order to be conservative in bracketing the age of the sample I use both for a time frame of 42.3-39.8 Mya.

Samples from this site were used in this study because of their rare preservational environment for *Nummulites* species; the clay-rich matrix has low permeability, which limits the free circulation of fluids to embedded fossil material thus limiting opportunity for diagenetic alteration to occur, and samples from clay-rich sediments are generally less altered than those from more carbonate-rich sites (Pearson Paul N. et al. 2001). SEM and element mapping were carried

out on tests of all included taxa to check for alteration (Casazza, unpublished), and only specimen with exceptional preservation were included.

Specimen preparation

Megalospheric (asexually produced) and microspheric (sexually produced) forms of *N. gizehensis* were ground on a horizontal wet diamond grinder to expose equatorial sections, rinsed with deionized water to remove any residue, and dried over night at 60°C.

Sediment from the original bulk sample was sprinkled over a gridded tray, and *Cibicides* sp. and *Uvigerina* sp. were picked using a binocular microscope and fine paint brush, and placed in a micropaleontological slide.

N. gizehensis were chosen for subsampling based on the degree of test alteration (see chapter 2). To increase sample size, some specimen with minimal alteration in the outermost whorls were included, however only the unaltered, inner whorls were subsampled for isotope testing. Larger rotaliid foraminifera grow by adding chambers in a spiral formation, and as each chamber is produced an additional veneer of calcite is added to the previous chamber (Wefer et al. 1981). In an effort to capture the isotopic signature of a single growth period without contamination from calcite produced at a later time, a scalpel was used to scrape calcite material from the interior of chamber walls.

Subsampling was done on a line transect from the proloculus to the outermost preserved whorl, skipping at least every other whorl. For microspheric specimen 3-10 subsamples were taken per individual, and for megalospheric specimen 1-4 subsamples. In Microspheric forms the proloculus was too small to provide sufficient sample size for isotope testing, so proloculi were combined with whorls 1-4 in a single subsample. Proloculi of megalospheric forms comprise a single subsample (Figure 2).

Although high-resolution sampling that closely follows the growth pattern of the *Nummulites* test such as that used by Purton and Brasier (1999) provides detailed information about annual temperature cycles and *Nummulites* life history, the cost of isotopic testing makes this a practical method only for studies that include a few individual specimen. To determine the average isotopic signature for a whole population it is necessary to include as many individuals as

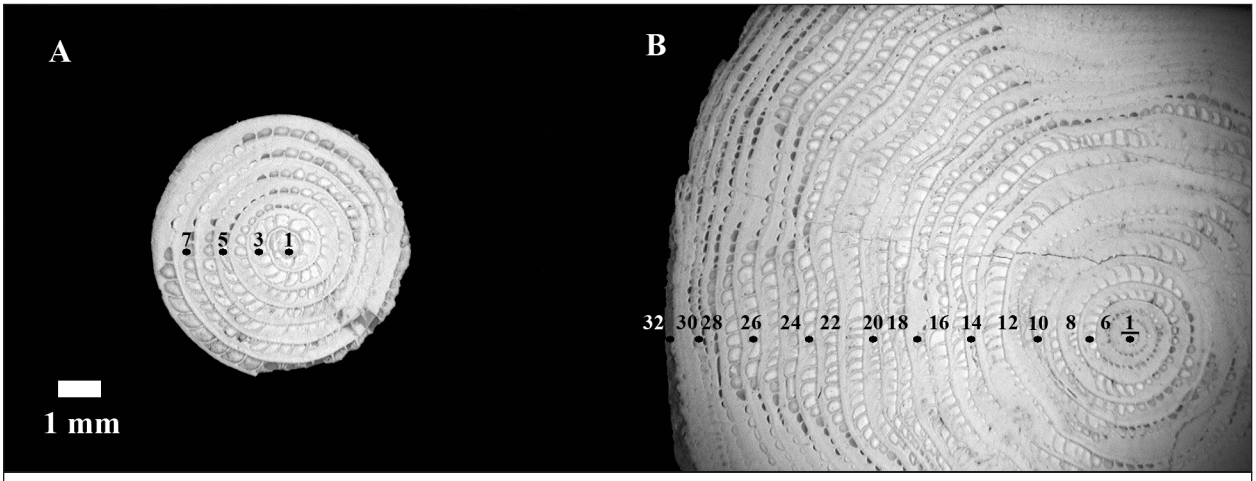

Figure 2. Generalized sub-sampling schemes for *N. gizehensis*. Sub-samples are identified by whorl number counted from proloculus to test margin. A) In megalospheric forms 1-4 subsamples were collected including the proloculus. B) In microspheric forms 3-10 subsamples were collected. The first sub-sample includes the proloculus and whorls 1-4.OK

possible. Sampling along a transect provides adequate resolution to capture the ontogenetic trend in δ13C and the range of temperatures experienced of the individual organisms' lifetime while permitting the inclusion of more individuals in the study.

For the small foraminiferal taxa *Uvigerina* spp. and *Cibicides* spp., individual tests were visually inspected and only those with high luster, white tests were included for analysis (see chapter 2). 15 or more specimen less than 100 μm in size were used to create bulk samples sufficient in size for isotopic analysis.

Isotope analysis

Samples containing about 10 to 100 microgram calcite were used for both carbon and oxygen isotope analyses, which were determined using a GV IsoPrime mass spectrometer with Dual-Inlet and MultiCarb systems in the Laboratory for Environmental and Sedimentary Isotope Geochemistry (LESIG) at Department of Earth and Planetary Science, University of California at Berkeley. Several replicates of one international standard NBS19 and two lab standards were measured along with samples for each run. The overall external analytical precision is +0.04‰ for $\delta^{13}C$ and +0.07‰ for $\delta^{18}O$**.** All values are reported as per mil deviations from the PDB standard in the δ-notation:

$$\delta = \frac{R_{sample} - R_{standard}}{R_{standard}} \text{ x } 1000‰ \quad (1)$$

where R is the ratio of heavier to lighter isotope ($^{18}O/^{16}O$ and $^{13}C/^{12}C$).

Calculation of fossil equilibrium calcite

Corrections for Cibicides spp. and Uvigerina spp.

No foraminifera record $\delta^{13}C$ in isotopic equilibrium with seawater, however $\delta^{13}C$ of *Cibicides* spp. provides a reliable estimate of dissolved carbon (HCO_3) in ambient seawater (Duplessey et al. 1984), and this can be used to calculate $\delta^{13}C$ in isotopic equilibrium with seawater. Duplessey et. al. (1984) found $\delta^{13}C$ of *Cibicides* differed from that of HCO_3 (in ambient sea water) by +0.07‰ +/- 0.04, results within experimental error and in agreement with those of earlier workers (Belanger et al. 1981, Graham et al. 1981). In this study I followed their recommendations and used measured $\delta^{13}C$ values of *Cibicides* spp. as a proxy for $\delta^{13}C$ of ambient seawater during calcification without correction. Measured $\delta^{13}C$ values of *Uvigerina* spp. are normalized to those of *Cibicides* spp.(Duplessey et al. 1984, Hagen and Keigwin 2002, Poli et al. 2010).

Uvigerina spp. record $\delta^{18}O$ in isotopic equilibrium with ambient seawater (Duplessey et al. 1984, Shackleton N. J. 1974, Woodruff et al. 1980) and are widely used for paleotemperature reconstructions. A correction factor of +0.64‰ is applied to the measured $\delta^{18}O$ of *Cibicides* spp. to provide values consistent with calcite in isotopic equilibrium with seawater (Duplessey et al. 1984, Shackleton Nicholas J. and Opdyke 1973).

Paleotemperature

Water temperature at the time of calcification was calculated for all taxa using the equation from Shackleton (1974),

$$T(°C) = 16.9 - 4.38\ (\delta_c - \delta_w)^2 \qquad (2)$$

where δc is the $\delta^{18}O$ of the measured (and corrected) foraminiferal calcite and δw is the $\delta^{18}O$ of ambient seawater at the time of calcification.

Estimates for the $\delta^{18}O$ of Eocene seawater range from a low value of −1.20‰ (Shackleton N. J. and Kennett 1975) to a high of −0.75‰ (Pearson Paul N. et al. 2001), and include −1‰ (Zachos et al. 1994) and −0.98‰ (Bralower et al. 1995). In this study I use −0.75‰ in order to make temperature results comparable to results found by Pearson et. al. (2001) on exceptionally well preserved benthic foraminifera from similar environments (low latitude shelf environments) and from the same time period as the samples in this study (42 +/- 1.6 mya to 39 +/-0.9 mya).

Equilibrium calcite

To make the isotopic results of this study comparable to previously published studies on rotaliid foraminifera, the measured $\delta^{13}C$ of *Cibicides* spp. and corrected δ13C of *Uvigerina* spp. were used to calculate a $\delta^{13}C$ value for calcite in isotopic equilibrium with seawater. I applied the fractionation equation derived by Emrich et al. (1970):

$$\epsilon_{CB} = \delta^{13}C\ HCO^-_3 + 1.85 + 0.035\ (T - 20\ °C) \pm 0.23‰ \qquad (3)$$

to calculate an average value for equilibrium calcite. To calculate the lower limit of the range a correction of +1.62‰ (i.e.1.85 - 0.23‰) was applied to the $\delta^{13}C$ values of all *Cibicides* spp. and *Uvigerina* spp., and +2.08‰ was applied for the upper limit. A temperature of 28°C was used for fossil seawater (see *Theoretical Temperature Salinity range* for explanation).

Theoretical Temperature Salinity range

The $\delta^{18}O$ values found in *N. gizehensis* yielded temperatures that were very low (mean = 11°C). This is 10°C colder than average temperatures found from *Cibicides* spp. and *Uvigerina* spp., and much colder than any sea surface temperatures found for tropical Eocene seas. Many factors can affect $\delta^{18}O$ of foraminiferal calcite, however in this instance salinity is likely responsible; $\delta^{18}O$ values are known to become more positive with increasing salinity yielding falsely low temperatures. (See the discussion for lines of evidence leading to this conclusion).

To successfully calculate the true temperatures experienced by the *N. gizehensis*, the salinity of surrounding seawater must be known. Although this isn't possible, a strong linear relationship exists between salinity and the $\delta^{18}O$ of seawater (Arbuszewski et al. 2010, Rostek et al. 1993, Schmidt 1999), and this empirically derived relationship can be used in conjunction with

Table 1. Facing page. Measured and corrected values for carbon and oxygen isotopes in Eocene benthic foraminifera. Correction to $\delta^{18}O$ of *Cibicides* spp. = +0.65‰; Correction to $\delta^{13}C$ of *Uvigerina* spp. = +0.76‰.

Specimen: taxon and ID #	sample name	measured $\delta^{18}O$‰	corr. $\delta^{18}O$‰	measured $\delta^{13}C$‰	corr. $\delta^{13}C$‰
Nummulites gizehensis (microspheric) - NB1	NB1A	0.13	-	-1.24	-
	NB1B	1.13	-	-0.72	-
	NB1C	0.92	-	-0.70	-
	NB1D	0.99	-	-0.75	-
	NB1E	1.13	-	-0.80	-
	NB1G	1.02	-	-1.02	-
	NB1H	0.41	-	-0.93	-
	NB1I	1.15	-	-0.93	-
N. gizehensis (microspheric) - NB19	NB19A	0.94	-	-0.96	-
	NB19B	0.93	-	-0.86	-
	NB19C	-0.31	-	-1.52	-
	NB19D	0.95	-	-1.04	-
	NB19E	0.77	-	-0.82	-
	NB19F	1.29	-	-0.92	-
	NB19G	0.95	-	-0.90	-
	NB19H	1.09	-	-0.97	-
N. gizehensis (microspheric) - NB21	NB21A	0.66	-	-0.86	-
	NB21B	0.72	-	-1.04	-
	NB21C	1.19	-	-0.75	-
	NB21D	1.06	-	-0.81	-
	NB21E	0.88	-	-0.94	-
	NB21F	0.39	-	-0.74	-
N. gizehensis (microspheric) - NB2	NB2B	0.60	-	-0.88	-
	NB2D	0.78	-	-0.94	-
	NB2E	1.17	-	-0.68	-
N. gizehensis (microspheric) - NB15	NB15A	0.33	-	-0.84	-
	NB15B	0.87	-	-0.72	-
	NB15C	0.98	-	-0.77	-
	NB15D	0.48	-	-0.62	-
	NB15E	-0.68	-	-1.68	-
N. gizehensis (microspheric) - NB31	NB31B	-0.02	-	-1.66	-
	NB31C	0.62	-	-1.03	-
	NB31D	0.47	-	-0.88	-
	NB31E	0.69	-	-1.18	-
	NB31F	0.61	-	-1.04	-
	NB31G	0.89	-	-1.12	-
N. gizehensis (microspheric) - NB32	NB32A	0.06	-	-1.14	-
	NB32C	0.90	-	-0.93	-

Specimen: taxon and ID #	sample name	measured $\delta^{18}O$‰	corr. $\delta^{18}O$‰	measured $\delta^{13}C$‰	corr. $\delta^{13}C$‰
N. gizehensis (microspheric) - NB32	NB32D	0.66	-	-0.93	-
	NB32E	0.89	-	-1.09	-
	NB32F	0.41	-	-1.40	-
N. gizehensis (microspheric) - NB35	NB35A	1.02	-	-0.97	-
	NB35B	0.97	-	-0.79	-
	NB35C	0.50	-	-1.04	-
	NB35D	0.46	-	-1.05	-
	NB35E	-0.84	-	-1.79	-
	NB35F	0.66	-	-1.36	-
N. gizehensis (microspheric) - NB34	NB34A	0.85	-	-0.86	-
	NB34B	1.13	-	-0.78	-
	NB34C	0.58	-	-1.04	-
	NB34D	0.84	-	-0.86	-
	NB34E	0.58	-	-1.06	-
	NB34F	-1.00	-	-1.71	-
	NB34G	0.22	-	-1.13	-
	NB34H	-0.18	-	-1.52	-
	NB34I	0.84	-	-1.27	-
	NB34J	0.34	-	-1.42	-
N. gizehensis (megalospheric) - NA12	NA12A	0.30	-	-0.81	-
	NA12B	0.75	-	-0.71	-
	NA12C	0.36	-	-1.18	-
N. gizehensis (megalospheric) - NA13	NA15A	0.44	-	-0.64	-
	NA15B	0.59	-	-0.60	-
	NA15C	0.55	-	-0.87	-
N. gizehensis (megalospheric) - NA20	NA20A	0.25	-	-0.89	-
	NA20B	0.74	-	-0.74	-
	NA20C	0.66	-	-1.09	-
N. gizehensis (megalospheric) - NA17	NA17A	-0.15	-	-0.64	-
	NA17B	0.46	-	-0.72	-
N. gizehensis (megalospheric) - NA7	NA7B	0.75	-	-0.88	-
N. gizehensis (megalospheric) - NA34	NA34A	0.75	-	-0.81	-
	NA34C	-0.23	-	-1.39	-
	NA34B	1.08	-	-1.05	-
N. gizehensis (megalospheric) - NA35	NA35A	0.76	-	-0.91	-
	NA35B	0.84	-	-0.91	-
	NA35C	0.65	-	-1.26	-
N. gizehensis (megalospheric) - NA30	NA30A	-0.40	-	-1.35	-

Specimen: taxon and ID #	sample name	measured $\delta^{18}O$‰	corr. $\delta^{18}O$‰	measured $\delta^{13}C$‰	corr. $\delta^{13}C$‰
N. gizehensis (megalospheric) - NA30	NA30B	1.03	-	-0.87	-
	NA30C	0.77	-	-1.24	-
	NA30D	0.66	-	-1.37	-
N. gizehensis (megalospheric) - NA31	NA31A	-0.62	-	-0.96	-
	NA31B	0.42	-	-1.35	-
	NA31C	0.53	-	-1.12	-
Cibicides spp. (bulk)	CB1	-2.71	-2.07	0.65	-
Cibicides spp. (bulk)	CB2	-2.19	-1.55	0.62	-
Cibicides spp. (bulk)	CB3	-2.73	-2.09	0.80	-
Cibicides spp. (bulk)	CB4	-2.47	-1.83	0.73	-
Cibicides spp. (bulk)	CB5	-2.77	-2.13	0.66	-
Cibicides spp. (bulk)	CB6	-2.02	-1.38	0.66	-
Cibicides spp. (bulk)	CB7	-2.37	-1.73	0.53	-
Cibicides spp. (bulk)	CB8	-2.73	-2.09	0.37	-
Cibicides spp. (bulk)	CB9	-2.25	-1.61	0.61	-
Uvigerina spp. (bulk)	UV1	-1.77	-	0.00	0.76
Uvigerina spp. (bulk)	UV2	-1.68	-	-0.12	0.64
Uvigerina spp. (bulk)	UV3	-1.68	-	-0.12	0.64
Uvigerina spp. (bulk)	UV4	-1.15	-	-0.02	0.74
Uvigerina spp. (bulk)	UV5	-1.32	-	-0.26	0.50
Uvigerina spp. (bulk)	UV6	-1.48	-	-0.16	0.60
Uvigerina spp. (bulk)	UV7	-1.23	-	-0.09	0.67
Uvigerina spp. (bulk)	UV8	-1.45	-	-0.33	0.43

$\delta^{18}O$ in *N. gizehensis* to produce a theoretical range of temperatures at different salinities.

Empirically derived equations from Rostek (1993) and Schmidt (1999) are in close agreement for tropical seas:

$$\delta^{18}O_{seawater} = 9.24 + 0.28S \quad (4)$$

and,

$$\delta^{18}O_{seawater} = 7.7 + 0.22S \quad (5)$$

respectively, where $\delta^{18}O_{seawater}$ is the $\delta^{18}O$ of seawater (not calcite in equilibrium with seawater) and S is the salinity of seawater. Starting with the assumption that the $\delta^{18}O$ of the fossil seawater is -0.75 per mil at a normal marine salinity of 35‰ (Pearson Paul N. et al. 2001), a range of seawater $\delta^{18}O$ values was generated for increasing salinities up to 60‰ using both equation (4) and (5). These ranges of values were then substituted into Shackleton's paleotemperature equation (equation 2 above) using only the minimum and maximum $\delta^{18}O$ values recorded by the *N. gizehensis* to create two overlapping ranges of salinity and temperature. These ranges show the temperatures that would have been experienced by *N. gizehensis* at different salinities.

The mean temperature calculated for the smaller taxa was assumed to be a minimum annual temperature experienced by *N. gizehensis,* and the maximum annual temperature was taken to be the corresponding maximum theoretical temperature. The average of these (28°C) was used to calculate the $\delta^{13}C$ of fossil equilibrium calcite.

$\delta^{13}C$ shift

Previously published data on the $\delta^{13}C$ values of extant symbiont-bearing rotaliid foraminifera relative to equilibrium calcite values were used to calculate expected mean shifts (Saraswati 2007, Saraswati et al. 2004, Wefer et al. 1981, Zimmerman et al. 1983), values were published as means rather than raw values; these means are treated as independent data sets in order to be consistent with other published data. The mean shift of values in this study was compared to those of published studies to see if they fell within the expected range.

$\delta^{13}C$ over ontogeny

For all microspheric and megalospheric *N. gizehensis* linear regression analyses of on-

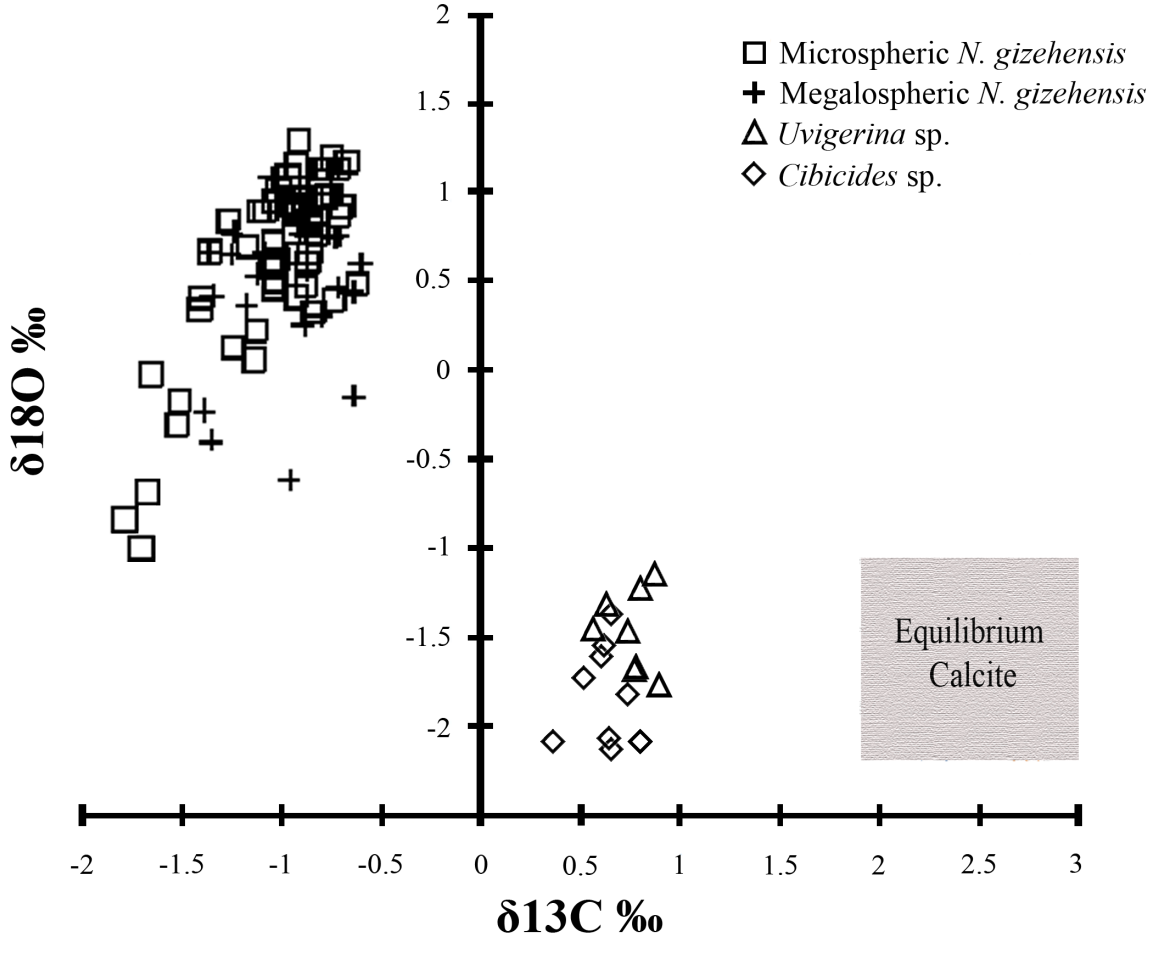

Figure 3. Graph of $\delta^{13}C$ and $\delta^{18}O$ for all sampled taxa. Measured values are shown for microspheric and megalospheric *N. gizehensis*; *Uvigerina* spp. and *Cibicides* spp. are corrected values (see text); The range of Equilibrium Calcite values is calculated according to Emrich (1970) (see text for details).

togenetic sequences were carried out for $\delta^{13}C$ values. Positive slopes were interpreted as a trend of increasing $\delta^{13}C$ and negative slopes were interpreted as a trend of decreasing $\delta^{13}C$ over ontogeny.

Sample Set	n	X +/- SD (%)
$\delta^{18}O$ Microspheric *N. gizehensis*	57	0.36 ± 0.50
$\delta^{18}O$ Megalospheric *N. gizehensis*	25	0.48 ± 0.43
$\delta^{18}O$ *Cibicides* spp.	9	-1.83 ± 0.28
$\delta^{18}O$ *Uvigerina* spp.	8	-1.47 ± 0.23
$\delta^{13}C$ Microspheric *N. gizehensis*	57	-1.02 ± 0.28
$\delta^{13}C$ Megalospheric *N. gizehensis*	25	-0.97 ± 0.25
$\delta^{13}C$ *Cibicides* spp.	9	0.62 ± 0.12
$\delta^{13}C$ *Uvigerina* spp.	8	0.62 ± 0.11

Table 2. Mean and standard deviation of $\delta^{18}O$ and $\delta^{13}C$ values for megalospheric and microspheric forms of *N. gizehensis*, and adjusted values for *Cibicides* spp. and *Uvigerina* spp.

Statistics

Many statistical methods for detecting differences between samples rely on the assumption that the samples are drawn from populations with a normal distribution. In order to determine whether these parametric tests were appropriate all eight sample sets were first checked for normal distribution using the Shapiro-Wilk test: $\delta^{18}O$ of microspheric *N. gizehensis*, $\delta^{18}O$ of megalospheric *N. gizehensis*, $\delta^{18}O$ of *Uvigerina* sp., $\delta^{18}O$ of *Cibicides* sp., $\delta^{13}C$ of microspheric *N. gizehensis,* $\delta^{13}C$ of megalospheric *N. gizehensis,* $\delta^{13}C$ of *Uvigerina* sp., and $\delta^{13}C$ of *Cibicides* sp. Test results can be adversely affected by data sets containing multiple points of the same value with the Shapiro-Wilk test, however this is not the case for the samples tested here, and the Shapiro-Wilk test has been shown to be the most appropriate one for this purpose (D'Agostino and Stevens 1986).

Sample sets with normal distributions were compared using a two-tailed T-test; an f-test was also done to check for differences in variance. When the sample sets being compared lacked a normal distribution the non-parametric Mann-Whitney and Kruskal-Wallace tests were applied, which detect whether samples are taken from populations with equal medians; the Kolmogorov-Smirnoff test was also used to check for overall equal distribution of the samples. Because non-parametric tests increase the probability of Type II errors (accepting a false null), in cases where one of the sample sets is normal and one isn't, both the parametric and non-parametric tests were applied to check the robustness of results.

All statistical tests were performed in PAST, a paleontological software package for statistical analysis (Hammer et al. 2001).

Results

$\delta^{13}C$ and δ18O

The measured and corrected δ18O and $\delta^{13}C$ values for every sample are reported in Table 1, and the means and standard deviations for corrected values are given in Table 2. The offset for $\delta^{13}C$ in *Uvigerina* spp. relative to *Cibicides* spp. was +0.76‰. All *N. gizehensis* show a mean positive shift in δ18O and a negative shift in $\delta^{13}C$ relative to the Vienna PeeDee Belemnite standard, while corrected *Uvigerina* sp. and *Cibicides* sp. show a mean negative shift in δ18O and a positive shift in $\delta^{13}C$. A plot of isotope values shows two distinct clusters; micro- and megalospheric *N. gizehensis* forming one, and the smaller, asymbiotic taxa forming the other (Figure 3).

Of the eight data sets tested, only three are likely drawn from a non-normal distribution

of values: δ18O of microspheric *N. gizehensis*, δ18O of megalospheric *N. gizehensis* and $\delta^{13}C$ of microspheric *N. gizehensis* (Table 3).

Sample Set	n	W	*p*	H_0
$\delta^{18}O$ Microspheric *N. gizehensis*	57	.8634	$1.22x10^{-5}$	Rejected
$\delta^{18}O$ Megalospheric *N. gizehensis*	25	.8814	.007	Rejected
$\delta^{18}O$ *Cibicides* spp.	9	.8937	.218	Not Rejected
$\delta^{18}O$ *Uvigerina* spp.	8	.9387	.597	Not Rejected
$\delta^{13}C$ Microspheric *N. gizehensis*	57	.8909	$9.33x10^{-5}$	Rejected
$\delta^{13}C$ Megalospheric *N. gizehensis*	25	.9318	.095	Not Rejected
$\delta^{13}C$ *Cibicides* spp.	9	.9304	.485	Not Rejected
$\delta^{13}C$ *Uvigerina* spp.	8	.9389	.600	Not Rejected

Table 3. Shapiro-Wilk test for normal distribution. H_0 = Sample was taken from a population with normal distribution.

δ18O values recorded in megalospheric forms of *N. gizehensis* fall within the range of values recorded by microspheric forms of *N. gizehensis* (see figure 3), but the two sets of values have significantly different medians (Mann-Whitney test, U=514, *p*=.046 and Kruskal-Wallace test, H=3.998, *p*=.046) and significantly different distributions (Kolmogorov-Smirnov test, D=.37614, *p*=.012).

Unlike δ18O values, $\delta^{13}C$ values recorded in megalospheric forms of *N. gizehensis* are not significantly different than values recorded in microspheric forms of *N. gizehensis*. Parametric tests fail to reject the null hypothesis of same means (two-tailed t-test, t=.76996, *p*=.44) and same variance (f-test, f=1.25, *p*=.57) and non-parametric tests fail to reject the null hypothesis of same medians (Mann-Whitney test, U=648, *p*=.52 and Kruskal-Wallace test, H=.4221, *p*=.52) and overall equal distributions (Kolmogorov-Smirnov test, D=.17404, *p*=.66).

δ18O values recorded in *Uvigerina* sp. and *Cibicides* sp. are overlapping (see figure 3) with similar variance (f-test, f=1.25, *p*=.57), but with significantly different means (two-tailed t-test, t=2.8914, *p*=.011).

Paleotemperature and salinity

All calculated paleotemperatures are reported in Table 4. Paleotemperatures calculated from *Uvigerina* spp. and *Cibicides* spp. give a mean of 21°C +/- 1.41°C SD, a value in close agreement with low-latitude shelf environments of the Middle Eocene (Pearson Paul N. et al. 2001).

Those calculated from *N. gizehensis* give a mean of 11.25°C +/- 2.00°C SD. This is much colder than any temperatures reported for low latitude Eocene waters, and much colder than habitats for modern *Nummulites* spp.

Figure 4 shows the theoretical temperature ranges likely experienced by *N. gizehensis* at different salinities.

Equilibrium calcite and photosymbiosis

$\delta^{13}C$ values in *Uvigerina* spp. and *Cibicides* spp. are in close agreement with previously reported $\delta^{13}C$ for the early middle Eocene (Stott et al. 1996, Zachos et al. 1994), although slightly

Table 4. All Paleotemperatures calculated from measured $\delta^{18}O$ of *N. gizehensis* and *Uvigerina* spp. and corrected $\delta^{18}O$ of *Cibicides* spp. according to Shackleton (1974) and assuming the $\delta^{18}O$ of middle Eocene seawater to be -0.75‰ (Pearson 2001).

Specimen: taxon and ID #	sample name	$\delta^{18}O‰$	Temperature (°C)
Nummulites gizehensis (microspheric) - NB1	NB1A	0.13	13.13
	NB1B	1.13	9.00
	NB1C	0.92	9.85
	NB1D	0.99	9.59
	NB1E	1.13	9.02
	NB1G	1.02	9.48
	NB1H	0.41	11.94
	NB1I	1.15	8.94
N. gizehensis (microspheric) - NB19	NB19A	0.94	9.79
	NB19B	0.93	9.82
	NB19C	-0.31	14.97
	NB19D	0.95	9.75
	NB19E	0.77	10.49
	NB19F	1.29	8.38
	NB19G	0.95	9.73
	NB19H	1.09	9.18
N. gizehensis (microspheric) - NB21	NB21A	0.66	10.93
	NB21B	0.72	10.68
	NB21C	1.19	8.77
	NB21D	1.06	9.31
	NB21E	0.88	10.02
	NB21F	0.39	12.04
N. gizehensis (microspheric) - NB2	NB2B	0.60	11.17
	NB2D	0.78	10.43
	NB2E	1.17	8.84
N. gizehensis (microspheric) - NB15	NB15A	0.33	12.31
	NB15B	0.87	10.07
	NB15C	0.98	9.62
	NB15D	0.48	11.65
	NB15E	-0.68	16.60
N. gizehensis (microspheric) - NB31	NB31B	-0.02	13.77
	NB31C	0.62	11.10
	NB31D	0.47	11.69
	NB31E	0.69	10.79
	NB31F	0.61	11.15
	NB31G	0.89	9.98
N. gizehensis (microspheric) - NB32	NB32A	0.06	13.43
	NB32C	0.90	9.94

Specimen: taxon and ID #	sample name	$\delta^{18}O‰$	Temperature (°C)
N. gizehensis (microspheric) - NB32	NB32D	0.66	10.93
	NB32E	0.89	9.98
	NB32F	0.41	11.97
N. gizehensis (microspheric) - NB35	NB35A	1.02	9.46
	NB35B	0.97	9.65
	NB35C	0.50	11.60
	NB35D	0.46	11.75
	NB35E	-0.84	17.29
	NB35F	0.66	10.91
N. gizehensis (microspheric) - NB34	NB34A	0.85	10.13
	NB34B	1.13	9.02
	NB34C	0.58	11.27
	NB34D	0.84	10.20
	NB34E	0.58	11.25
	NB34F	-1.00	17.99
	NB34G	0.22	12.76
	NB34H	-0.18	14.42
	NB34I	0.84	10.19
	NB34J	0.34	12.23
N. gizehensis (megalospheric) - NA12	NA12A	0.30	12.39
	NA12B	0.75	10.55
	NA12C	0.36	12.16
N. gizehensis (megalospheric) - NA13	NA15A	0.44	11.84
	NA15B	0.59	11.20
	NA15C	0.55	11.36
N. gizehensis (megalospheric) - NA20	NA20A	0.25	12.60
	NA20B	0.74	10.60
	NA20C	0.66	10.92
N. gizehensis (megalospheric) - NA17	NA17A	-0.15	14.30
	NA17B	0.46	11.74
N. gizehensis (megalospheric) - NA7	NA7B	0.75	10.54
N. gizehensis (megalospheric) - NA34	NA34A	0.75	10.54
	NA34C	-0.23	14.67
	NA34B	1.08	9.22
N. gizehensis (megalospheric) - NA35	NA35B	0.84	10.18
	NA35A	0.76	10.50
	NA35C	0.65	10.98
N. gizehensis (megalospheric) - NA30	NA30A	-0.40	15.37

Specimen: taxon and ID #	sample name	$\delta^{18}O$‰	Temperature (°C)
N. gizehensis (megalospheric) - NA30	NA30B	1.03	9.43
	NA30C	0.77	10.45
	NA30D	0.66	10.92
N. gizehensis (megalospheric) - NA31	NA31A	-0.62	16.34
	NA31B	0.42	11.92
	NA31C	0.53	11.44
Cibicides spp. (bulk)	CB1	-2.07	22.85
Cibicides spp. (bulk)	CB2	-1.55	20.48
Cibicides spp. (bulk)	CB3	-2.09	22.93
Cibicides spp. (bulk)	CB4	-1.83	21.74
Cibicides spp. (bulk)	CB5	-2.13	23.15
Cibicides spp. (bulk)	CB6	-1.38	19.69
Cibicides spp. (bulk)	CB7	-1.73	21.29
Cibicides spp. (bulk)	CB8	-2.09	22.95
Cibicides spp. (bulk)	CB9	-1.61	20.76
Uvigerina spp. (bulk)	UV1	-1.77	21.48
Uvigerina spp. (bulk)	UV2	-1.68	21.06
Uvigerina spp. (bulk)	UV3	-1.68	21.06
Uvigerina spp. (bulk)	UV4	-1.15	18.68
Uvigerina spp. (bulk)	UV5	-1.32	19.44
Uvigerina spp. (bulk)	UV6	-1.48	20.15
Uvigerina spp. (bulk)	UV7	-1.23	19.03
Uvigerina spp. (bulk)	UV8	-1.45	20.03

more positive than for values found by Pearson (2001). Calculated $\delta^{13}C$ values for calcite in equilibrium with seawater yield a range from 2.27‰ to 3.16‰, with a mean of 2.75‰. The mean $\delta^{13}C$ of all *Nummulites* samples shows a negative shift of 3.75‰ relative to the mean of calcite in equilibrium with seawater (Figure 5), putting it solidly in the expected range for symbiont-bearing rotaliid foraminifera (Table 5).

Seven of the nine subsampled microspheric *N. gizehensis* show increasing $\delta^{13}C$ over ontogeny (Figure 6). Two of the microspheric forms and all eight of the subsampled megalospheric forms show the opposite; $\delta^{13}C$ becomes more negative over the individuals lifetime.

Discussion

The *N. gizehensis* in this study show a negative $\delta^{13}C$ shift of 3.75‰ relative to the calculated contemporary fossil equilibrium calcite. This falls within the expected range for rotaliid foraminifera hosting photosynthesizing endosymbionts. The results for $\delta^{13}C$ over ontogeny are more ambiguous, but do not rule out symbiosis. However, given the large number of variables that can potentially affect stable isotopes in foraminiferal calcite and the complications inherent

in of working with fossil material, a thorough review of each assumption and calculation as well as all alternative interpretations is necessary.

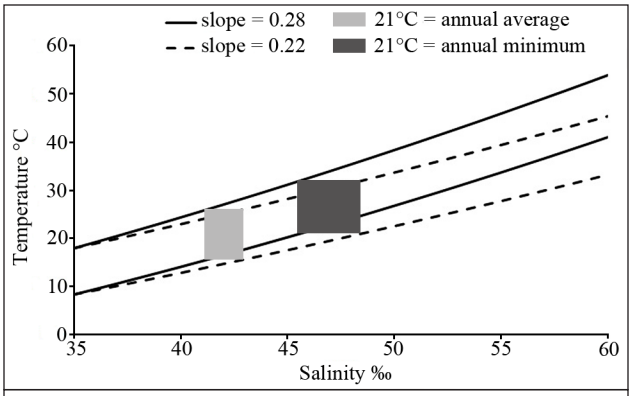

Figure 4. Temperature/salinity ranges experienced by *N. gizehensis* assuming the average temperature recorded by *Cibicides* spp. and *Uvigerina* spp. (21°C) is the annual average temperature, or the annual minimum.

Fossil equilibrium calcite

Two variables must be known in order to calculate the $\delta^{13}C$ of calcite in equilibrium with seawater: the $\delta^{13}C$ of HCO_3 in the seawater and seawater temperature, neither of which can be directly measured in the case of a fossil environment. However, good proxies for these measurements exist and are present in the study sample.

Cibicides spp. are known to record $\delta^{13}C$ very close to that of HCO_3 in surrounding seawater (Duplessey et al. 1984) and are commonly used for this in reconstructions of marine paleoenvironments. Measured $\delta^{13}C$ values of *Uvigerina* spp. can be normalized to those of *Cibicides* spp. The offsets calculated by other workers include +0.9‰ (Duplessey et al. 1984), +1.1‰ (Poli et al. 2010), and 1.5‰ (Hagen and Keigwin 2002). The calculated offset in this study is +0.76‰, which is somewhat lower than previously found offsets, but still closer to Duplessey's original offset than the highest offset found (differences of 0.14‰ vs. 0.20‰ respectively). Also, even when the larger offset of Duplessey's +0.9‰ is applied to *Uvigerina* spp., the alternative values for a fossil equilibrium calcite still results in a shift that falls within the expected range for photosymbiotic rotaliids.

Uvigerina spp. are among the best studied and most widely used proxies for reconstructing paleotemperatures because they record $\delta^{18}O$ in isotopic equilibrium with seawater (Duplessey et al. 1984, Shackleton N. J. 1974, Woodruff et al. 1980). *Cibicides* spp. can also be used for $\delta^{18}O$ in isotopic equilibrium by applying a correction factor of +0.64‰ (Duplessey et al. 1984, Shackleton Nicholas J. and Opdyke 1973). When this correction is applied the *Cibicides* spp. show values in close agreement with the *Uvigerina* spp. (see Figure 3). Although these two data sets still show a significant difference in their means, it's a difference of 0.4‰, resulting in a mean temperature difference of 1.64°C. The correction was derived using modern *Cibicides* spp. and *Uvigerina* spp., so it is possible that the biological fractionation of $\delta^{18}O$ is slightly different in the fossil taxa used here; this could be explained by differences in seasonal reproduction or in respiration rates between the two taxa and their modern counterparts. Given that there is always some time-averaging in sediments, the two taxa could represent conditions at slightly different time periods, however the *N. gizehensis* included in this study co-occur with the smaller taxa and therefore likely represent the same averaged time period.

Even taking these considerations into account, for the purposes of this study the results for $\delta^{18}O$ and $\delta^{13}C$ in the *Cibicides* spp. and *Uvigerina* spp. are in good agreement with each other, and with previously reported values for benthic foraminifera from similar environments of the middle Eocene (Pearson Paul N. et al. 2001, Stott et al. 1996, Zachos et al. 1994).

Despite this good agreement between expectation and the asymbiotic taxa, they are only useful if they represent temperature conditions also experienced by the *N. gizehensis*. Extant symbiotic rotaliid species show an approximate -2.0‰ shift in $\delta^{18}O$ relative to equilibrium calcite

(Buchardt and Hansen 1977, Wefer et al. 1981), therefore this is the expectation that best fits the hypothesis that *N. gizehensis* hosted symbionts. However, values reported in Table 2 clearly show that this expectation is not met; *N. gizehensis* show a strong positive shift relative to the $\delta^{18}O$ of equilibrium calcite as recorded by *Uvigerina* spp. and *Cibicides* spp. (>2‰). Many factors, both biotic and abiotic, affect $\delta^{18}O$ in foraminiferal calcite. Each can be examined in the context of this study.

$\delta^{18}O$ of Nummulites gizehensis

Variables effecting $\delta^{18}O$ of calcium carbonate

The most significant factors effecting $\delta^{18}O$ in calcium carbonate are both environmental in nature: the $\delta^{18}O$ of ambient seawater, (covered separately below) and temperature. The temperatures calculated from the *N. gizehensis* are much lower than those calculated from co-occurring asymbiotic taxa, and they are also anomalously low for Eocene surface water (a mean of 11°C vs. previous reports of 15-23°C, which may even be cooler than the true temperatures (Pearson Paul N. et al. 2001). Therefore, they most likely do not provide a reliable temperature record.

Other factors effecting $\delta^{18}O$ in calcium carbonate include changes with ontogeny or gametogenesis, and changes due to photosynthesis or respiration. Unlike some planktonic species which show enrichment in heavier isotopes with age, there doesn't appear to be any ontogenetic trend in $\delta^{18}O$ of these *N. gizehensis* that could account for the strong positive shift. Rather there appears to be an oscillation of values like those found in previous studies (Brasier and Green 1993, Purton and Brasier 1999) that were interpreted as reflecting seasonal temperature cycles. Likewise gametogenic calcite is not an issue for benthic foraminifera because they do not migrate vertically in the water column. The presence of photosynthetic symbionts in larger foraminifera, both miliolids and rotaliids, results in a negative shift in $\delta^{18}O$ rather than enrichment.

Publication	N	Mean $\delta^{13}C$ in symbiotic rotaliids (‰)	$\delta^{13}C$ of contemporary equilibrium calcite (‰)	Mean shift (‰)
Zimmerman, 1983	4	0.32	3.73	-3.41
Zimmerman, 1983	4	0.50	3.73	-3.23
Zimmerman, 1983	4	0.12	3.73	-3.61
This Publication	**84**	**-1.0**	**2.75**	**-3.75**
Zimmerman, 1983	4	-0.08	3.73	-3.81
Zimmerman, 1983	4	-0.08	3.73	-3.81
Zimmerman, 1983	4	-0.20	3.73	-3.93
Saraswati, 2007	11	-0.23	3.95	-4.18
Wefer, 1981	44	-0.19	4.35	-4.29
Zimmerman, 1983	3	-0.60	3.73	-4.33
Saraswati, 2004	10	-0.44	4.0	-4.44
Zimmerman, 1983	4	-0.97	3.73	-4.70

Table 5. Summary of calculated mean shifts for extant symbiotic rotaliid foraminifera from contemporary equilibrium calcite from previously published literature. Table lists values from smallest to largest shift and includes results for this publication.

Aragonite tends to be slightly enriched relative to calcite, however *Nummulites* spp. secrete low Mg calcite tests. Oxygen used in respiration is depleted relative to ambient dissolved oxygen (by 21‰ in near-shore environments), and if respiratory products are incorporated during calcification then calcium carbonate tests can show depleted $\delta^{18}O$ values (Rohling and Cooke 1999). Again, this fails to account for a strong positive shift.

In summary, the positive shift seen in *N. gizehensis* is unlikely to be accounted for by fractionation during calcification alone. From this comes the inference that although the *N. gizehensis, Uvigerina* spp. and *Cibicides* spp. examined in this study were distributed throughout a single sample, they calcified under different ambient conditions.

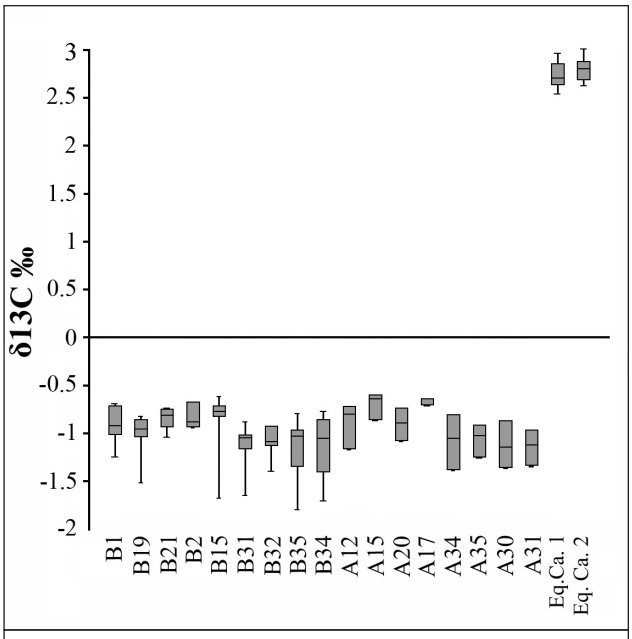

Figure 5. Box plot of $\delta^{13}C$ for individual specimen of *N. gizehensis*, and calculated equilibrium calcite values: B-sample names are microspheric specimen, A-samples are megalospheric; Eq. Ca.1 is equilibrium calcite values calculated from *Cibicides* spp. and Eq. Ca. 2 are calculated from corrected *Uvigerina* spp. Boxes are 25-75 percent quartiles, horizontal bar indicates median, vertical bars indicate minimum and maximum values.

Variables effecting $\boldsymbol{\delta^{18}O}$ *of seawater*

In the global water cycle, lighter isotopes of oxygen (^{16}O) are preferentially evaporated, leaving behind heavier isotopes of oxygen (^{18}O). This results in $\delta^{18}O$ values that vary between reservoirs, geographic locations and time periods. Global ice volume plays a major role in the $\delta^{18}O$ of seawater, with values getting heavier with increasing ice volume, however because all the taxa come from a single sample it is reasonable to assume that ice volume did not change significantly during its deposition. Likewise, although proximity to sea ice margins can cause seasonal effects in the $\delta^{18}O$ of seawater, it's an unlikely explanation for the southern Tethys margin of the middle Eocene.

Local freshwater input from rivers or high levels of precipitation can result in lighter $\delta^{18}O$ values, leading to "warmer" calculated temperatures, although this is less of an influence in tropical climates because local precipitation is close to the $\delta^{18}O$ of seawater. Furthermore, because *Uvigerina* spp. and *Cibicides* spp. yield values consistent with expectation, and because *Uvigerina* spp. are rarely found shallower than 75 m the smaller taxa were probably not influenced by freshwater inputs yielding falsely "warm" results.

High evaporation rates have the inverse effect, causing the $\delta^{18}O$ of seawater to become heavier as ^{16}O is preferentially lost to the atmosphere. This effect is consistent with heavier than expected values in *N. gizehensis.* Figure 4 shows a theoretical range of temperatures and salinities calculated using the $\delta^{18}O$ of both microspheric and megalospheric forms of *N. gizehensis* and the equations of Rostek et al. (1993) and Schmidt (1999). Whether 21°C (as calculated from *Uvigerina* spp. and *Cibicides* spp.) is assumed to be an average annual temperature or an annual minimum, the corresponding salinities are feasible for semi-enclosed coastal marine environments in arid, low-latitude regions; a lowest possible salinity of 41‰ using Rostek et. al.'s equation (1993) and assuming 21°C is an annual average, and a highest possible salinity of 48‰ using Schmidt's equation (1999) and assuming 21°C is an annual minimum. These salinities are

also consistent with salinity ranges for modern Nummulites which have tolerances in the range of 30-45‰ (Hallock and Glenn 1986). Beavington-Penney and Racey (2004) report the highest diversity assemblages for living rotaliids in this salinity range, indicating that low diversity assemblages (such as the one studied here) may be found in higher salinities.

Given the very low likelihood of other potential factors that can affect $\delta^{18}O$ in calcium carbonate and seawater, and the reasonable fit with salinity expectations given the temperature data available, higher salinity most likely accounts for the positive shift found in *N. gizehensis.* If this is true, however, why would this effect be absent in the co-occurring *Uvigerina* spp. and *Cibicides* spp?

Observed $\delta^{18}O$ differences and their implications for temperature data

Multiple scenarios can account for the differences found in the $\delta^{18}O$ of *N. gizehensis* and the *Uvigerina* spp. and *Cibicides* spp. collected in the same sample; all of them require either a

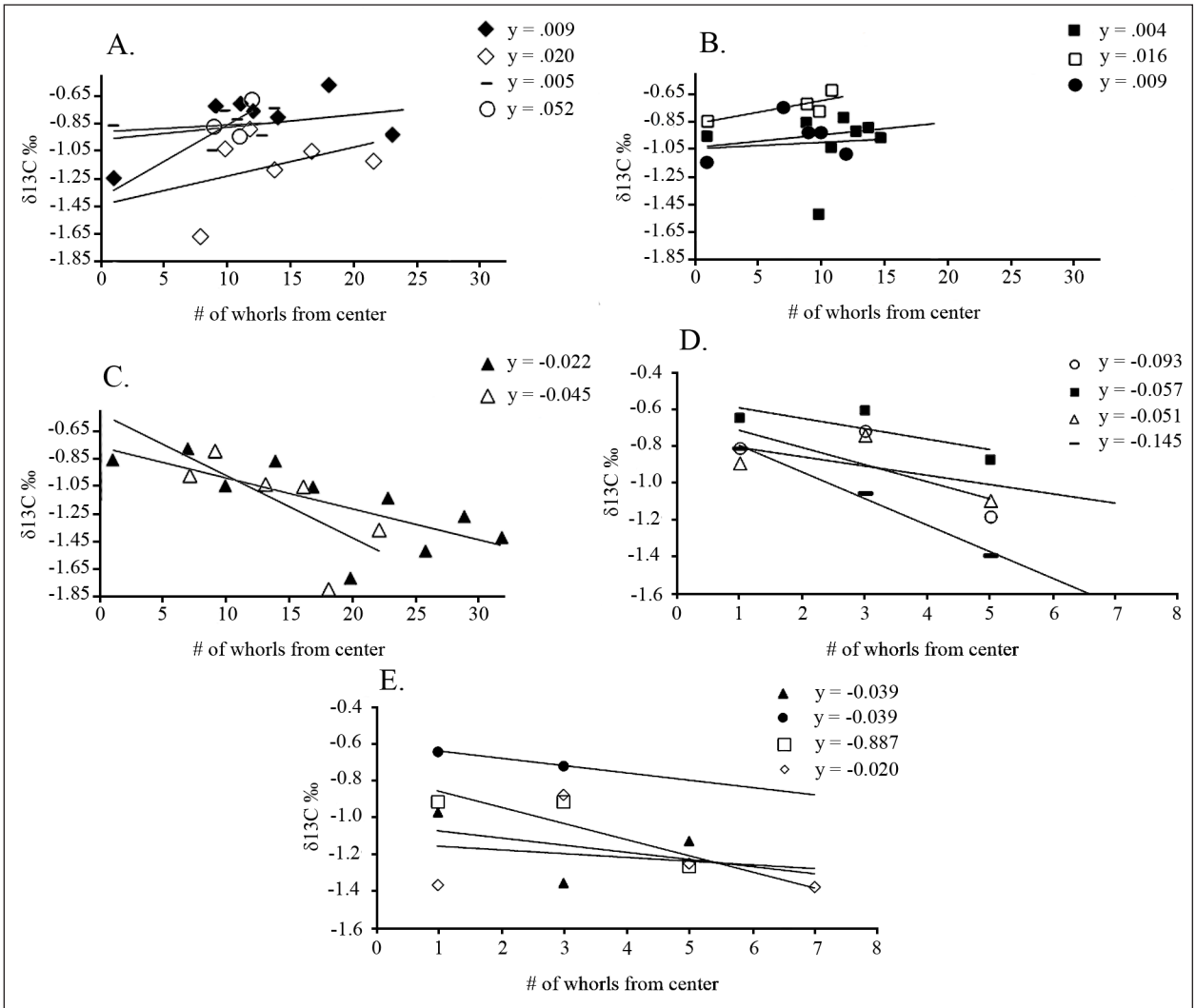

Figure 6. $\delta^{13}C$ over ontogeny in *N. gizehensis*. A. and B. show a trend of increasing $\delta^{13}C$ with increasing age in seven subsampled microspheric individuals. C. Shows a trend of decreasing $\delta^{13}C$ with increasing age in two microspheric individuals. D. and E. show decreasing $\delta^{13}C$ in all subsampled megalospheric individuals.

difference in timing of growth between taxa, and/or the post-mortem transport of taxa. Here I eliminate scenarios that are highly improbable in light of other available information. The remaining scenarios can then be used to inform temperature estimates used in the calculation of equilibrium calcite, and to generate predictions about the $\delta^{13}C$ of all taxa.

$\delta^{18}O$ values indicate that *N. gizehensis* were living in a location that experienced very high evaporation rates and the formation of hypersaline waters, which is most consistent with a semi-enclosed coastal environment, while *Uvigerina* spp. and *Cibicides* spp. reflect typical open shelf conditions for low-latitude middle Eocene seas. The transport of *N. gizehensis* offshore from a shallow, near-shore environment is perhaps the most expected explanation, however it is inconsistent with the geologic context of the sample (see Figure 7). Most significantly, the *N. gizehensis* bank from which the sample was collected is made up of whole tests in life position (parallel to the bedding plane), rather than the primarily broken tests found in transported deposits. The argument against transport of the *N. gizehensis* is further strengthened by the thinness of the tests, which would have been particularly susceptible to breakage during transport. Furthermore their preservation in a very fine-grained matrix is consistent with a very low-energy environment, while storm deposits would include larger grain sizes.

Another possible explanation is that smaller taxa were mixed into the nummulite bank by bioturbation after local conditions had changed significantly, such as might be expected with rising sea level. Field notes (Strougo, pers. comm.) indicate that "the plane of demarcation between the clay below and the nummulites above is sharp with no apparent evidence of bioturbation (burrowing, mottling, etc.). A few hundred meters northeast of this clay pit the nummulites seemingly were overlain by another bed of variegated clays." The lack of evidence to support bioturbation makes this another unlikely candidate.

Although less expected, the transport of smaller taxa onshore is more probable. During coastal upwelling events, onshore-directed shelf bottom currents are vigorous enough to transport particles up to sand size (Huhn et al. 2007). With the exception of *N. gizehensis* tests, all of the sediment in the sample is sand-sized or smaller, which is consistent with transport of smaller taxa by upwelling.

The difference in $\delta^{18}O$ might also be explained by seasonal differences in growth. *Nummulites* sp. have been found to grow for years (Purton and Brasier 1999, Sarangi et al. 2001) while *Uvigerina* spp. and *Cibicides* spp. may calcify their tests over weeks or months. Therefore, if all of these taxa lived in the same location and *Uvigerina* spp. and *Cibicides* spp. represent conditions during a single season, those conditions might still be represented in the tests of the larger foraminifera, which is clearly not the case. It is also possible that no overlap in values exists because the conditions conducive to *Uvigerina* spp. and *Cibicides* spp. growth actually inhibit or prevent growth in *N. gizehensis.* The dwindling number of *N. gizehensis* $\delta^{18}O$ values as they approach those of *Uvigerina* spp. and *Cibicides* spp. could support this idea (see Figure 3), although it certainly doesn't confirm it.

Only two of the potential scenarios reviewed above can account for the difference observed in $\delta^{18}O$ between *N. gizehensis* and the smaller taxa, and both of these provide the same temperature predictions. Whether smaller taxa were transported during upwelling events or calcified only during a single season, *N. gizehensis* calcify during periods of increased salinity, which is caused by high evaporation rates associated with high temperatures, while *Uvigerina* spp. and *Cibicides* spp. calcify in typical shelf conditions around 21°C at normal marine salinities. Both scenarios predict that 21°C is approximately the lowest temperature likely experienced by *N.*

gizehensis. This estimate can therefore be used as a lower boundary on the calculated salinity/ temperature graph and to find an average annual temperature experienced by *N. gizehensis* for the calculation of contemporary fossil equilibrium calcite.

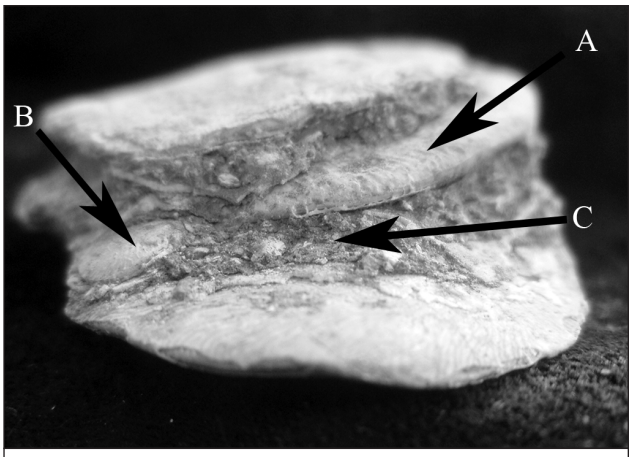

Figure 7. Photographs of the original field site do not exist, however a fragment of the original sample illustrates descriptions from field notes. Arrow A. points to a thin, unbroken test of a microspheric *N. gizehensis* oriented parallel to two other thin, unbroken microspheric forms. Arrow B shows the likewise parallel orientation of a megalospheric form, And arrow C shows the fine grained sediment intercalated with the *N. gizehensis* from which *Cibicides* spp. and *Uvigerina* spp. were collected.

$\delta^{13}C$ and photosymbiosis

Any observed differences in $\delta^{13}C$ between *N. gizehensis, Cibicides* spp. and *Uvigerina* spp. must be considered in light of the differences found in $\delta^{18}O$. If these taxa did not calcify under the same temperature conditions and perhaps not even in the same location, alternative explanations may be possible for the observed 3.75‰ negative shift in the $\delta^{13}C$ of *N. gizehensis.* The factors that can affect $\delta^{13}C$ are reviewed here in the context of the possible depositional scenarios discussed above.

Variables affecting $\delta^{13}C$ of calcium carbonate

Similar to the case for $\delta^{18}O$, the most important factors affecting $\delta^{13}C$ in calcium carbonates are environmental: the $\delta^{13}C$ of ambient seawater (covered separately below), and the ratios of carbon species (pH) during calcification. Given the relative stability of carbon species in ocean water on shorter time scales, no major shifts in seawater chemistry can be assumed to have occurred between the deposition of *N. gizehensis* and the smaller taxa.

Metabolic CO_2 is depleted in ^{13}C, so utilization of metabolic CO_2 in test formation can result in $\delta^{13}C$ values more negative than expected for equilibrium calcite. However, in non-symbiotic foraminifera, once the effects of differences in the $\delta^{13}C$ of ambient seawater in microhabitats is subtracted out, the resulting negative shift due to respiration alone is relatively small (Fontanier et al. 2006, Woodruff et al. 1980) and cannot account for the large negative shift seen here in *N. gizehensis.*

Variables affecting $\delta^{13}C$ of seawater

Average $\delta^{13}C$ values vary between carbon reservoirs, with carbonates having an average value around 0‰, terrestrial organic carbon -26‰, and marine organic carbon -22‰. Organics are so depleted in heavier carbon isotopes because there is a strong preference for lighter isotopes in photosynthesis. Therefore, the $\delta^{13}C$ of seawater depends most strongly on the location in the water column. Surface water is enriched in ^{13}C because lighter isotopes are bound in organisms, while water close to the bottom is lighter due to the rerelease of ^{12}C by decaying organics. Pore water values are increasingly negative with sediment depth as buried organic material continues to decay. The amount of organic matter raining down to the seafloor determines how depleted bottom and pore water will be, thus distance from coastal areas (where productivity tends to be

highest as a result of runoff from land) and local currents can also influence $\delta^{13}C$.

For benthic foraminifera, $\delta^{13}C$ is controlled primarily by the foraminifera's microhabitat on or within the sediment (Fontanier et al. 2006). Some species of *Uvigerina* and *Cibicides* are known to be endobenthic, living just below the sediment/water interface (Duplessey et al. 1984, Fontanier et al. 2006). This would result in a slightly negative shift in these smaller taxa, which is the opposite of the findings here. The $\delta^{13}C$ found for *Uvigerina* spp. and *Cibicides* spp. are in agreement with previously reported $\delta^{13}C$ values for the Eocene (Stott et al. 1996, Zachos et al. 1994).

All extant larger rotaliids are epibenthic, a necessity to access adequate sunlight for their symbionts. If extinct rotaliids such as *N. gizehensis* lacked symbionts, perhaps they were endobenthic, and deep infaunal microhabitats can produce strong negative shifts in productive areas, such as those found for *Globobulimina* spp. in the Bay of Biscay (Fontanier et al. 2006). However this hypothesis is highly unlikely in light of the observed $\delta^{18}O$ values. The *N. gizehensis* record high-salinity conditions, which implies little to no runoff from land, and very low productivity. Even if *N. gizehensis* lived buried deep in sediments (itself unlikely given their thin, flat morphology), and even if *Uvigerina* spp. and *Cibicides* spp. lived farther offshore (and thus farther from an area of higher productivity) the observed negative shift in $\delta^{13}C$ is too great to be caused by pore-water effects in a very low productivity location; Langer (1995) found that asymbiotic foraminifera living in low-oxygenated, organic-rich sediments had $\delta^{13}C$ values that overlapped with those of symbiotic rotaliids.

Endosymbiosis

The presence of photosynthesizing endosymbionts is the best supported and most likely explanation for the observed 3.75‰ shift in the $\delta^{13}C$ of *N. gizehensis*. The shift found here is toward the lower end of ranges found in extant taxa. This is consistent with deeper water depths (Langer 1995), which is supported by the thin tests of observed in *N. gizehensis*. The presence of photosynthesizing endosymbionts is also consistent with a hypersaline, low-productivity environment responsible for anomalously high $\delta^{18}O$ values, where symbiotic organisms such as larger foraminifera and corals flourish.

The expected ontogenetic trend of heavier $\delta^{13}C$ with increasing age is also seen in seven of nine subsampled microspheric *N. gizehensis* (Figure 6), but the opposite is found in all of the subsampled megalospheric forms. This doesn't rule out symbiosis, however, because the trend is only weakly supported in the literature and no comparisons have been done between sexually and asexually reproduced populations (microspheric and megalospheric forms, respectively). The extant rotaliid species *Heterostegina depressa* and *Calcarina spengleri* showed increasingly heavier $\delta^{13}C$ over ontogeny, but another rotaliid, *Operculina* sp. showed the opposite (Wefer et al. 1981). Isotope analysis of whole tests of the extinct *Nummulites prestwichianus* showed more positive $\delta^{13}C$ values with increasing test size, much like *Heterostegina depressa* (Brasier and Green 1993). However, it's unclear if this analysis included megalospheric forms, and unlike *N. gizehensis,* there is almost no size difference between megalospheric and microspheric forms in *N. prestwichianus* (Brasier and Green 1993).

As photosynthetic rates increase more metabolic CO_2 is incorporated in the test, thus $\delta^{13}C$ values become more negative (Erez 1978). Increasingly heavy $\delta^{13}C$ values over the course of ontogeny is commonly attributed to slowing growth rates with increasing age, and has been noted

in corals and planktonic foraminifera as well as extant rotaliid foraminifera (Wefer et al. 1981). The shorter lifespan and rapid asexual reproduction of megalospheric forms relative to the giant, long-lived, sexually reproduced microspheric forms (see figure 2 for a size comparison) may account for the observed difference in $\delta^{13}C$ over ontogeny.

Conclusions

This study used stable isotope techniques to test for the presence of photosynthetic endosymbionts in an extinct rotaliid Eocene Foraminifer, *Nummulites gizehensis*. Expectations derived from extant species were that, in endosymbionts (1) $\delta^{13}C$ test values should be 3-5‰ more negative than $\delta^{13}C$ of contemporary "fossil" equilibrium calcite, and (2) increasing $\delta^{13}C$ values over ontogeny. The first expectation was fulfilled, providing strong support for the hypothesis of symbiosis in *N. gizehensis.* Observations consistent with the second expectation prevailed for most microspheric individuals, but not for the smaller, shorter lived megalospheric individuals.

An alternative explanation that the 3-5‰ difference between *N. gizehensis* and equilibrium calcite is due to a difference in ratios of carbon species during the time of calcification was rejected because all of the included taxa co-occur in a single sample and carbon species ratios are relatively constant in seawater over short time scales. Similarly, the incorporation of metabolic CO_2 without photosynthesis results in negative shifts that are much less than 3-5‰. Differences due to productivity predict more negative values for endobenthic calcite relative to epibenthic calcite because of pore water effects, and benthic calcite secreted in higher productivity areas vs. lower productivity areas. A 3-5‰ shift due to pore water effects is unlikely because some species of *Uvigerina* and *Cibicides* are known to be endobenthic while all extant *Nummulites* are known to be epibenthic and their discoid morphology is inconsistent with an epibenthic microhabitat; this predicts more negative values in *Uvigerina* spp. and *Cibicides* spp. A 3-5‰ difference due to local productivity would require *N. gizehensis* to be living in a low-oxygen, organic rich environment, which is inconsistent with the high salinities indicated by the $\delta^{18}O$ values recorded by *N. gizehensis.* High salinity requires negligible rainfall and runoff from land, which also results in low nutrient, low productivity conditions.

Observed values of $\delta^{18}O$ in *N. gizehensis* are interpreted to result from high salinities, because alternative explanations can be rejected. Temperatures calculated from *N. gizehensis* $\delta^{18}O$ values are anomalously low for low-latitude Eocene surface water, and the warmer temperatures recorded by *Uvigerina* spp. and *Cibicides* spp. are in good agreement with previously reported temperatures for open shelf conditions in low-latitude middle Eocene seas. $\delta^{18}O$ shifts due to ontogenetic changes, gametogenesis or aragonitic material do not apply in the case of *N. gizehensis,* and respiration effects would cause a negative shift rather than a positive one. Likewise shifts due to changes in global ice volume, or proximity to sea ice margins are not applicable in this case. It is also unlikely that freshwater input caused *Uvigerina* spp. and *Cibicides* spp. to record "warmer" temperatures, both because they are in good agreement with previously reported values, and because *Uvigerina* spp. do not occur at depths shallower than 75 meters, and are thus unlikely to be strongly affected by freshwater runoff. Finally, calculated salinity and temperature ranges are consistent with temperature and salinity ranges of extant, symbiotic *Nummulites*. These interpretations are consistent with symbiont-bearing *N. gizehensis* living in a nearshore, saline environment with onshore transport of *Uvigerina* spp. and *Cibicides* spp. during upwelling events, or with seasonal differences in timing of growth between *N. gizehensis* and the smaller

taxa.

This study provides the first clear isotopic evidence for symbiosis in an extinct, larger foraminifera. In the future, more species must be tested in order to demonstrate that symbiosis was common throughout extinct larger taxa. Likewise, the evolution of symbiosis in foraminifera might be illuminated through isotopic testing of smaller, suspected precursor taxa and the earliest appearances of larger taxa.

References

Arbuszewski J, deMenocal P, Kaplan A, Farmer EC. 2010. On the fidelity of shell-derived δ18Oseawater estimates. Earth and Planetary Science Letters 300: 185-196.

Beavington-Penney S, Racey A. 2004. Ecology of extant nummulitids and other larger benthic foraminifera: applications in palaeoenvironmental analysis. Earth-Science Reviews 67: 219-265.

Belanger PE, Curry WB, Matthews RK. 1981. Core-top evaluataion of benthic foraminifera isotopic ratios for paleo-oceanographic interpretations. Palaeogeography, Palaeoclimatology, Palaeoecology 33: 205-220.

Berggren WA, Pearson PN. 2005. A revised tropical to subtropical Paleogene planktonic foraminiferal zonation. Journal of Foraminiferal Research 35: 279-298.

—. 2006. Tropical to subtropical planktonic foraminiferal zonation of the Eocene and Oligocene. Pages 29-40 in Pearson PN, Olsson RK, Huber BT, Hemleben C, Berggren WA, eds. Atlas of Eocene Planktonic Foraminifera. Greenville, North Carolina.

Berggren WA, Kent DV, Swisher CC, Aubrey MP. 1995. A revised Cenozoic geochronology and chronostratigraphy. Society of Economic Paleontologists and Mineralogists, Special Publication 54: 129-212.

Bralower TJ, Zachos JC, Thomas E, Parrow M, Paull CK, Kelly DC, Premoli Silva I, Sliter WV, Lohmann KC. 1995. Late Paleocene to Eocene paleoceanography of the Equitorial Pacific Ocean: stable isotopes recorded at Ocean Drilling Program site 865, Allison Guyot. Paleoceanography 10: 841-865.

Brasier MD, Green OR. 1993. Winners and losers: stable isotopes and microhabitats of living Archaiadae and Eocene *Nummulites* (larger foraminifera). Marine Micropaleontology 20: 267-276.

Buchardt B, Hansen HJ. 1977. Oxygen isotope fractionation and algal symbiosis in benthic foraminifera from the Gulf of Elat, Israel. Bulletin of the Geological Society of Denmark 26: 185-194.

Cande SC, Kent DV. 1995. Revised calibration of teh geomagnetic polarity timescale for the Late Cretaceous and Cenozoic. Journal of Geophysical Research 100: 6093-6095.

Cowen R. 1988. The role of algal symbiosis in reefs through time. Palaios 3: 221-227.

D'Agostino RB, Stevens MA. 1986. Goodness-of-Fit Techniques. New York: Marcel Dekker.

D'Hondt S, Zachos J, Schultz G. 1994. Isotopic signals and photosymbiosis in Late Paleocene planktonic foraminifera. Paleobiology 20: 391-406.

Duguay LE. 1983. Comparative laboratory and field studies on calcification and carbon fixation in foraminiferal-algal associations. Journal of Foraminiferal Research 13: 252-261.

Duplessey J-C, Shackleton NJ, Matthews RK, Prell W, Ruddiman WF, Caralp M, Hendy CH. 1984. 13C record of benthic foraminifera in the Last Interglacial ocean: implications for the carbon cyucle and the global deep water circulation. Quaternary Research 21: 225-243.
Emrich K, Ehhalt DH, Vogel JC. 1970. Carbon isotope fractionation during the precipitation of calcium carbonate. Earth and Planetary Science Letters 8: 363-371.
Erez J. 1978. Vital effect on stable-isotope somposition seen in foraminifera and coral skeletons. Nature 273: 199-202.
Fontanier C, Mackensen A, Jorissen FJ, Anschutz P, Licari L, Griveaud C. 2006. Stable oxygen and carbon isotopes of live benthic foraminifera from the Bay of Biscay: Microhabitat impact and seasonal variability. Marine Micropaleontology 58: 159-183.
Graham DW, Corliss BH, Bender ML, Keigwin LDJ. 1981. Carbon and oxygen isotopic disequilibria of Recent deep-sea benthic Foraminifera. Marine Micropaleontology 6: 483-497.
Hagen S, Keigwin LD. 2002. Sea-surface temperature variability and deep water reorganisation in the subtropical North Atlantic during isotope stage 2-4. Marine Geology 189: 145-162.
Hallock P. 1985. Why are larger foraminifera large? Paleobiology 11: 195-208.
—. 1999. Symbiont-bearing foraminifera. Pages 123-139 in Gupta BKS, ed. Modern Foraminifera. Dordrecht, The Netherlands: Kluwer Academic Press.
Hallock P, Glenn CE. 1986. Larger Foraminifera: a tool for paleoenvironmental analysis of Cenozoic carbonate. Palaios 1: 55-64.
Hammer O, Harper DAT, Ryan PD. 2001. PAST: paleontological statistics software package for education and data analysis. Palaeontologia Electronica 4: 9.
Hottinger L. 1982. Larger Foraminifera, giant cells with a historical background. Naturwissenschaften 69: 361-371.
Hottinger L, Dreher D. 1974. Differentiation of protoplasm in Nummulitidae (Foraminifera) from Elat, Red Sea. Marine Biology 25: 41-61.
Houston RM, Huber BT. 1998. Evidence of photosymbiosis in fossil taxa? Ontogenetic stable isotope trends in some Late Cretaceous planktonic foraminifera. Marine Micropaleontology 34: 29-46.
Houston RM, Huber BT, Spero HJ. 1999. Size-related isotopic trends in some Maastrichtian planktic foraminifera: methodological comparisons, intraspecific variability, and evidence of photosymbiosis. Marine Micropaleontology 36: 169-188.
Huhn K, Paul A, Seyferth M. 2007. Modeling sediment transport patterns during an upwelling event. Journal of Geophysical Research 112.
Langer MR. 1995. Oxygen and carbon isotopic composition of recent larger and smaller foraminifera from the Madang Lagoon (Papua new Guinea). Marine Micropaleontology 26: 215-221.
Lee JJ. 2006. Algal symbiosis. Symbiosis 42: 63-75.
Lee JJ, Hallock P. 1987. Algal symbiosis as the driving force in the evolution of larger foraminifera. Annals of the New York Academy of Sciences 503: 330-347.
Lee JJ, McEnery ME, Kahn EG, Schuster FL. 1979. Symbiosis and the evolution of larger foraminifera. Micropaleontology 25: 118-140.
Lee JJ, Sang K, ter Kuile B, Strauss E, Lee PJ, Faber WWJ. 1991. Nurtional and related experiments on laboratory maintenance of three species of symbiont-bearing, large foraminifera. Marine Biology 109: 417-425.
Leutenegger S. 1984. Symbiosis in benthic foraminifera: specificity and host adaptations. Journal of Foraminiferal Research 14: 16-35.

Loeblich ARJ, Tappan H. 1988. Foraminiferal Genera and Their Classification. New York: Van Nostrand Reinhold.
Luterbacher HP, et al. 2004. The Paleogene Period. Pages 384-408 in Gradstein FM, Ogg JG, Smith AG, eds. A Geologic Time Scale. Cambridge: Cambridge University Press.
McEnery ME, Lee JJ. 1981. Cytological and fine structural studies of three species of symbiont-bearing larger foraminifera from the Red Sea. Micropaleontology 27: 71-83.
Norris RD. 1996. Symbiosis as an evolutionary innovation in the radiation of Paleocene planktic foraminifera. Paleobiology 22: 461-480.
Pearson P, Shackleton N, Hall M. 1993. Stable isotope paleoecology of middle Eocene planktonic foraminifera and multi-species isotope stratigraphy, DSDP site 523, South Atlantic. Journal of Foraminiferal Research 23: 123-140.
Pearson PN, Ditchfield PW, Singano J, Harcourt-Brown KG, Nicholas CJ, Olsson RK, Shackleton NJ, Hall MA. 2001. Warm tropical sea surface temperatures in the Late Cretaceous and Eocene epochs. Nature 413: 481-487.
Pochon X, LaJeunesse TC, Pawlowski J. 2004. Biogeographic partitioning and host specialization among foraminiferan dinoflagellate symbionts (Symbiodinium; Dinophyta). Marine Biology 146: 17-27.
Poli MS, Meyers PA, Thunnell RC. 2010. The western North Atlantic record of MIS 13 to 10: changes in primary productivity, organic carbon accumulation and benthic foraminiferal assemblages in sediments from teh Blake Outer Ridge (ODP Site 1058). Palaeogeography, Palaeoclimatology, Palaeoecology 295: 89-101.
Purton LMA, Brasier MD. 1999. Giant protist Nummulites and its Eocene environment: life span and habitat insights from $\delta^{18}O$ abd $\delta^{13}C$ data from *Nummulites* and *Venericardia*, Hampshire basin, UK. Geology 27: 711-714.
Richardson SL. 2001. Endosymbiont change as a key innovation in the adaptive radiation of Soritida (Foraminifera). Paleobiology 27.
Rohling EJ, Cooke S. 1999. Stable oxygen and carbon isotope ratios in foramiferal carbonate. Pages 239-258 in Gupta BKS, ed. Modern Foraminifera. Dordrecht, The Netherlands: Kluwer Academic Press.
Ross CA. 1974. Evolutionary and ecological significance of large calcareous foraminifera (Protozoa), Great Barrier Reef. Proceedings of the Second International Symposium On Coral Reefs 1: 327-333.
Rostek F, Ruhland G, Labeyrie LD, Lancelot Y, Bard E. 1993. Reconstructing sea surface temperature and salinity using $\delta^{18}O$ and alkenone records. Nature 364: 319-321.
Sarangi S, Sarkar A, Sarin MM, Bhattacharya SK, Ebihara M, Ray AK. 2001. Growth rate and life span of Eocene/Oligocene *Nummulites* tests: inferences from Sr/Ca ratio. Terra Nova 13: 264-269.
Saraswati PK. 2007. Symbiont-bearing benthic foraminifera of Lakshadweep. Indian Journal of Marine Science 36: 351-354.
Saraswati PK, Seto K, Nomura R. 2004. Oxygen and carbon isotopic variation in co-existing larger foraminifera from a reef flat at Akajima, Okinawa, Japan. Marine Micropaleontology 50: 339-349.
Schmidt GA. 1999. Error analysis of paleosalinity calculations. Paleoceanography 14: 422-429.
Shackleton NJ. 1974. Attainment of isotopic equilibrium between ocean water and benthonic foraminifera genus *Uvigernia*: isotopic changes in the ocean during the last glacial. Colloques

Internationaux du C.N.R.S. Les methodes quantitative d'etude des variations du climat au cours du Pleistocene: 203-209.
Shackleton NJ, Opdyke ND. 1973. Oxygen isotope and paleomagnetic stratigraphy of equitorial pacifc core V28-238: oxygen isotope temperatures and ice volumes on a 10^5 year and 10^6 year sclae. Quaternary Research 3: 39-55.
Shackleton NJ, Kennett JP. 1975. Paleotemperature history of the Cenozoic and the initiation of Antarctic glaciation: oxygen and carbon isotope analysis in DSDP sites 277, 279, and 281. Initial Reports of the Deep Sea Drilling Project 29: 743-755.
Song Y, Black RG, Lipps JH. 1994. Morphological optimization in the largest living foraminifera: implication from finite element analysis. Paleobiology 20: 14-26.
Stanley GDJ, Swart PK. 1995. Evolution of the coral-zooxanthellae symbiosis during the Triassic: a geochemical approach. Paleobiology 21.
Stott LD, Sinha A, Thiry M, Aubrey M-P, Berggren WA. 1996. Global δ13C changes across the Paleocene-Eocene boundary: criteria for terrestrial-marine correlations. Pages 381-399 in Knox RW, Corfield RM, Dunay RE, eds. Correlation of the Early Paleogene in Northwest Europe, vol. 101. London: The Geological Society.
Strougo A. 2008. The Mokkattamian Stage: 125 years later. Middle East Research Center , Ain Shams University, Earth Science Series 22: 47-108.
Tappan H, Loeblich ARJ. 1988. Foraminiferal evolution, diversification, and extinction. Journal of Paleontology 62: 695-714.
Wade BS, Al-Sabouni N, Hemleben C, Kroon D. 2007. Symbiont bleaching in fossil planktonic foraminifera. Evolutionary Ecology 22: 253-265.
Wade BS, Pearson PN, Berggren WA, Pälike H. 2011. Review and revision of Cenozoic tropical planktonic foraminiferal biostratigraphy and calibration to the geomagnetic polarity and astronomical time scale. Earth-Science Reviews 104: 111-142.
Wefer G, Killingley JS, Lutze GF. 1981. Stable isotopes in recent larger foraminifera. Palaeogeography, Palaeoclimatology, Palaeoecology 33: 253-270.
Williams DF, Rottger R, Schmaljohann R, Keigwin L. 1981. Oxygen and carbon isotopic fractionation and algal symbiosis in the benthic foraminiferan *Heterostegina depressa*. Palaeogeography, Palaeoclimatology, Palaeoecology 33: 231-251.
Woodruff F, Savin SM, Douglas RG. 1980. Biological fractionation of oxygen and carbon isotopes by recent benthic foraminifera. Marine Micropaleontology 5: 3-11.
Zachos JC, Stott LD, Lohmann KC. 1994. Evolution of early Cenozoic marine temperatures. Paleoceanography 9: 353-387.
Zimmerman MA, Williams DF, Rottger R. 1983. Symbiont-influenced isotopic disequilibrium in *Heterostegina depressa*. Journal of Foraminiferal Research 13: 115-121.

IV. Pleistocene Reefs of the Egyptian Red Sea

Abstract

Coral reefs are endangered globally, and predicting their response to changing environmental conditions is a priority for researchers and managers. The fossil record of Red Sea fringing reefs provides a unique opportunity to study the history of coral survival and recovery in the context of environmental catastrophe. Coral assemblage data from eight emerged fossil reef terraces on the Egyptian coast are described and used to determine if and how coral assemblages change from Middle to Late Pleistocene, and Late Pleistocene to modern reefs. The first Red Sea occurrence of *Favites micropentagona* is reported from the Middle Pleistocene. Coral taxa are constant over the studied time period, as are coral assemblages, despite likely extinctions of coral species over two-thirds of the Red Sea basin during glacial low-stands. A less saline but still hostile southern Red Sea may have acted as a refuge for small communities of salinity-tolerant taxa during these extinction events, and provided the early settlers for subsequent recolonization events. If populations of corals can be sustained, even in marginal and geographically limited habitat, they retain the potential to re-establish themselves with restored water quality and available substrate.

Introduction

Coral reefs world-wide are under threat from over-fishing, coastal development and pollution run-off from land, as well changes in ocean temperature and chemistry resulting from anthropogenic climate change (Wilkinson 2008). With rising concerns about the future of coral reef ecosystems has come increased efforts to predict their fate under varying climate predictions (see review by Donner et al. 2009). Modern ecological studies of reefs seeking to predict future response are limited to analyses at the scale of decades, which may not be indicative of ecological trends at longer time scales (Denny et al. 2004, Pandolfi 2011). The fossil record provides unique opportunities to study diversity on longer time scales, and under different environmental conditions (Jackson Jeremy B. C. and Erwin 2006, Pandolfi 2011), making it a valuable resource for understanding coral response to a changing planet.

The Red Sea provides a unique natural laboratory to study the history of coral survival and recovery in the context of environmental catastrophe. Fossil coral terraces from interglacials of the Middle and Late Pleistocene occur along-side modern day fringing reefs all along the Red

Sea coast (Plaziat et al. 2008). These preserved stages of reef growth are punctuated by times when the Red Sea experienced hypersaline conditions hostile to life (Almogi-Labin 1982, Almogi-Labin et al. 1998, Badawi et al. 2005, Fenton et al. 2000, Hemleben et al. 1996, Thunnell et al. 1988), as a response to glacial periods. This study is a biological survey of these Pleistocene assemblages from the Egyptian coast, and aims to determine if and how coral reefs of the Red Sea changed in response to dramatic environmental change. This history is of particular interest not only for its implications for the future of coral reefs, but also for what it can tell us about the adaptive history of Red Sea corals, which tolerate temperatures and salinities known to be fatal to populations living in other locations (Sheppard C. R. C. and Sheppard 1991).

Geologic setting

The Red Sea is a long, narrow, marginal sea at the western most extent of the Indo-Pacific. It stretches over 2000 km from N 30° at the Gulf of Suez to N 13° at its southern limit, the Straits of Bab-el-Mandeb. The basin is almost completely enclosed by land, bordered to the east by the Arabian Peninsula, the African continent to the west, Sinai Peninsula to the north. It is connected to the Indian Ocean via the Gulf of Aden through the straits of Bab El Mandeb in the south, which at just 20 km across and 137 m deep at the Hanish sill(Werner and Lange 1975) limits water mass exchange. This limited exchange combined with a lack of fresh water input and the surrounding hot and arid climate accounts for an average surface salinity of 40 -41‰. It is an active, maritime rift system overlying the divergent plate boundary between the African and Arabian plates, and connecting the East African Rift Valley to the southwest, to the Dead Sea rift to the northeast.

During interglacial high-stands of the Pleistocene (as well as the present) extensive fringing reefs developed along the coasts of the Red Sea. Today, emerged reef terraces running parallel to the modern coastline are a nearly continuous feature of the entire Red Sea (El Moursi et al. 1994, Gvirtzman et al. 1977, Plaziat et al. 2008, Plaziat et al. 1998). On the Egyptian coast Late Pleistocene terraces dated to the Marine Isotope Stage (MIS) 5e (Plaziat et al. 2008) form a low cliff along the water line. In most locations they appear as two obvious terraces, the lower at approximately 1.5 m above mean sea level and the upper terrace approximately 4 meters. This is near to their original elevation because the Egyptian coast south of the Gulf of Suez has been tectonically stable over the Late Pleistocene (Plaziat et al. 1998). These terraces have been interpreted as 3 terraces representing independent stages of reef growth by some authors (El Moursi et al. 1994), however an exhaustive review of uranium series dates by Plaziat et. al. (2008) find both terraces belong to MIS 5e, and the platform morphology a result of erosion. Wadis (erosional valleys) running perpendicular to the coast form breaks in the terraces and modern fringing reefs, allowing access to the outcrop face.

Middle Pleistocene reefs occur farther inland, and at elevations up to 50 m as a result of sea level change and tectonic uplift (El-Asmar 1997, El Moursi et al. 1994, Gvirtzman et al. 1977, Plaziat et al. 2008, Plaziat et al. 1998). These have been attributed to MIS 7 and 9, and a limited number of uranium series dates have placed them at around 200,000 years b.p. (MIS 7) with some ages over 300,000 years b.p. (MIS 9) (El-Asmar 1997, El Moursi et al. 1994, Gvirtzman 1994, Hoang and Taviani 1991, Plaziat et al. 2008).

Based on elevation and preservation, it is possible that this study includes terraces from MIS 5, MIS 7 and MIS9. However, given the uncertainty of ages on the older terraces, they are

referred to the Late or Middle Pleistocene only. The underlying assumption is that the terraces studied here are separated by a single glacial period (MIS 6) with the understanding that it may be an underestimation of the spanned time period. This is a more conservative assumption than the alternative because dates over 300,000 years b.p. are even less certain than those for MIS 7. For a thorough review of the geology of the Pleistocene reef terraces of the Egyptian coast and their dating see Plaziat et. al. (2008).

Paleontology of Red Sea reefs

The Pleistocene reef terraces of the Red Sea coast have attracted considerable geological study for their contribution to past sea level reconstructions (Gvirtzman 1994, Hemleben et al. 1996, Siddall et al. 2004, Thunnell et al. 1988), but much less work has focused on the biology of the reef fauna. Dullo (1990) describes Late Pleistocene fauna from the terraces of Saudi Arabia, and El-Sorogy (1997, 2008) describes the corals of Middle and Late Pleistocene fauna from the Sinai peninsula and Pleistocene of the Egyptian coast; Al-Rifaiy and Cherif (1988) provides a more limited description of corals from the coast of Jordan and likewise Bruggemann et al. (2004) mentions coral species in descriptions of terraces from the coast of Eritrea. The political and geographic climate of the region limit access to the outcrops, so these works provide a valuable resource for comparing the fossil fauna of the Red Sea to the modern fauna (see Table 4).

Methods

I explored potential field sites along the

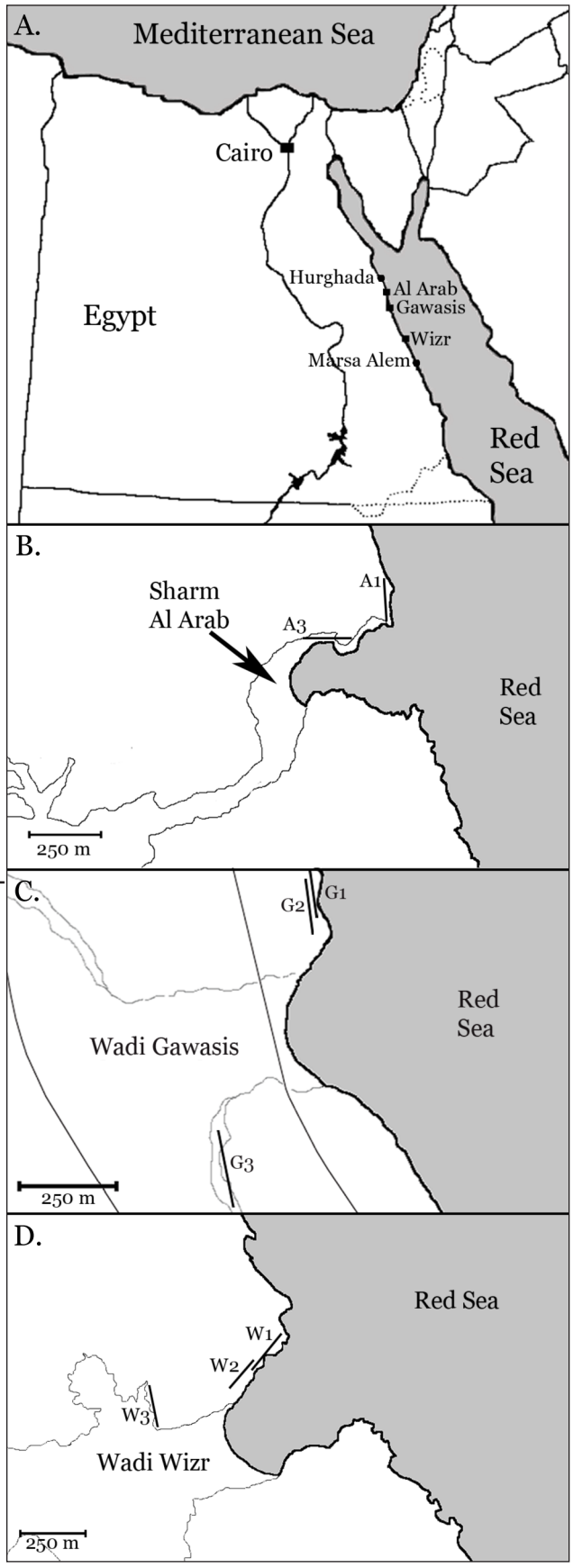

Figure 1. Field location maps. A, Egyptian coastline, showing field sites between Hurghada and Marsa Alem; B, Sharm Al Arab field site showing the location of fossil reef terraces. A1 is lower Late Pleistocene terrace, A3 is Middle Pleistocene terrace; C, Wadi Gawasis field site showing the location of fossil reef terraces. G1 is lower Late Pleistocene terrace, G2 is upper Late Pleistocene terrace, G3 is Middle Pleistocene terrace; D, Wadi Wizr field site showing the location of fossil reef terraces. W1 is lower Late Pleistocene terrace, W2 is upper Late Pleistocene terrace, W3 is Middle Pleistocene terrace.

Egyptian Red Sea coast between the cities of Hurghada (Al Ghardaqah) and Marsa Alem in a series of four field trips between February and May of 2007 using the work of El Moursi et. al. (1994) as a guide. Field sites were chosen based on three criteria: a) the presence of coral reef terraces representing Late and Middle Pleistocene interglacials, b) at least 100 meters of exposed outcrop for each terrace present, and c) safe and legal access to the outcrops. Three locations fulfilling these criteria were studied during four field trips from June 2007 to April 2008. These sites were Sharm Al Arab (26°57'58"N, 33°54'40"E), Wadi Gawasis (26°33'18"N, 34°02'06"E) and Wadi Wizr (25°47'08"N, 34°29'05"E).

Point transects were used to record coral assemblages on all examined terraces. A tape measure was laid along the terrace and photographs were taken at each meter mark to record the reef building coral species (the solitary corals of family Fungiidae were not included) or sediment type present; in some cases multiple species intersected a meter mark on the line transect, and in these cases all were photographed. Seven of the eight terrace transects contain gaps in transect data due to covered, absent or inaccessible stretches of the outcrop. Although continuous line transects (in which all species that intersect a line transect are recorded) are the preferred method for reef studies due to their frequent application to both living and fossil reefs, the point transect is more time efficient; a greater area of outcrop can be covered with fewer field workers (for a full review of methods see Perrin et al. 1995).

Two Late Pleistocene terraces found at approximately 1.5 m and 4 m above mean sea level (m.s.l.) respectively were studied at Wadi Gawasis and Wadi Wizr, and one Lower Pleistocene terrace at 1.5 m m.s.l. was studied at Sharm Al Arab. The Middle Pleistocene terraces studied at Sharm Al Arab and Wadi Wizr occur at approximately 6 m m.s.l. and the Middle Pleistocene terrace at Wadi Gawasis occurs at around 12 m m.s.l. (See Figure 1 for field site and transect locations). Specimens of the most commonly occurring reef species were collected and deposited at the University of California Museum of Paleontology (coral specimen #s 557184 - 557253, other invertebrate specimen #s 557273 - 557391).

Corals were identified to the lowest taxonomic level using Ditlev (1980), Scheer and Pillai (1983), Sheppard C. R. C. and Sheppard (1991), Veron (2000) and photographic plates from Dullo (unpublished). In the case of very weathered specimens from the Middle Pleistocene terraces corals were embedded in epoxy under vacuum, and longitudinal and latitudinal thin sections were prepared from the better preserved interiors to aid in identification.

Transect data was used to calculate estimates of percent coral cover, species abundances, Shannon diversity index and Margalef diversity index. Sediment type (course, medium and fine) and outcrop orientation were used to determine the degree of hydrodynamic exposure, and coral assemblages and habitat preferences of coral species were used to define reef zones (paleodepths could not be measured directly due to outcrop erosion). Hierarchical agglomerative cluster analyses (unweighted pair-group average (UPGMA)) using a Bray-Curtis dissimilarity index (Bray and Curtis 1957) were carried out on raw species abundances, proportional species abundances and on presence absence data. These were used to assess the stability of reef assemblages across glaciations events, however the small sample size involved (n=8) makes interpretations of the results suggestive rather than definitive.

The Bray-Curtis dissimilarity index was used because it has been shown to be one of the most robust measures of distance in taxonomic data sets (Faith et al. 1987). Raw species abundance data was transformed to proportions (species counts were divided by the total count for each transect) to minimize the effect of differences in sampling between transects. The analysis

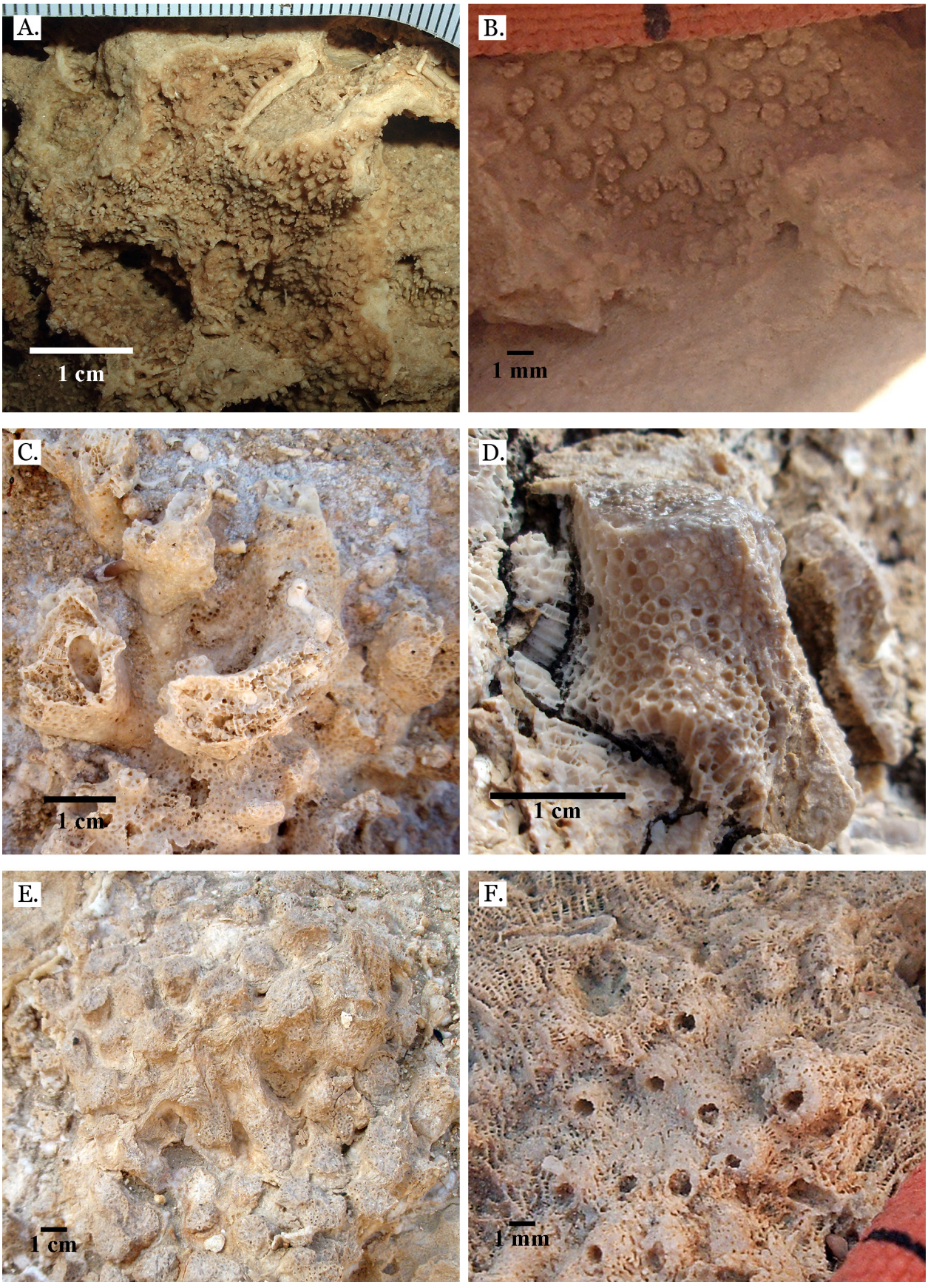
A.
1 cm
B.
1 mm
C.
1 cm
D.
1 cm
E.
1 cm
F.
1 mm

was also run on presence-absence data because the Bray-Curtis coefficient is calculated from differences in species abundances, so dominant species will have the most influence on values; transforming data to presence-absence removes this effect, and also makes results comparable to other reef studies that use presence-absence rather than abundance data. SIMPER analysis was used to identify taxa responsible for cluster differences. All statistical tests were performed in PAST, a paleontological software package for statistical analysis (Hammer et al. 2001).

Results

Taxonomy

Fifty-three species in 25 genera and 11 families were identified (Figures 2 - 18). Thirty -six of these were identified with a high degree of confidence and 9 were given tentative identifications due to poorer preservation. Six were recognizable as distinct from other taxa present, but only identifiable to the generic (6) or family (2) level. Specimen of the genera *Acropora* and *Porites* were not identified to the species level because they could not be consistently identified throughout transects, and were instead treated as single species in analyses, leading to an underestimation of true diversity.

Only two of the identified taxa have not been reported from the modern Red Sea (Table 4). *Favites micropentagona* was identified from a Middle Pleistocene terrace with high confidence; this is the first report of this species from the Red Sea. *Pavona minuta* was identified from a Late Pleistocene terrace, although it may be Holocene aged. It was also reported from the Late Pleistocene of Saudi Arabia (Dullo 1990). A species resembling *Pavona bipartita* was found on a Middle Pleistocene terrace which would also be a first report of this species from the Red Sea, however preservation is too poor to identify the specimen with confidence.

Pleistocene corals of Sharm Al Arab, Wadi Gawasis and Wadi Wizr

In the taxonomic descriptions below, rare taxa are defined as those species occurring ≤ 5 times across all examined transects.

Family ASTROCOENIDAE Koby, 1890

Genus *Stylocoeniella* Yabe & Sugiyama, 1935

Stylocoeniella guentheri (Basset-Smith, 1890)
(Figure 1A, B)

Remarks: Only preserved as a mold, but growth form and corallite structure are preserved; branching form, corallites have diameter <1 mm with 6 septa reaching the styliform columella, Calices are flush with coenosteum; identification is tentative.
Occurrence: Middle Pleistocene, Egypt (This study); extant in the Red Sea.

Figure 2. Facing Page. A, *Stylocoeniella guentheri* mold from Middle Pleistocene Wadi Wizr; B, *Stylocoeniella guentheri* mold from Middle Pleistocene Sharm Al Arab; C *Pocillopora damicornis* from Late Pleistocene Wadi Gawasis; D, *Pocillopora damicornis* from Late Pleistocene Wadi Wizr; E, *Acropora sp*. A from Late Pleistocene Wadi Wizr; F, *Acropora* sp. A from Late Pleistocene Sharm Al Arab.

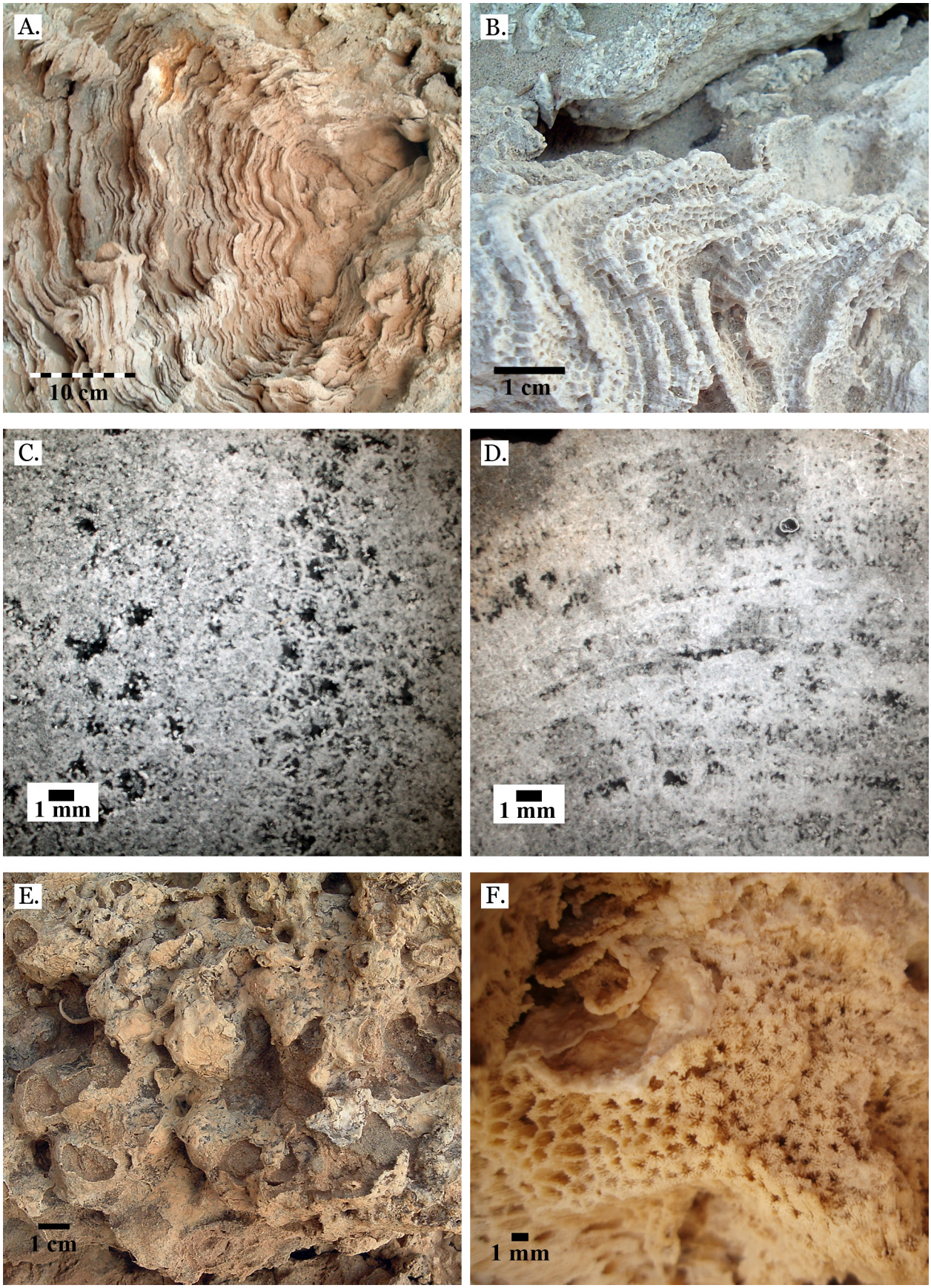
A.
10 cm
B.
1 cm
C.
1 mm
D.
1 mm
E.
1 cm
F.
1 mm

Family POCILLOPORIDAE Gray, 1842

Genus *Pocillopora* Lamarck, 1816

Pocillopora damicornis (Linneaus, 1758)
(Figure 1C,D)

Remarks: Third most common taxon in this study.
Occurrence: Middle Pleistocene of Egypt (this study) and Sinai (El-Sorogy 1997); Late Pleistocene of Egypt (this study), Sinai (El-Sorogy 1997), and Saudi Arabia (Dullo 1990), extant in the Red Sea.

Family ACROPORIDAE Verrill, 1902

Genus *Acropora* Oken, 1815

Acropora sp. A
(Figure 1E,F)

Remarks: Not enough detail is preserved to identify to the species level with confidence.
Occurrence: Middle and Late Pleistocene of Egypt (this study).

Family PORITIDAE Gray, 1842

Genus *Porites* Link, 1807

Porites spp.
(Figures 2A-F, 3A-F)

Remarks: 47% of all individual transect points identified in this study are *Porites,* making it the most abundant genus by a large margin. Given the difficulties inherent in the taxonomy of the group and the inconsistent preservation within and between terraces, identifications were not made to the species level. However, based on gross morphologies and a few well preserved corallum, *P. columnaris*, *P. nodifera* and *P. solida* are likely well represented.
Occurrence: Middle and Late Pleistocene of Egypt (this study).

Genus *Goniopora* de Blainville, 1830

Goniopora sp. A
(Figure 4A,B)

Remarks: Only common on Middle Pleistocene terrace of Wadi Gawasis; large (>1 meter) colonies, columnar growth, with corallite diameters ~2-3mm. Not enough information preserved for

Figure 3. A, Massive *Porites* sp. from Middle Pleistocene Wadi Gawasis; B, Close up of massive *Porites* sp. from Middle Pleistocene Sharm Al Arab; C, Latitudinal thin section of *Porites* sp. from Middle Pleistocene; D, Longitudinal thin section of *Porites* sp. from Middle Pleistocene; E, Robust branching *Porites* sp. from Middle Pleistocene Wadi Gawasis; F. *Porites* sp. from Middle Pleistocene Wadi Wizr.

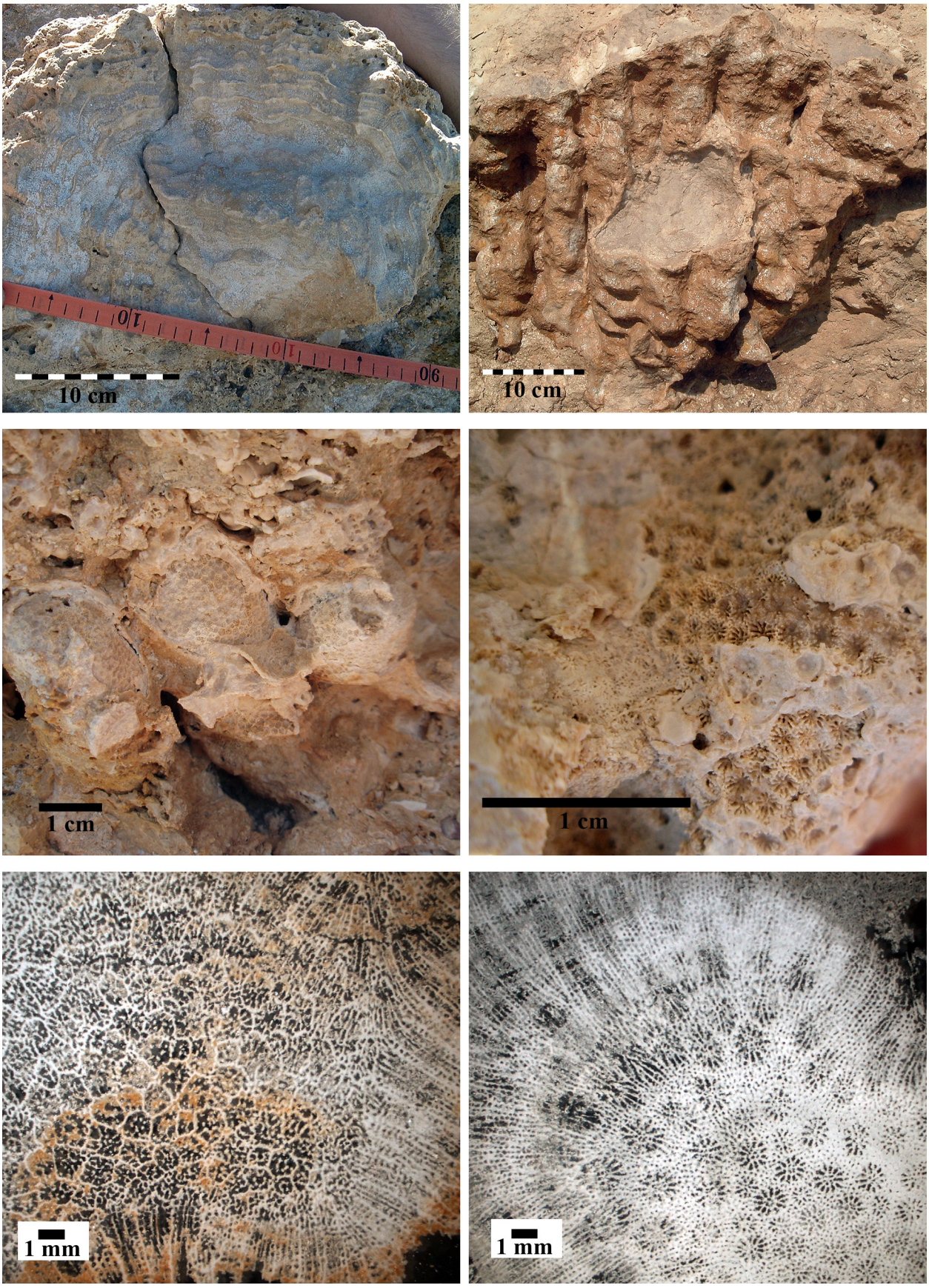
10 cm
10 cm
1 cm
1 cm
1 mm
1 mm

confident identification to species level, however most likely *G. savignyi*.
Occurrence: Middle Pleistocene of Egypt (this study).

Family SIDERASTREIDAE Vaughan & Wells, 1943

Genus *Siderastrea* Vaughan & Wells, 1943

Siderastrea savignyana (Milne Edwards & Haime, 1850)
(Figure 4C)

Remarks: Rare in this study; polygonal corallites 2-4 mm in diameter with septa forming an acute ridge on walls; identification is tentative.
Occurrence: Middle Pleistocene of Egypt (this study); Late Pleistocene of Egypt (this study), Sinai (El Sorogy 1997) and Saudi Arabia (Dullo 1990); extant in the Red Sea.

Family AGARICIIDAE Gray, 1842

Genus *Pavona* Lamarck, 1801

Pavona cactus (Forskal, 1775)
(Figure 4D, E)

Remarks: Rare in this study; distinctive.
Occurrence: Late Pleistocene of Egypt (this study) and Saudi Arabia (Dullo 1990); extant in the Red Sea.

Pavona decussata (Dana, 1846)
(Figure 4F)

Remarks: Rare in this study; distinctive.
Occurrence: Middle Pleistocene of Egypt (this study) and Sinai (El Sorogy 1997); extant in the Red Sea.

Pavona minuta (Wells, 1956)
(Figure 5A)

Remarks: Rare in this study; encrusting growth form with small, shallow corallites. Excellent preservation of sole specimen suggests it may be a Holocene aged overgrowth on the Late Pleistocene terrace.
Occurrence: Late Pleistocene or Holocene of Egypt (this study) and Late Pleistocene of Saudi Arabia (Dullo 1990); not reported from the modern Red Sea.

Figure 4. Facing page. A, Massive *Porites* sp. from Late Pleistocene Wadi Gawasis; B, Robust branching *Porites* sp. from Late Pleistocene Wadi Wizr; C, Branches of *Porites* sp. from Late Pleistocene Wadi Wizr; D, *Porites* sp. from Late Pleistocene Sharm Al Arab; E, Thin section of *Porites* sp. from Late Pleistocene; F, Thin section of *Porites* sp. from Late Pleistocene.

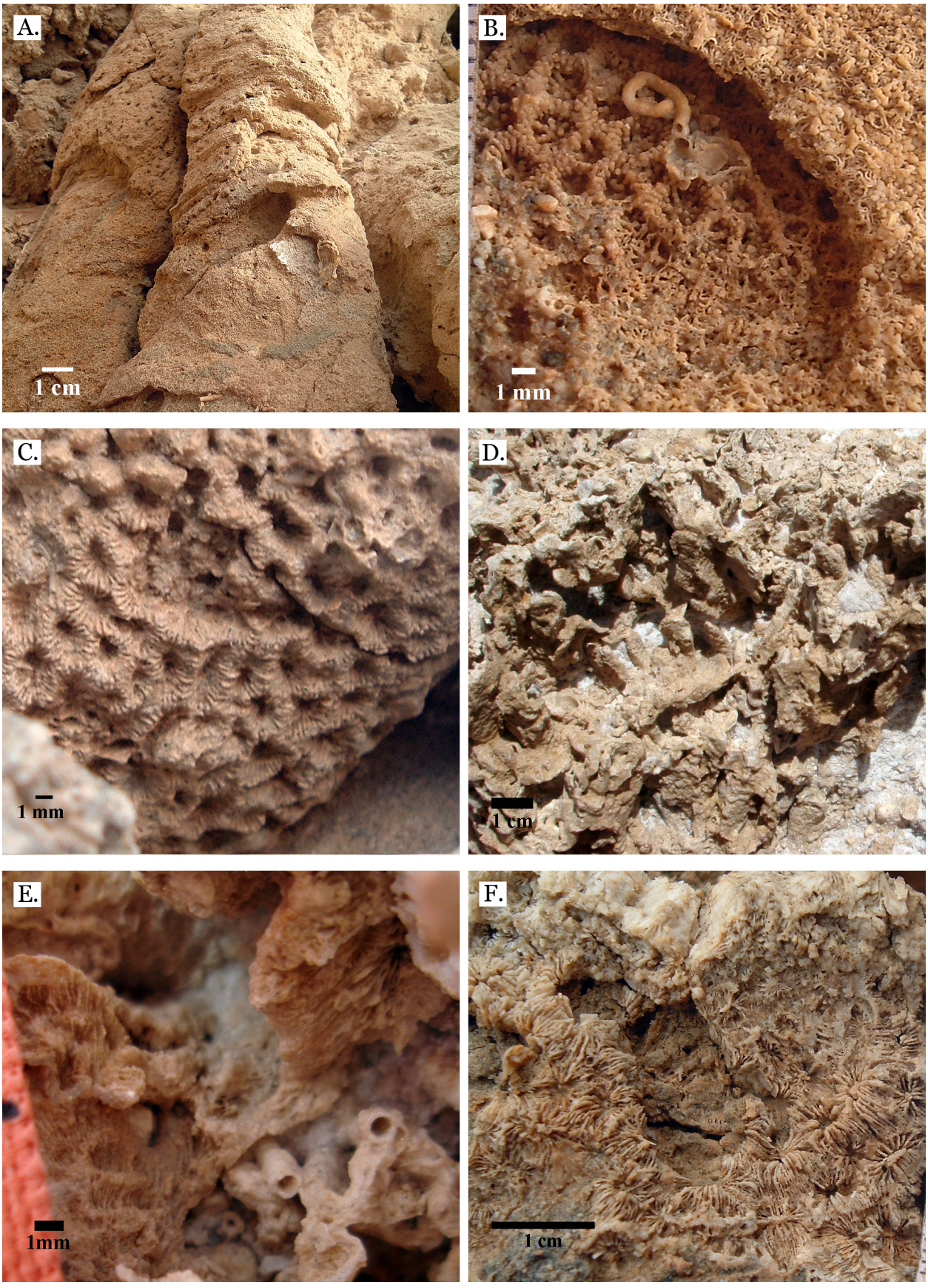
A.
1 cm
B.
1 mm
C.
1 mm
D.
1 cm
E.
1mm
F.
1 cm

Pavona c.f. *bipartita* (Nemenzo, 1980)
(Figure 5B)

Remarks: Rare in this study and very poorly preserved; identification is tentative.
Occurrence: Middle Pleistocene of Egypt (this study); not reported from the modern Red Sea.

Pavona venosa (Ehrenberg, 1834)
(Figure 5C)

Remarks: Rare in this study; distinctive.
Occurrence: Late Pleistocene of Egypt (this study); extant in the Red Sea.

Pavona maldivensis (Gardiner, 1905)
(Figure 5D)

Remarks: Rare in this study; Platy growth form.
Occurrence: Late Pleistocene of Egypt (this study); extant in the Red Sea.

Pavona frondifera (Lamark, 1816)
(Figure 5E,F)

Remarks: Rare in this study; distinctive.
Occurrence: Late Pleistocene of Egypt (this study); extant in the Red Sea.

Pavona sp. A
(Figure 6A,B)

Remarks: Rare in this study; only preserved as a mold, but recognizable as *Pavona* from the distinctive thamnasteroid form with star-like septo-costae pattern.
Occurrence: Middle Pleistocene of Egypt (this study).

Genus *Gardineroseris* Scheer & Pillai, 1974

Gardineroseris planulata (Dana, 1846)
(Figure 6C)

Remarks: Rare in this study and poorly preserved; many fine septo-costae, corallites separated by acute walls.
Occurrence: Middle Pleistocene of Egypt (this study); Late Pleistocene of Saudi Arabia (Dullo 1990); extant in the Red Sea.

Family OCULINIDAE Gray, 1847

Figure 5. Facing page. A, *Goniopora* sp. A from Middle Pleistocene Wadi Gawasis; B, *Goniopora* sp. A from Middle Pleistocene Wadi Gawasis; C, *Siderastrea savignyana* from Middle Pleistocene Wadi Gawasis; D, *Pavona cactus* from Late Pleistocene Sharm Al Arab; E, *Pavona cactus* from Late Pleistocene Sharm Al Arab; F, *Pavona decussata* from Middle Pleistocene Wadi Gawasis.

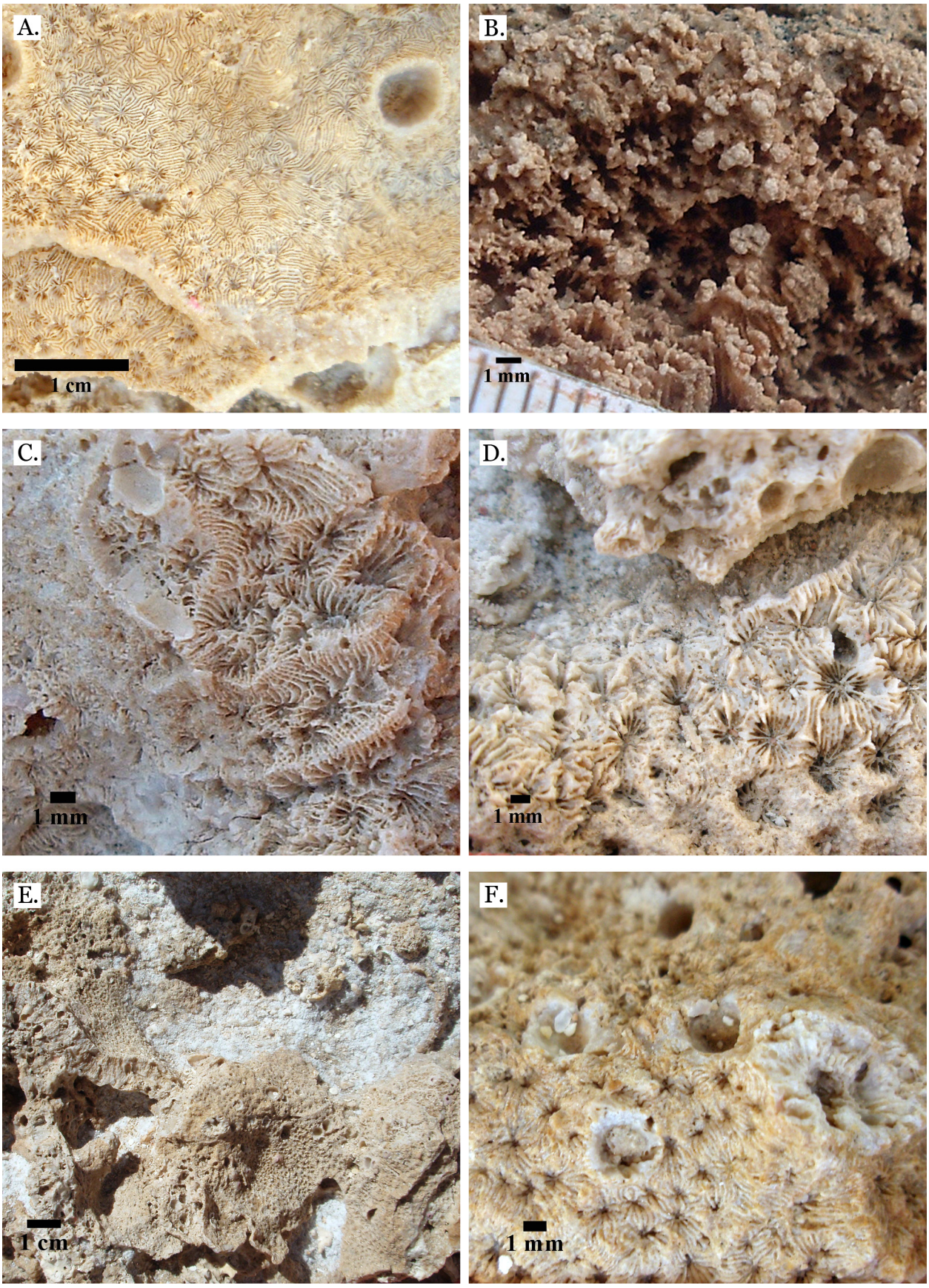
A.
1 cm
B.
1 mm
C.
1 mm
D.
1 mm
E.
1 cm
F.
1 mm

Genus *Galaxea* Oken, 1815

Galaxea fascicularis (Linnaeus, 1767)
(Figure 6D-F)

Remarks: Distinctive, and the second most common taxon in this study.
Occurrence: Middle Pleistocene of Egypt (this study) and Sinai (El Sorogy 1997); Late Pleistocene of Egypt (this study), Sinai (El Sorogy 1997), Saudi Arabia (Dullo 1990) and Eritrea (Bruggemann et al. 2004); extant in the Red Sea.

Galaxea astreata (Lamarck, 1816)
(Figure 7A)

Remarks: Rare in this study; similar to *G. fascicularis* but with widely spaced corallites 2-3 mm in diameter.
Occurrence: Late Pleistocene of Egypt (this study) and Saudi Arabia (Dullo 1990); extant in the Red Sea.

Family MUSSIDAE Ortmann, 1890

Genus *Acanthastrea* Edwards & Haime, 1848

Acanthastrea echinata (Dana, 1846)
(Figure 7B,C)

Remarks: Rare in this study; rounded corallites with thick walls and spiny septa.
Occurrence: Late Pleistocene of Egypt (this study) and Saudi Arabia (Dullo 1990); extant in the Red Sea.

Acanthastrea rotundoflora
(Figure 7D)

Remarks: Rare in this study; corallite walls are very thick.
Occurrence: Late Pleistocene of Egypt (this study); extant in the Red Sea.

Genus *Lobophyllia* Blainville, 1830

Lobophyllia hemprichii (Ehrenberg, 1834)
(Figure 7E,F)

Remarks: Phaceloid, septa thicker at walls and tapering toward columella.
Occurrence: Late Pleistocene of Egypt (this study) and Saudi Arabia (Dullo 1990); extant in the Red Sea.

Figure 6. Facing page. A, *Pavona minuta* from Wadi Wizr, Late Pleistocene or Holocene; B, *Pavona* c.f. *bipartita* from Middle Pleistocene Wadi Gawasis; C, *Pavona venosa* from Late Pleistocene Sharm Al Arab; D, *Pavona maldivensis* from Late Pleistocene Sharm Al Arab; E, *Pavona frondifera* from Late Pleistocene Wadi Gawasis; F, *Pavona frondifera* from Late Pleistocene Wadi Gawasis.

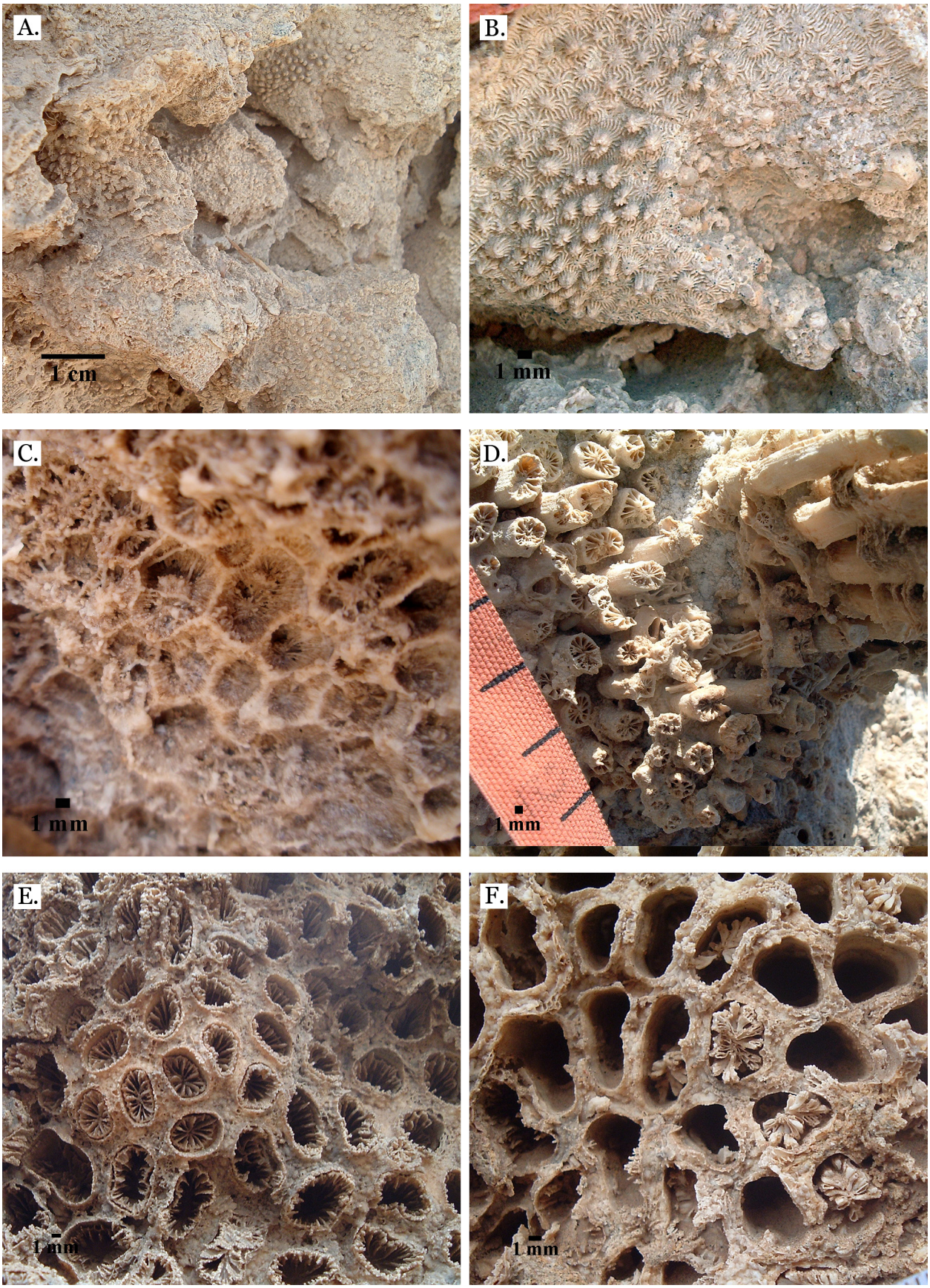
A.
1 cm
B.
1 mm
C.
1 mm
D.
1 mm
E.
1 mm
F.
1 mm

Family MERULINIDAE Verrill, 1866

Genus *Hydnophora* Fischer de Waldheim, 1807

Hydnophora microconus (Lamarck 1816)
(Figure 8A)

Remarks: Distinctive.
Occurrence: Late Pleistocene of Egypt (this study), Sinai (El Sorogy 1997), Saudi Arabia (Dullo 1990) and Eritrea (Bruggemann et al. 2004); extant in the Red Sea.

Family FAVIIDAE Gregory, 1900

Genus *Caulastrea* Dana 1846

Caulastrea tumida Matthai, 1928
(Figure 8B)

Remarks: Rare in this study; phaceloid, short corallites 12-15 mm in diameter.
Occurrence: Late Pleistocene of Egypt (this study); extant in the Red Sea.

Genus *Erythrastrea* Scheer & Pillai, 1983

Erythrastrea flabellata Scheer & Pillai, 1983
(Figure 8C,D)

Remarks: Rare in this study; flabello-meandroid, valleys ~ 10 mm across with trabecular columella.
Occurrence: Late Pleistocene of Egypt (this study); extant in the Red Sea.

Genus *Favia* Oken, 1815

Favia stelligera (Dana, 1846)
(Figures 8E-F, 9A-D)

Remarks: Columnar growth form, corallites ~2 mm in diameter; frequently occurs in stands several meters across. On Middle Pleistocene terraces can be very poorly preserved and identifiable only by thin section.
Occurrence: Middle Pleistocene of Egypt (this study); Late Pleistocene of Egypt (this study), Sinai (El Sorogy 1997) and Saudi Arabia (Dullo 1990); extant in the Red Sea.

Figure 7. Facing page. A, *Pavona* sp. A mold from Middle Pleistocene Sharm Al Arab; B, *Pavona* sp. A mold from Middle Pleistocene Sharm Al Arab; C, *Gardineroseris planulata* from Middle Pleistocene Wadi Wizr; D, *Galaxea fascicularis* from Late Pleistocene Sharm Al Arab; E, *Galaxea fascicularis* from Middle Pleistocene Wadi Gawasis; F, Very poorly preserved *Galaxea fascicularis* from Middle Pleistocene Wadi Gawasis.

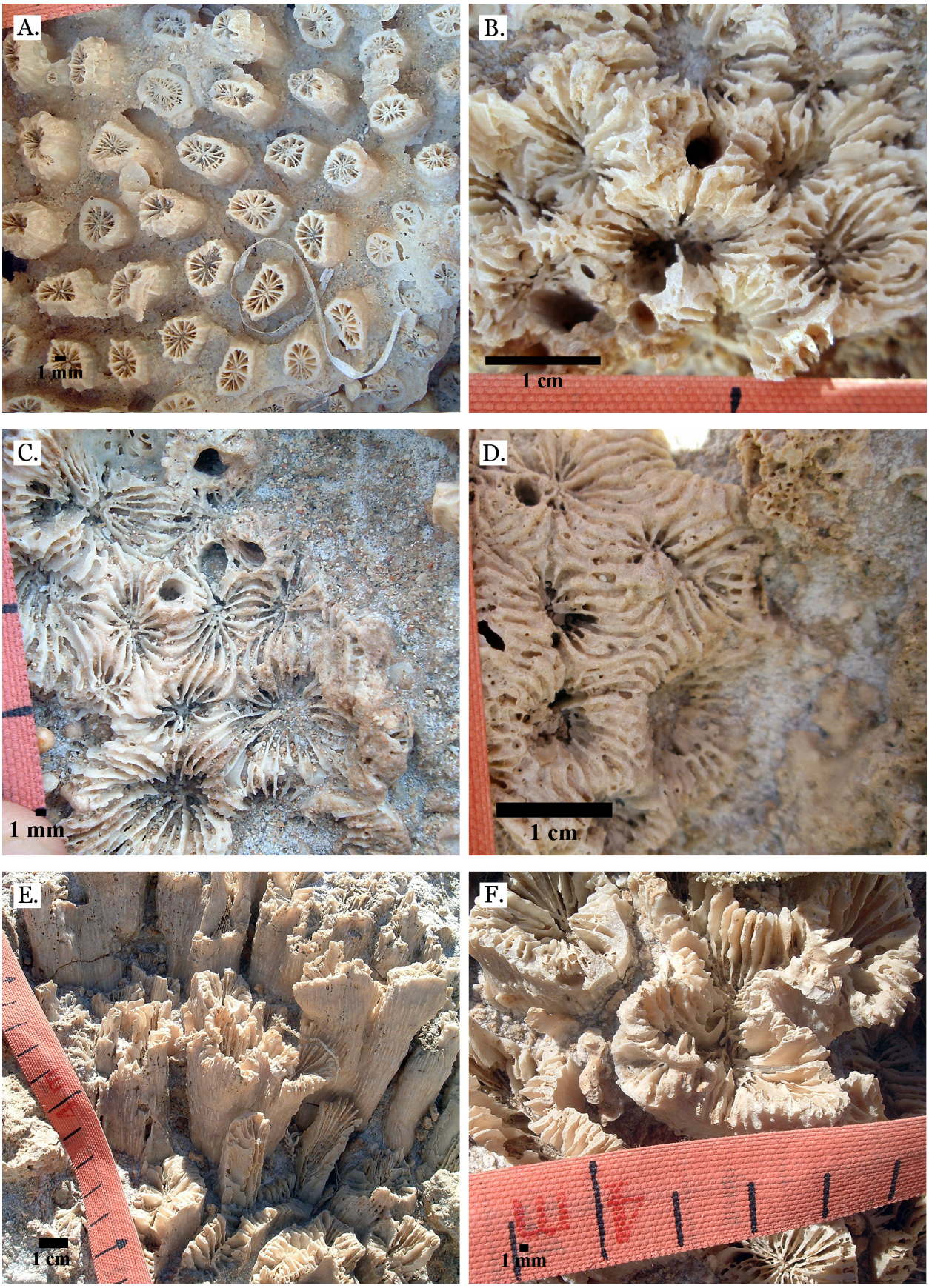
A.
1 mm
B.
1 cm
C.
1 mm
D.
1 cm
E.
1 cm
F.
1 mm

Favia pallida (Dana, 1846)
(Figures 9E-F, 10A-B)

Remarks: Massive growth form, rounded corallites.
Occurrence: Middle Pleistocene of Egypt (this study) and Sinai (El Sorogy 1997); Late Pleistocene of Egypt (this study), Sinai (El Sorogy 1997) and Saudi Arabia (Dullo 1990); extant in the Red Sea.

Favia speciosa Dana, 1846
(Figure 10C,D)

Remarks: Massive growth form, corallites are rounded to irregularly shaped and are sometimes very closely packed, sometimes more widely spaced.
Occurrence: Middle Pleistocene of Egypt (this study) and Sinai (El Sorogy 1997); Late Pleistocene of Egypt (this study), Sinai (El Sorogy 1997), Saudi Arabia (Dullo 1990) and Jordan (Al-Rifaiy and Cherif 1988); extant in the Red Sea.

Favia favus (Forskal, 1775)
(Figure 10E)

Remarks: Rare species in this study; massive growth form, corallites 10-15 mm in diameter with widely spaced septa; identification is tentative.
Occurrence: Late Pleistocene of Egypt (this study) and Saudi Arabia (Dullo 1990); extant in the Red Sea.

Favia matthai Vaughan, 1918
(Figure 10F)

Remarks: Rare in this study; massive growth form, closely packed corallites 10-14 mm in diameter with thick septa.
Occurrence: Late Pleistocene of Egypt (this study); extant in the Red Sea.

Favia sp. A
(Figure 11A,B)

Remarks: Only preserved as a single mold; plocoid with ~5 mm corallite diameter and spiny septo-costae. Not enough information preserved for confident identification to species level.
Occurrence: Middle Pleistocene of Egypt (this study).

Genus *Favites* Link, 1807

Favites pentagona (Esper, 1794)
(Figure 11C,D)

Figure 8. Facing page. A, *Galaxea astreata* from Late Pleistocene Wadi Gawasis; B, *Acanthastrea echinata* from Late Pleistocene Wadi Gawasis; C, *Acanthastrea echinata* from Late Pleistocene Wadi Gawasis; D, *Acanthastrea rotundoflora* from Late Pleistocene Wadi Gawasis; E, *Lobophyllia hemprichii* from Late Pleistocene Wadi Gawasis; F, *Lobophyllia hemprichii* from Late Pleistocene Wadi Gawasis.

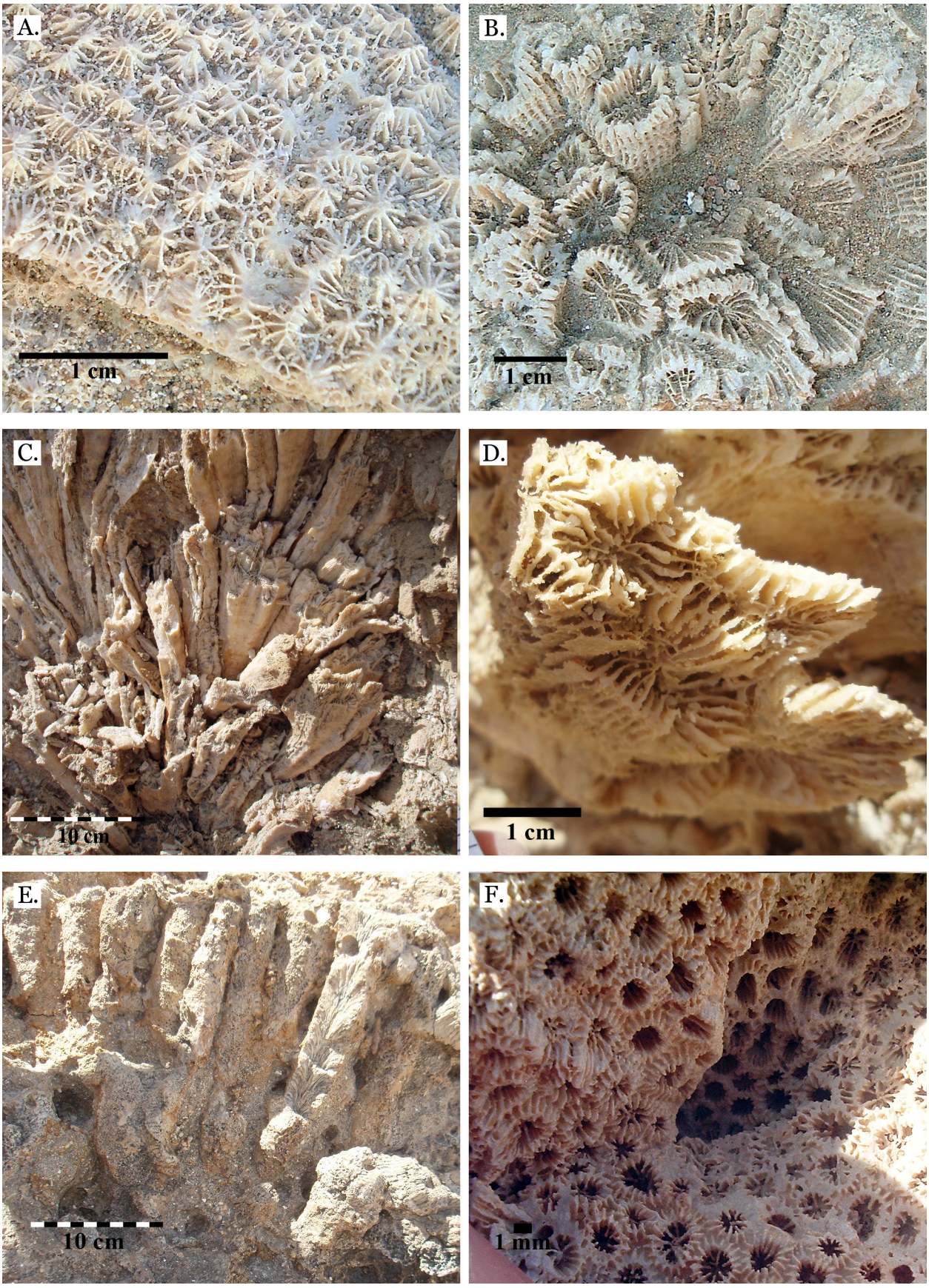
A.
1 cm
B.
1 cm
C.
10 cm
D.
1 cm
E.
10 cm
F.
1 mm

Remarks: Ceroid, mostly pentagonal corallites 5-8 mm in diameter.
Occurrence: Middle Pleistocene of Sinai (El Sorogy 1997); Late Pleistocene of Egypt (this study), Sinai (El Sorogy 1997), Saudi Arabia (Dullo 1990) and Eritrea (Bruggemann et al. 2004).

Favites abdita (Ellis & Solander, 1786)
(Figure 11E)

Remarks: Rare in this study.
Occurrence: Late Pleistocene of Egypt (this study), Saudi Arabia (Dullo 1990) and Jordan (Al Rifaiy 1988); extant in the Red Sea.

Favites paraflexuosa Veron, 2000
(Figure 11F)

Remarks: Identification is tentative.
Occurrence: Late Pleistocene of Egypt (this study); extant in the Red Sea.

Favites flexuosa (Dana 1846)
(Figure 12A)

Remarks: Rare in this study.
Occurrence: Late Pleistocene of Egypt (this study) and Saudi Arabia (Dullo 1990); extant in the Red Sea.

Favites vasta (Klunzinger, 1879)
(Figure 12B)

Remarks: Identification is tentative.
Occurrence: Late Pleistocene of Egypt (this study); extant in the Red Sea.

Favites micropentagona (Veron, 2000)
(Figures 12C-F, 13A-B)

Remarks: Massive growth form, pentagonal corallites 3-4 mm in diameter.
Occurrence: Late Pleistocene of Egypt (this study); not reported from the modern Red Sea.

Favites sp. A
(Figure 13C,D)

Remarks: Only preserved as a single mold; massive growth form, ceroid corallites 6-10 mm in diameter with many fine septa, not enough information preserved to identify to the species level.
Occurrence: Middle Pleistocene of Egypt (this study).

Figure 9. Facing page. A, *Hydnophora microconus* from Late Pleistocene Wadi Gawasis; B, *Caulastrea tumida* from Late Pleistocene Sharm Al Arab; C, *Erythrastrea flabellata* from Late Pleistocene Wadi Wizr; D, *Erythrastrea flabellata* from Late Pleistocene Wadi Wizr; E, *Favia stelligera* from Late Pleistocene Wadi Gawasis; F, *Favia stelligera* from Late Pleistocene Sharm Al Arab.

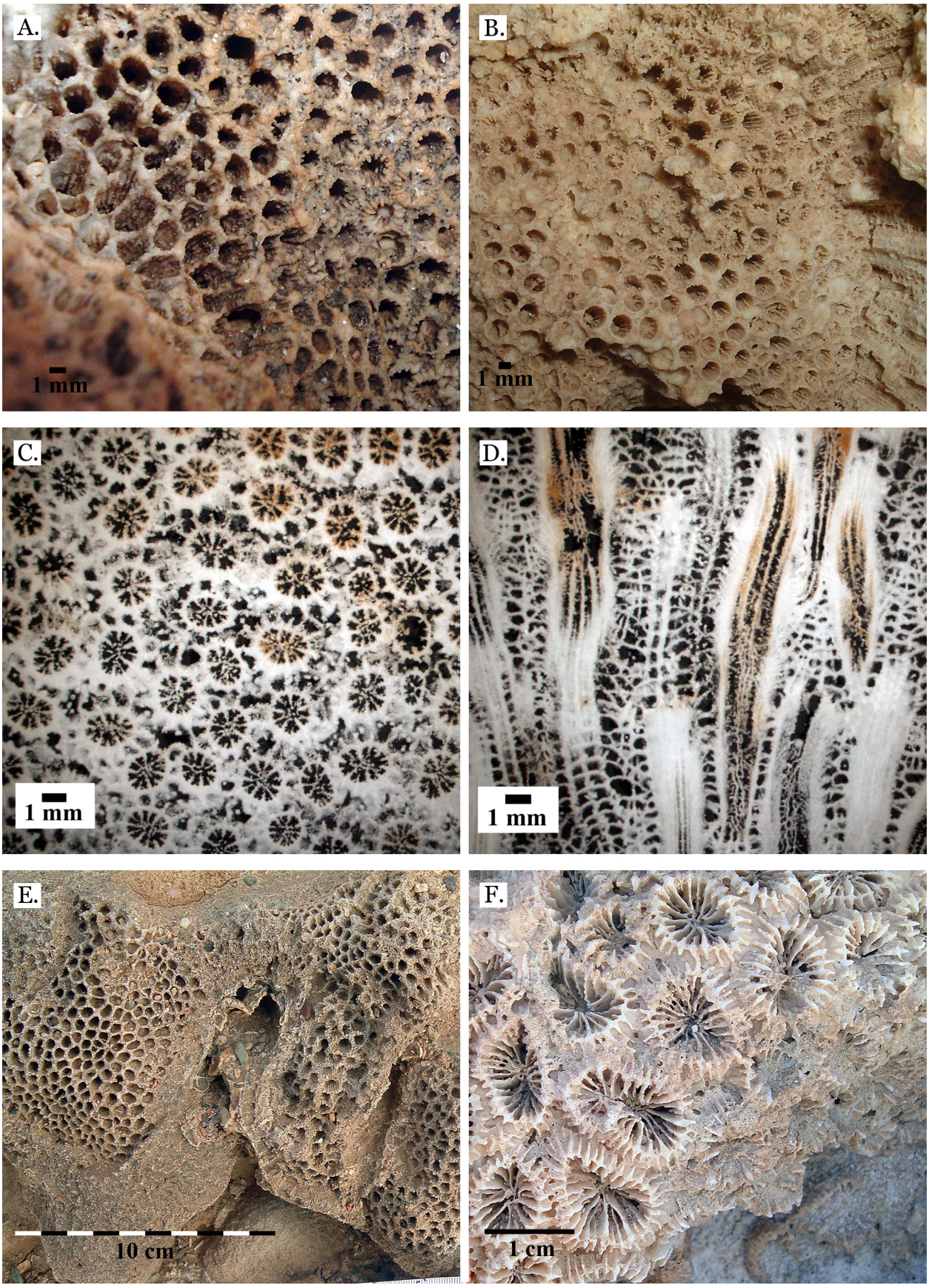
A.
1 mm
B.
1 mm
C.
1 mm
D.
1 mm
E.
10 cm
F.
1 cm

Genus *Goniastrea* Edwards & Haime, 1848

Goniastrea retiformis (Lamarck, 1816)
(Figure 13E)

Remarks: Rare in this study and poorly preserved; recognizable by polygonal corallites, ~4 mm across with acute walls; identification is tentative.
Occurrence: Middle Pleistocene of Egypt (this study); Late Pleistocene of Saudi Arabia (Dullo 1990) and Eritrea (Bruggemann et al. 2004); extant in the Red Sea.

Goniastrea pectinata (Ehrenberg, 1834)
(Figure 13F)

Remarks: Has well-developed paliform lobes; identification is tentative.
Occurrence: Late Pleistocene of Egypt (this study), Saudi Arabia (Dullo 1990) and Eritrea (Bruggemann et al. 2004); extant in the Red Sea.

Goniastrea sp. A
(Figure 14A)

Remarks: Rare in this study; ceroid, corallites 4-6 mm in diameter with very thick walls and thin septa; not enough information present to identify to the species level.
Occurrence: Middle Pleistocene of Egypt (this study).

Genus *Platygyra* Ehrenberg, 1834

Platygyra daedalea (Ellis & Solander, 1786)
(Figure 14B)

Remarks: Massive growth form, meandroid, valleys long and sinuous and 5-7 mm wide, columella is trabecular and continuous.
Occurrence: Late Pleistocene of Egypt (this study), Saudi Arabia (Dullo 1990) and Jordan (Al-Rifaiy and Cherif 1988); extant in the Red Sea.

Platygyra lamellina (Ehrenberg, 1834)
(Figure 14C)

Remarks: Rare in this study; massive growth form, meandroid, valleys ~ 3 mm wide with very thick walls and well developed columella.
Occurrence: Late Pleistocene of Egypt (this study) and Eritrea (Bruggemann et al. 2004); extant in the Red Sea.

Figure 10. Facing page. A, *Favia stelligera* from Middle Pleistocene Wadi Wizr; B, Very poorly preserved *Favia stelligera* from Middle Pleistocene Wadi Wizr; C, Latitudinal thin section of *Favia stelligera* from Middle Pleistocene; D, Longitudinal thin section of *Favia stelligera* from Middle Pleistocene; E, *Favia pallida* from Middle Pleistocene Wadi Gawasis; F, *Favia pallida* from Late Pleistocene Sharm Al Arab.

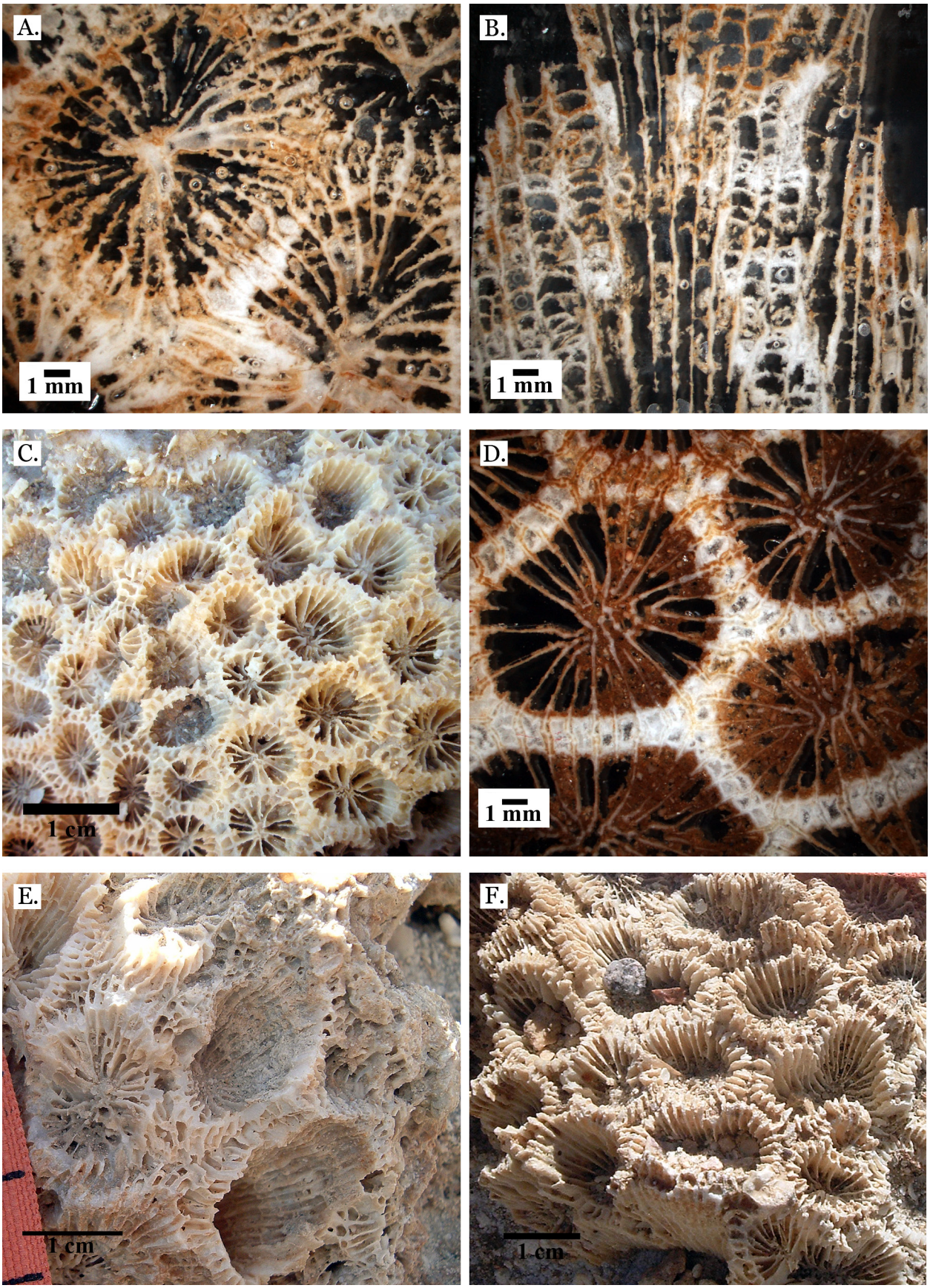
A.
1 mm
B.
1 mm
C.
1 cm
D.
1 mm
E.
1 cm
F.
1 cm

Platygyra sinensis (Edwards & Haime, 1849)
(Figure 14D)

Remarks: Rare in this study; massive growth form, meandroid, short valleys 2-3 mm wide with thin walls and septa.
Occurrence: Middle and Late Pleistocene of Egypt (this study); extant in the Red Sea.

Platygyra acuta Veron 2000
(Figure 14E)

Remarks: Massive growth form, sub-meandroid, short valleys ~5 mm wide, thick walls with acute edge and trabecular columella.
Occurrence: Late Pleistocene of Egypt (this study); extant in the Red Sea.

Genus *Leptoria* Edwards & Haime, 1848

Leptoria phrygia Ellis & Solander, 1786
(Figure 14F)

Remarks: Massive growth form, meandroid, long valleys ~ 3 mm wide, lamellar columella with evenly spaced septa.
Occurrence: Middle Pleistocene of Egypt (this study) and Sinai (El Sorogy 1997); Late Pleistocene of Egypt (this study), Sinai (El Sorogy 1997), and Saudi Arabia (Dullo 1990); extant in the Red Sea.

Genus *Montastrea* Blainville, 1830

Montastrea curta (Dana, 1846)
(Figure 15A-D)

Remarks: Very poorly preserved; flat to spherical growth form, corallite diameter 4-8 mm; identifiable from thin section.
Occurrence: Middle Pleistocene of Egypt (this study); extant in the Red Sea.

Genus *Leptastrea* Edwards & Haime, 1848

Leptastrea pruinosa Crossland, 1952
(Figure 15E)

Remarks: Rare in this study; angular corallites.
Occurrence: Late Pleistocene of Egypt (this study); extant in the Red Sea.

Figure 11. Facing page. A, Latitudinal thin section of *Favia pallida* from Middle Pleistocene; B, Longitudinal thin section of *Favia pallida* from Middle Pleistocene; C, *Favia speciosa* from Late Pleistocene Wadi Gawasis; D, Latitudinal thin section of *Favia speciosa* Middle Pleistocene; E, *Favia favus* from Late Pleistocene Sharm Al Arab; F, *Favia matthai* from Late Pleistocene Wadi Gawasis.

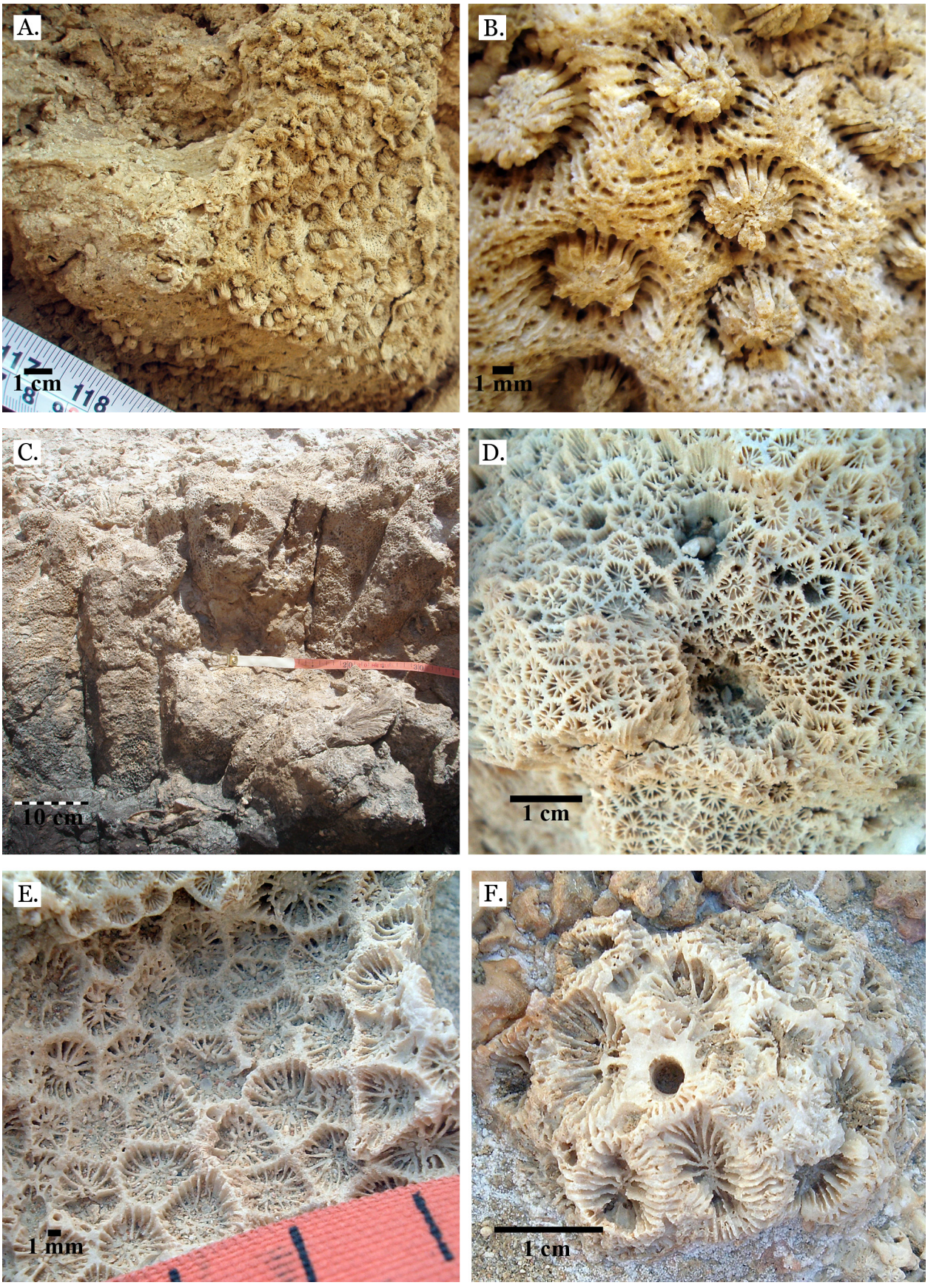
A.
1 cm
B.
1 mm
C.
10 cm
D.
1 cm
E.
1 mm
F.
1 cm

Leptastrea bottae (Milne Edwards & Haime, 1849)
(Figure 15F)

Remarks: Round, closely packed projecting corallites ~ 3 mm in diameter, distinctive groove and tubercle structure.
Occurrence: Middle Pleistocene of Egypt (this study); Late Pleistocene of Egypt (this study), Eritrea (Bruggemann et al. 2004) and Jordan (Al-Rifaiy and Cherif 1988); extant in the Red Sea.

Genus Cyphastrea Edwards & Haime, 1848

Cyphastrea microphthalma (Lamarck, 1816)
(Figure 16A)

Remarks: Corallites 1-2 mm in diameter with spiny coenosteum
Occurrence: Middle Pleistocene of Egypt (this study); Late Pleistocene of Egypt (this study), Sinai (El Sorogy 1997) and Saudi Arabia (Dullo 1990); extant in the Red Sea.

Genus *Echinopora* Lamarck, 1816

Echinopora lamellosa Esper, 1795
(Figure 16B-E)

Remarks: Foliaceous growth form, corallites 2-3 mm in diameter, beaded septo-costae.
Occurrence: Middle Pleistocene of Egypt (this study); Late Pleistocene of Egypt (this study), Saudi Arabia (Dullo 1990) and Jordan (Al-Rifaiy and Cherif 1988); extant in the Red Sea.

Echinopora gemmacea Lamarck, 1816
(Figure 16F)

Remarks: Projecting corallites 3-4 mm in diameter, beaded septo-costae.
Occurrence: Late Pleistocene of Egypt (this study), Saudi Arabia (Dullo 1990) and Eritrea (Bruggemann et al. 2004); extant in the Red Sea.

UNKNOWN Faviid sp.
(Figure 17A)

Remarks: Preserved as a highly weathered mold, assigned to Faviidae based on resemblance to other Faviid molds observed on terraces, but not enough information preserved to identify below family level.
Occurrence: Middle Pleistocene of Egypt (this study).

Figure 12. Facing Page. A, Favia sp. A mold from Middle Pleistocene Wadi Wizr; B, *Favia* sp. A mold from Middle Pleistocene Wadi Wizr; C, *Favites pentagona* from Late Pleistocene Sharm Al Arab; D, *Favites pentagona* from Late Pleistocene Wadi Wizr; E, *Favites abdita* from Late Pleistocene Sharm Al Arab; F, *Favites paraflexuosa* from Late Pleistocene Wadi Gawasis.

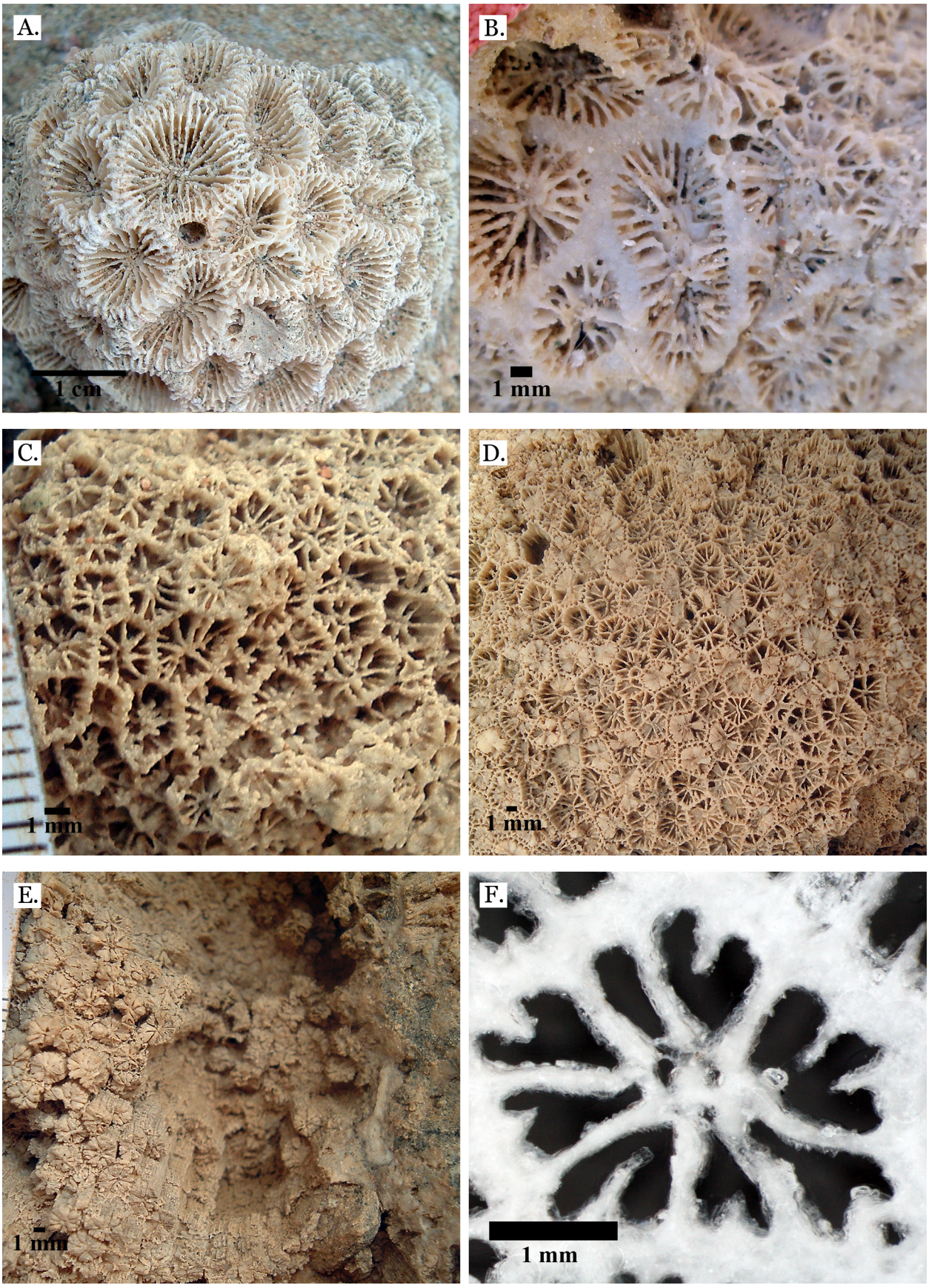
A.
1 cm
B.
1 mm
C.
1 mm
D.
1 mm
E.
1 mm
F.
1 mm

Family CARYOPHYLLIDAE Gray 1847

Genus *Gyrosmilia* Edwards & Haime, 1851

Gyrosmilia interrupta (Ehrenberg, 1834)
(Figure 17B,C)

Remarks: Rare in this study; highly exsert septa that form a thin ridge along the top of walls, steep valleys. In very weathered specimen the thin ridge is still visible along walls.
Occurrence: Middle and Late Pleistocene of Egypt (this study); extant in the Red Sea.

Diversity

The eight studied terraces represent 3 upper reef slopes, 2 shallow patch reef environments, and 3 shallow reef environments of indeterminate zone (Table 1). The highest diversity was found on the reef slope terraces in the most exposed environments (Wadi Al Arab Late Pleistocene and Wadi Gawasis Late Pleistocene lower terraces) and the lowest diversity found on the shallow patch reef terraces (Sharm Al Arab Middle Pleistocene and Wadi Wizr Middle Pleistocene terraces). Just three families, Faviidae, Poritidae and Oculinidae accounted for 90% of all transect point corals, and 60% of all species belonged to the family Faviidae. A detailed account of terrace diversity including dominant taxa per 10 meter segment is summarized in Figures 19 through 24. Species abundances for each terrace are presented in Table 2.

The most robust terrace clusters (i.e. occurring in all three analyses) comprise terraces of the same reef zone and degree of exposure, while only the presence-absence dendogram shows clustering by time period (Figure 25). However these "time clusters" are most likely related to differences in environment because all three Middle Pleistocene terraces represent sheltered environments, and the 5 Late Pleistocene terraces represent exposed or only partly sheltered environments. Distance between clusters in raw species abundances and proportional species abundances is driven by *Porites* spp. and *Galaxea fascicularis,* the two most frequently occurring taxa.

Discussion

The small number of terraces examined in this study (n=8) and the variability in reef environments they represent are inappropriate for an exhaustive quantitative comparison between Middle and Late Pleistocene coral assemblages of the Red Sea. However, the results of cluster analysis in combination with a qualitative review of transect data suggest that the differences in coral assemblages are a result of local environments rather than significant change or turn-over between the Middle and Late Pleistocene reefs. The coral taxa identified from the Middle and Late Pleistocene show no significant differences from each other or the taxa of the modern Red Sea, and clusters found using raw and proportional abundance as well as presence-absence data consistently reflect shared environment more than shared time period (Figure 25).

Figure 13. Facing page. A, *Favites flexuosa* from Late Pleistocene Wadi Gawasis; B, *Favites vasta* from Late Pleistocene Wadi Gawasis; C, *Favites micropentagona* from Middle Pleistocene Wadi Gawasis; D, *Favites micropentagona* from Middle Pleistocene Wadi Gawasis; E, *Favites micropentagona* mold from Middle Pleistocene Wadi Gawasis; F, Latitudinal thin section of *Favites micropentagona* from Middle Pleistocene.

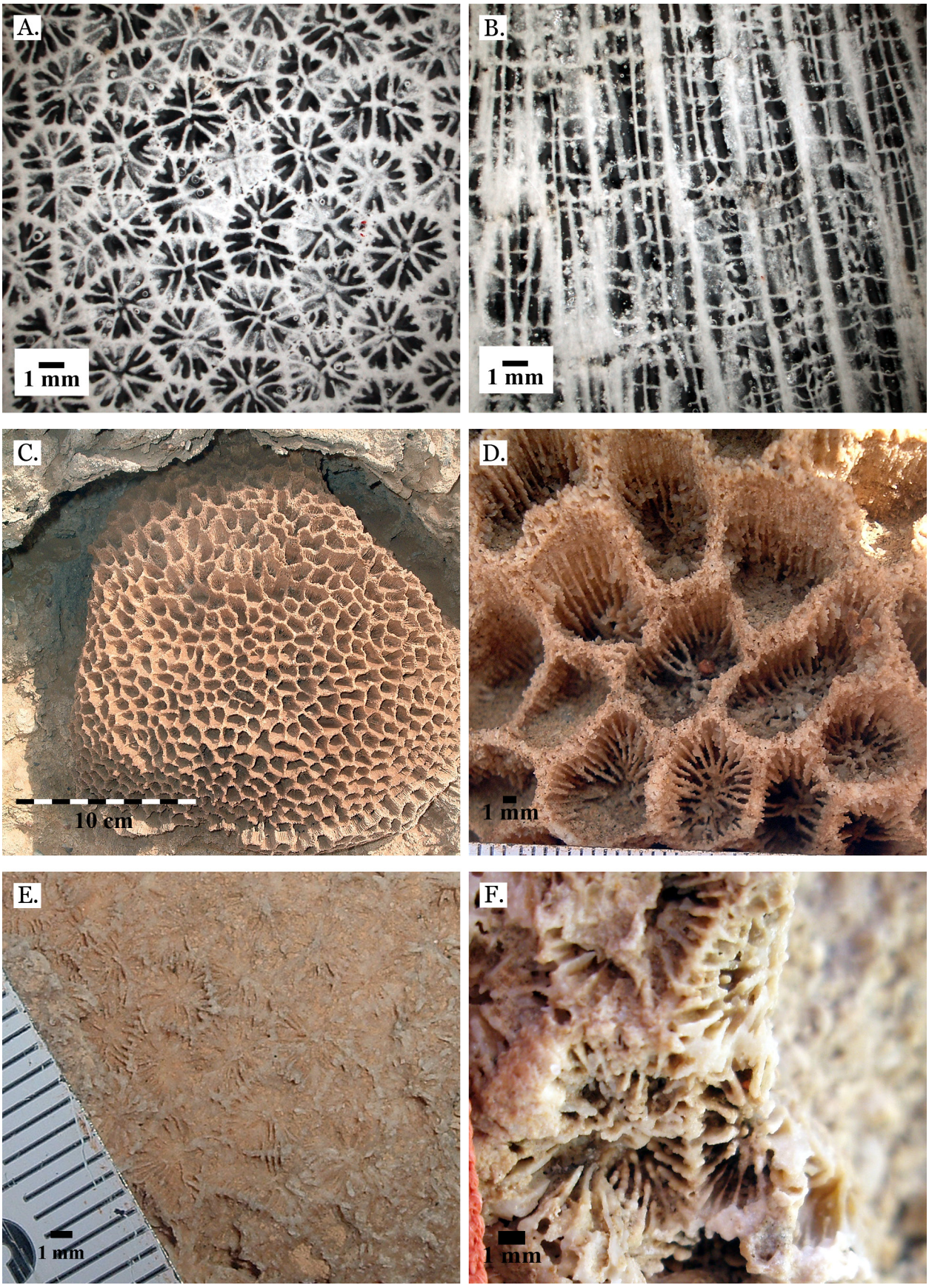
A.
1 mm
B.
1 mm
C.
10 cm
D.
1 mm
E.
1 mm
F.
1 mm

Location	Terrace	Environment	Reef Zone
Sharm Al Arab	Late Pleistocene, lower	Exposed	slope
Wadi Gawasis	Late Pleistocene, lower	Exposed	slope
Wadi Gawasis	Middle Pleistocene	Sheltered	slope
Sharm Al Arab	Middle Pleistocene	Sheltered	patch reefs
Wadi Wizr	Middle Pleistocene	Sheltered	patch reefs
Wadi Wizr	Late Pleistocene, lower	Partly sheltered	shallow, indeterminate
Wadi Wizr	Late Pleistocene, upper	Partly sheltered	shallow, indeterminate
Wadi Gawasis	Late Pleistocene, upper	Exposed	shallow, indeterminate

Table 1. Terrace reef zones

Taxonomy

Forty-two of the 45 coral species identified from Middle and Late Pleistocene reefs on the Egyptian coast are found in the modern Red Sea (Veron 2000), and the specimens that were only identified to family or genus level show no characters suggesting that they are either new or locally extinct species; in every case they resemble one or more species found on the modern Red Sea but simply lack enough detail for confident identification. The three species not found in the modern Red Sea include *Favites micropentagona, Pavona minuta* and a specimen bearing resemblance to *Pavona bipartita*.

Favites micropentagona was first described in 2000 (Veron 2000), making it a relatively new species. Originally recognized from locations within the Coral Triangle, it has since been identified in the Western Indian Ocean (Sheppard and Obura 2005) and the Gulf of Aden (DeVantier et al. 2004). It is possible that its current range extends into the Red Sea but it hasn't been recognized yet, or that it lived there during the Middle Pleistocene and has since gone locally extinct. *P. minuta* was reported from the Late Pleistocene of Saudi Arabia by Dullo (1990) suggesting it may be locally extinct, or that it occurs so rarely that it has gone unnoticed in surveys of living reefs. *P. minuta* also resembles *P. duerdeni*, a species that is found in the modern Red Sea but which has larger corallites and more exsert septo-costae. Thus another possibility is that these Pleistocene *P. minuta* are morphological variants of *P. duerdeni,* or that *P. minuta* in the modern Red Sea are routinely misidentified as *P. duerdeni*. The final specimen is too poorly preserved to have any confidence that it is in fact *P. bipartita*, so only future sampling of Middle Pleistocene reefs of the Red Sea region will determine of this species lived in the Red Sea during that time.

Montastrea curta and *Stylocoeniella guentheri* are the only two taxa to occur on all Middle Pleistocene terraces and none of the Late Pleistocene terraces, although both species occur on modern Red Sea reefs. Neither species has been reported from the Late Pleistocene elsewhere on the Red Sea, but given the limited sampling that has been done this is perhaps not surprising. *Favites pentagona* is the only taxa reported here that occurs on all Late Pleistocene terraces but no Middle Pleistocene terraces. However, *F. pentagona* has been reported from the Middle Pleistocene of the Sinai (El Sorogy 1997), and it also occurs on modern Red Sea reefs.

Figure 14. Facing page. A, Latitudinal thin section of *Favites micropentagona* from Middle Pleistocene; B, Longitudinal thin section of *Favites micropentagona* from Middle Pleistocene; C, *Favites* sp. A from Middle Pleistocene Wadi Gawasis; D, *Favites* sp. A from Middle Pleistocene Wadi Gawasis; E, *Goniastrea retiformis* from Middle Pleistocene Wadi Gawasis; F, *Goniastrea pectinata* from Late Pleistocene Wadi Gawasis.

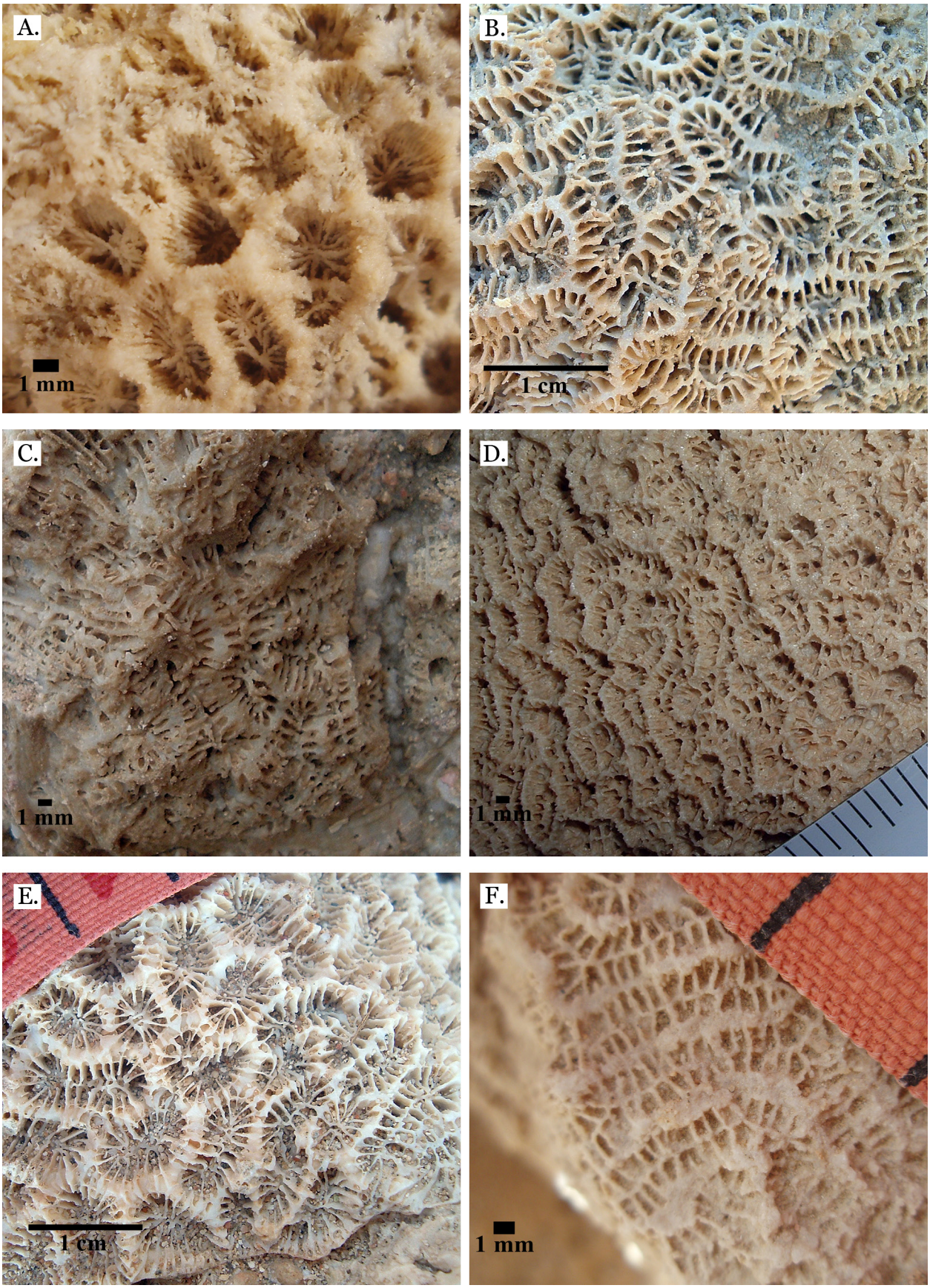
A.
1 mm
B.
1 cm
C.
1 mm
D.
1 mm
E.
1 cm
F.
1 mm

Diversity

Comparisons between Middle and Late Pleistocene

In modern marine systems, turbid water reefs (defined as those growing with high inputs of terrigenous sediment) are found mid-to-inner shelf with moderate to low water energy, or are relatively sheltered fringing reefs (Sanders and Baron-Szabo 2005). All of the fossil reef terraces studied here preserve near-shore reef environments, and sedimentation from land (in combination with reef zonation) is the factor most likely responsible for differences in diversity between terraces.

At intermediate levels of turbidity *Acropora* occurs only in minor abundances or disappears altogether (Acevedo et al. 1989, Loya 1976, Tudhope and Scoffin 1994). *Acropora* is completely absent or makes up less than 1% of coral cover on all the terraces except for the lower Late Pleistocene terrace of Sharm Al Arab (5.0%) and the upper Late Pleistocene terrace of Wadi Wizr (2.4%). Although these terraces are described as "exposed" and "partly sheltered" respectively in this paper, these are used as relative terms indicating greater or lesser exposure to wave and current action compared to other terraces in this study. Such low *Acropora* abundances are only reported for sheltered or semi-exposed environments in the modern northern Red Sea (Riegl and Velimirov 1994, Riegl and Piller 2000) indicating that all of the studied fossil reefs likely experienced turbidity from intermediate to high degrees.

The dominance of sediment resistant taxa such as *Porites* is another strong indicator of relatively high turbidity (Sanders and Baron-Szabo 2005, Stafford-Smith 1993, Tudhope and Scoffin 1994), and in the modern northern Red Sea *Porites* abundances of 25 to 85% have been reported for sheltered, near-shore environments (Heiss et al. 2005, Riegl and Velimirov 1994, Riegl and Piller 2000, Sheppard C. R. C. and Sheppard 1991). *Porites* abundance on the lower Late Pleistocene terrace of Sharm Al Arab is the lowest of all the studied terraces at 14.9%, further supporting that it experienced the least turbidity. The terrace itself sits above a modern fringing reef with a relatively narrow reef flat and steep slope that experiences moderately strong currents, indicating a similar morphology and degree of exposure for the fossil terrace. Waves, tides, currents and swells are all important for the passive removal of sediment from coral surfaces (Larcombe et al. 2001). The second lowest abundance of *Porites* is found on the lower Late Pleistocene terrace of Wadi Gawasis (21.2%), the other exposed reef slope environment.

All of the other terraces show *Porites* abundances over 40% and high abundances of other species with domal morphology (usually faviids) (Table 2). This is in good agreement with the domal coral assemblages described by (Montaggioni 2005), which occur on semi-exposed to sheltered shallow fore-reef zones, reef flats and back-reef slopes throughout the Indo-Pacific. Domal morphologies only require weak water motion to clear sediments, making them better able to persist in turbid environments (Sanders and Baron-Szabo 2005)).

The upper terrace of Late Pleistocene Wadi Gawasis has the second highest Porites abundance at 63.5%, as well as high abundances of domal Faviids and the stress tolerant *Pocillopora damicornis, Platygyra daedalea,* and *Cyphastrea microphthalma* (Sheppard C. R. C. and Sheppard 1991). Although in an exposed location, it was also shallower than the upper slope environment it sits above, possibly representing a shallow or intertidal reef flat or back reef. The

Figure 15. Facing page. A, *Goniastrea* sp. A from Middle Pleistocene Wadi Wizr; B, *Platygyra daedalea* from Late Pleistocene Sharm Al Arab; C, *Platygyra lamellina* from Late Pleistocene Wadi Gawasis; D, *Platygyra sinensis* from Middle Pleistocene Wadi Wizr; E, *Platygyra acuta* from Late Pleistocene Wadi Gawasis; F, *Leptoria phrygia* from Middle Pleistocene Sharm Al Arab.

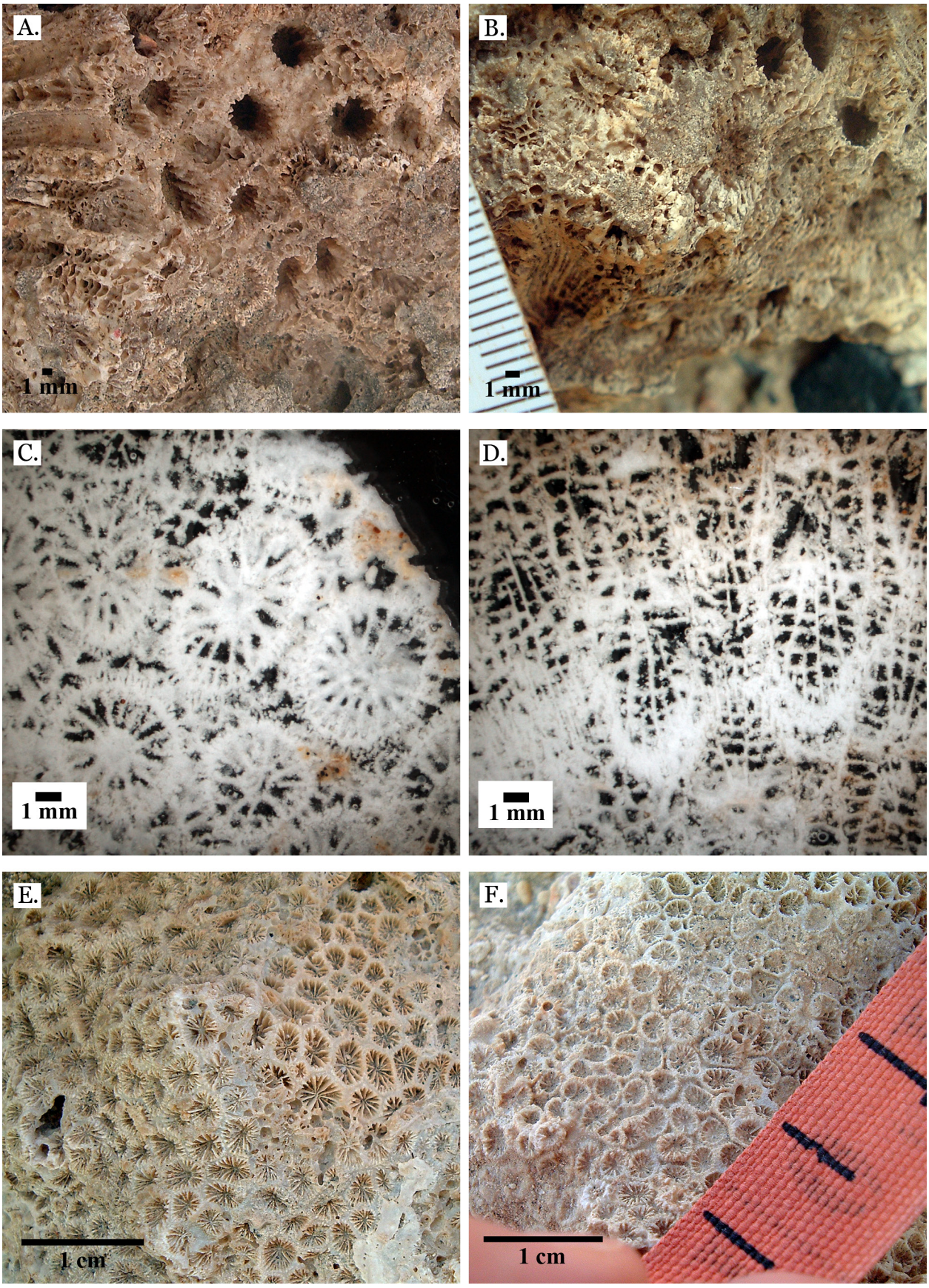
A.
1 mm
B.
1 mm
C.
1 mm
D.
1 mm
E.
1 cm
F.
1 cm

coral assemblage found here is consistent with exposure to stressors like temperature and salinity variations, heavy sedimentation and tide and wave action.

The Middle Pleistocene terrace of Wadi Gawasis, a sheltered slope environment, has the lowest *Porites* abundance after the two exposed reef environments (40.8%). Although in a sheltered environment compared to the upper terrace of Late Pleistocene Wadi Gawasis, as noted above the latter was very likely in a shallower, more stressful environment. In general, diversity is higher on reef slopes than on reef flats or back reefs (Perrin et al. 1995).

The Middle Pleistocene terraces of Sharm Al Arab and Wadi Wizr represent lagoonal patch reef environment, with low coral cover (67% and 60% respectively) and *Porites* dominated patch reefs (78.3% and 53.7% *Porites* abundances respectively). Wadi Wizr also has a high abundance of *Favia stelligera* (16.8%), which is common among shallow patch reefs(Sheppard Charles R. C. 1998).

The lower and upper terraces of Late Pleistocene Wadi Wizr have similar reef assemblages, particularly in the most abundant species *Porites*, and *Galaxea fascicularis* (49.6% and 50%, 18.9% and 16.4% respectively). Unlike the more exposed Wadi Gawasis, the terraces don't appear to preserve recognizable reef zones. Reduced ecological zonation is often seen in areas with high turbidity (Acevedo et al. 1989, Larcombe et al. 2001).

Diversity (as measured both by species richness and the Shannon and Margalef diversity indices) among the terraces reflects the reef zone and degree of turbidity of each environment (Figures 19-24). Exposed reef slopes have the highest diversity, followed closely by a sheltered reef slope; the sheltered patch reefs have the lowest diversity. The shallow reef flat or back reef at Wadi Gawasis is less diverse than the slope environment below it (consistent with expectation) but falls between the upper and lower Late Pleistocene terraces of Wadi Wizr. Although the Wadi Wizr terraces share similar assemblages, the upper terrace shows greater diversity than the lower terrace. This reduced zonation is perhaps expected for a sheltered, turbid bay environment (Acevedo et al. 1989, Larcombe et al. 2001).

Comparisons with the modern Red Sea

The coral taxa of the Middle and Late Pleistocene of the Red Sea are the same as those found in the modern Red Sea (Table 4), but do the communities of the Pleistocene show any differences from those found today? A number of factors can complicate comparisons between fossil and modern reef environments: time averaging on fossil reefs, differential preservation of taxa, difficulty inherent in identifying corals from living or weathered fossil specimen, as well as differences in sampling method. Despite these confounding factors, the Middle and Late Pleistocene terraces of this study bear close resemblance to fringing reefs of the modern Egyptian coast.

Sheppard C. R. C. and Sheppard (1991) provide the most extensive analysis of coral communities of the modern Red Sea. They surveyed 200 sites, estimating percent coral cover of all species by eye. As in this study, there were difficulties distinguishing similar species of *Acropora* and *Porites* (as well as *Montipora*, *Goniopora* and *Alveopora*) and these were treated as single species in ecological analyses (Sheppard C. R. C. and Sheppard 1991). Using cluster analysis they identified 13 distinct coral communities, some of which had subtypes.

Figure 16. Facing page. A, *Montastrea curta* from Middle Pleistocene Wadi Gawasis; B, Very poorly preserved *Montastrea curta* from Middle Pleistocene Wadi Gawasis; C, Latitudinal thin section of *Montastrea curta* from Middle Pleistocene; D, Longitudinal thin section of *Montastrea curta* from Middle Pleistocene; E, *Leptastrea pruinosa* from Late Pleistocene Wadi Gawasis; F, *Leptastrea bottae* from Late Pleistocene Sharm Al Arab.

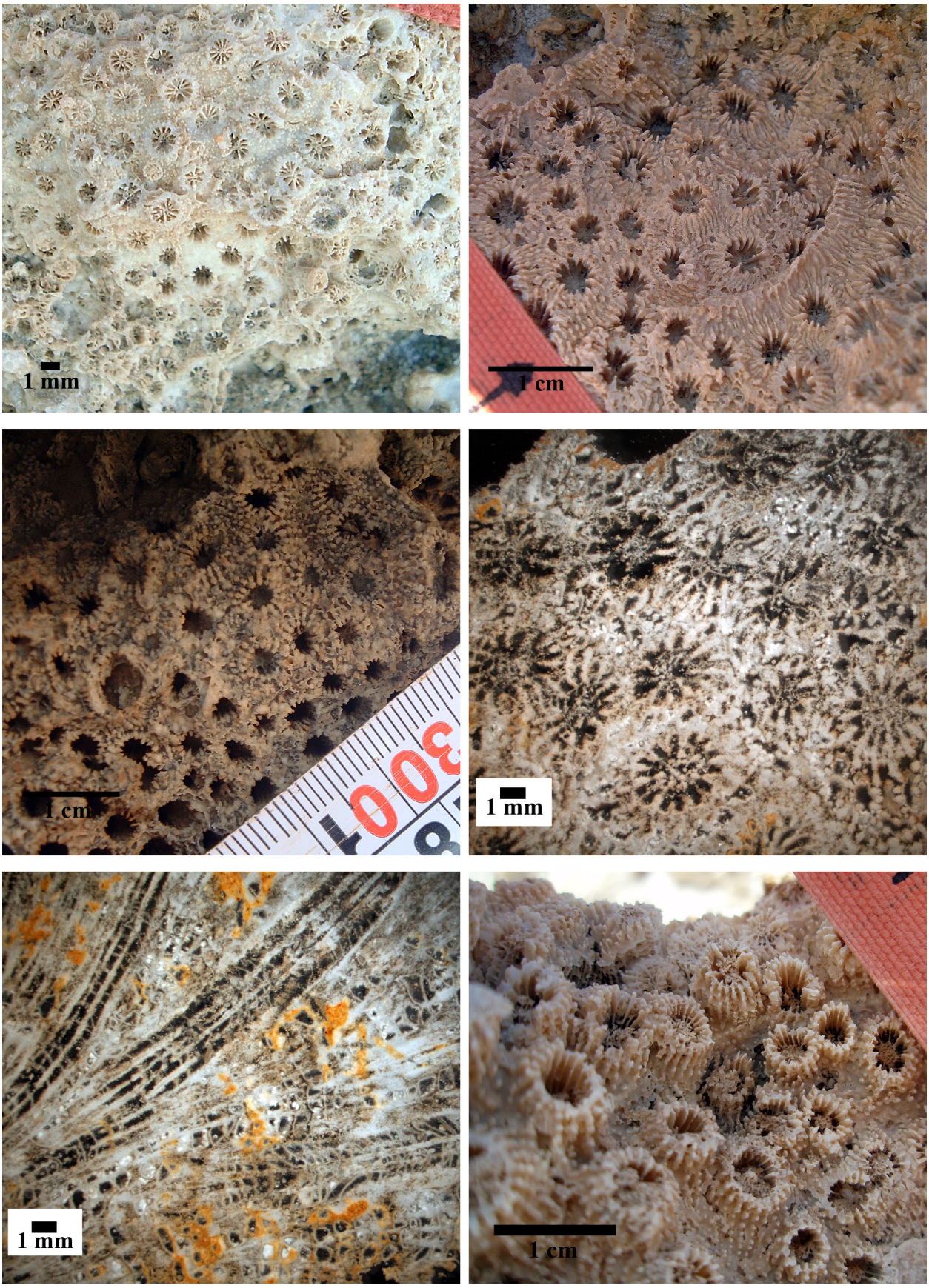
1 mm
1 cm
1 cm
1 mm
1 mm
1 cm

The Pleistocene reefs of this study more or less fit descriptions of their communities 4 and 6, and possibly community 11. Community 11 is a community described as very low diversity, and dominated by massive Porites; they occur in extremely sheltered, turbid, shallow environments in close proximity to mangroves (Sheppard C. R. C. and Sheppard 1991). Although this community is identified as restricted to the southern Red Sea, it accurately describes the Middle Pleistocene of Sharm Al Arab. It's unknown whether this terrace occurred in proximity to mangroves, but all other descriptors fit, and modern mangroves do occur along the modern Egyptian coast.

Community 4 is described as dominated by *Porites lutea* (47% - 85% cover), with Pocilloporidae and some *Pavona* species also being characteristic; it is found on fringing reefs in very sheltered bays and back reef slopes of patch reefs in the north and central Red Sea (Sheppard C. R. C. and Sheppard 1991). Both Late Pleistocene terraces of Wadi Wizr and the upper Late Pleistocene terrace of Wadi Gawasis are dominated by *Porites* (49.6% - 63.5%) with a high co-occurrence of *Pocillopora damicornis*; the main difference is that species of *Pavona* are absent. Sheppard C. R. C. and Sheppard (1991) surveyed reefs from the crest to 40 meters, with reef flats being excluded from analyses, while at least two of the terraces mentioned above very likely represent reef flats or very shallow back reef slopes of fringing reefs. There is also a great difference in the number of locations sampled between this study and the Sheppard C. R. C.and Sheppard (1991) study, which may also account for the absence of *Pavona*.

Community 6 is described as high diversity, dominated by faviids, together with "minor" families Mussidae, Merulinidae and Pectiniidae, but never dominated by any one species; it is found on reefs from 5 - 25 meters that are moderately to very exposed (Sheppard C. R. C. and Sheppard 1991). The lower Late Pleistocene terraces of Sharm Al Arab and Wadi Gawasis are high diversity with very high Faviid abundances. No species belonging to Pectiniidae were found in this study, but species of Mussidae and Merulinidae occur on both terraces (a difference that again, may be attributable to sampling). More significant perhaps is the very high abundances of *Porites* and *Galaxea fascicularis* that occur on the Pleistocene reefs.

Fossil reefs represent time averaged assemblages, and as a result have higher abundances of dominant sediment producing taxa, which may not have been the most abundant on the living reef (Edinger et al. 2001). Porites are not only dominant in shallow, sheltered areas throughout the Arabian region (Sheppard C. R. C. and Sheppard 1991), they are also known to be important frame-builders and therefore may be over-represented on fossil reefs.

G. fascicularis occurs in high abundances on all the Pleistocene terraces except for the patch reefs and the upper Late Pleistocene of Wadi Gawasis (potentially a reef flat), and this raises an interesting aspect of the Pleistocene reefs. Although it isn't listed as a dominant or even important taxa in the modern reef environments reviewed here (Heiss et al. 2005, Riegl and Velimirov 1994, Riegl and Piller 2000, Sheppard C. R. C. and Sheppard 1991), Sheppard C. R. C. and Sheppard (1991) state that in very turbid areas less than 5 meters deep it may be very abundant (as much as 50%). It may be that the Pleistocene terraces examined here were all very shallow and turbid. Another possibility is that as sea level fell and water became shallower and more turbid, *G. fascicularis* began to replace other less tolerant taxa. This might account for the very high *G. fascicularis* abundances in coral communities that are more diverse and tolerant

Figure 17. Facing page. A, *Cyphastrea microphthalma* from Late Pleistocene Wadi Gawasis; B, *Echinopora lamellosa* from Late Pleistocene Wadi Gawasis; C, *Echinopora lamellosa* from Middle Pleistocene Wadi Gawasis; D, Latitudinal thin section of *Echinopora lamellosa* from Middle Pleistocene; E, Longitudinal thin section of *Echinopora lamellosa* from Middle Pleistocene; F, *Echinopora gemmacea* from Late Pleistocene Sharm Al Arab.

than would be expected for a *G. fascicularis* dominated environment. This interpretation is also supported for the Late Pleistocene terraces because in many cases the contact where *G. fascicularis* is growing over another species corallum is evident, and no cases were observed where *G. fascicularis* is overgrown by another species.

Riegl and Velimirov (1994) surveyed exposed, sheltered and semi-exposed reefs around the northern Red Sea, and Heiss et. al. (2005) carried out a survey of fringing reefs in and around El Quadim Bay, El Quseir, Egypt. Both report Margalef diversity indices for exposed and sheltered sites, and Reigl and Velimirov (1994) also report on semi-exposed sites. The values found for the Pleistocene terraces classified as sheltered and semi-exposed are in general agreement with those found on modern Red Sea reefs, but the values for exposed sites were on average higher than those found on modern reefs (Table 3). Given that fossil reefs preserve a time-averaged assemblage it's expected that they will have higher diversity than life assemblages (Edinger et al. 2001). Conversely, the point-transect method used in this study underestimates diversity

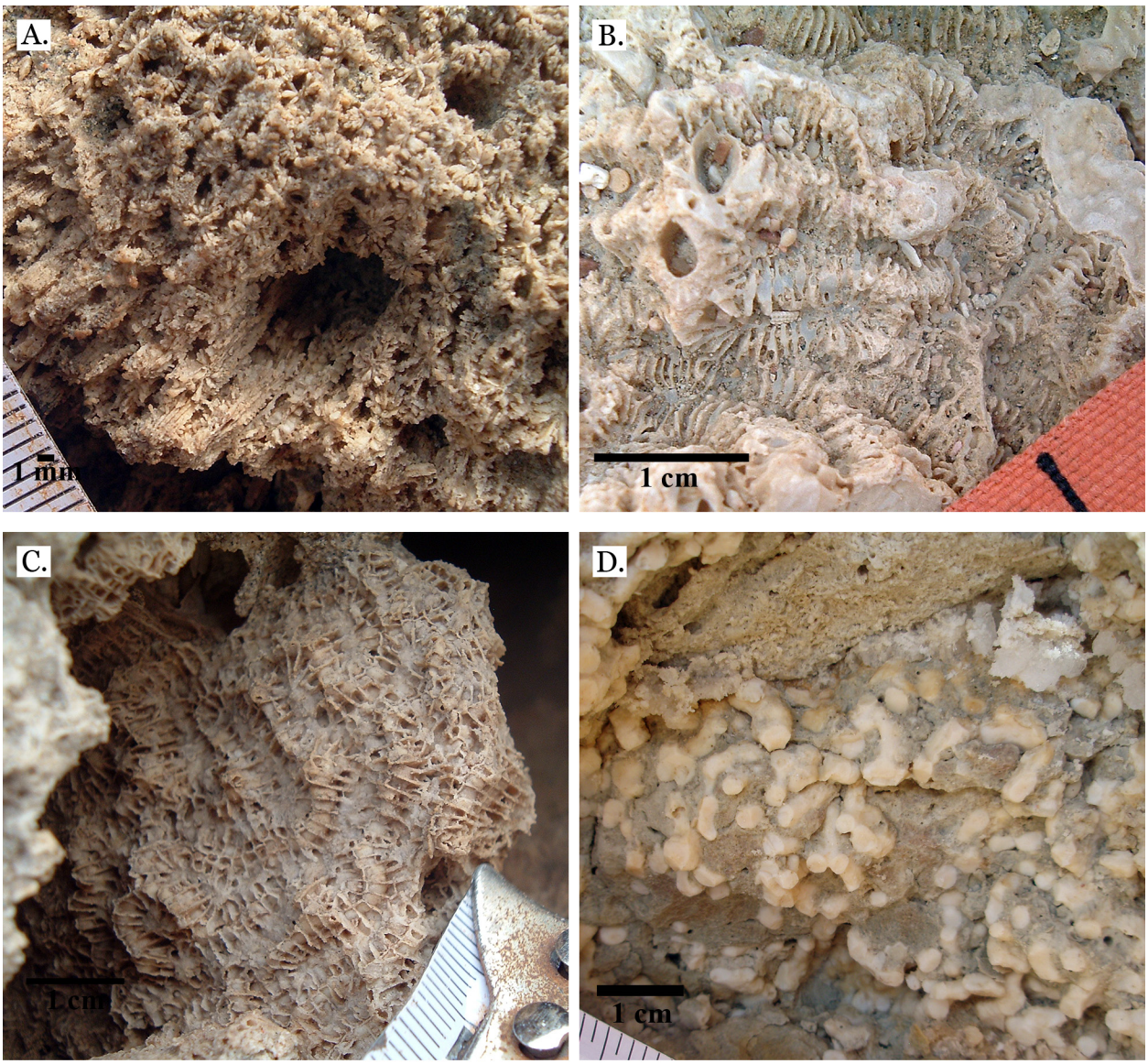

Figure 18. A, Unknown *Faviid* sp. from Middle Pleistocene Wadi Gawasis; B, *Gyrosmilia interrupta* from Late Pleistocene Sharm Al Arab; C, *Gyrosmilia interrupta* from Middle Pleistocene Wadi Gawasis; D, Coralline algae from Middle Pleistocene Wadi Wizr.

(Perrin et al. 1995), as does the compression of all *Porites* and *Acropora* species into single taxonomic units. The Margalef average for sheltered sites in this study may also be made artificially low by the Middle Pleistocene of Sharm Al Arab, a patch reef environment with excessively low diversity.

Coral cover percentages found in this study are much higher than for those found on modern fringing reefs of the Egyptian coast (Heiss et al. 2005, Riegl and Velimirov 1994, Sheppard C. R. C. and Sheppard 1991). This is very likely an artifact of sampling methods; surveys of modern reefs record live coral cover while fossil reefs represent a combined life-death assemblage. As a result these values are not comparable, and in this study were used only to help define and characterize fossil environments relative to each other.

Comparisons to the available survey data from the modern Red Sea indicate that the Pleistocene terraces studied here represent shallow, moderately to very sheltered, turbid water environments. The absence and very low abundances of *Acropora,* high abundances of *Porites*, *G. fascicularis* and other shallow water taxa, as well as the dominance of taxa with domal morphology are all consistent with modern shallow, sheltered, turbid environments (Heiss et al. 2005, Riegl and Velimirov 1994, Riegl and Piller 2000, Sheppard C. R. C. and Sheppard 1991). The difference seen between Pleistocene and modern assemblages are attributable to expected

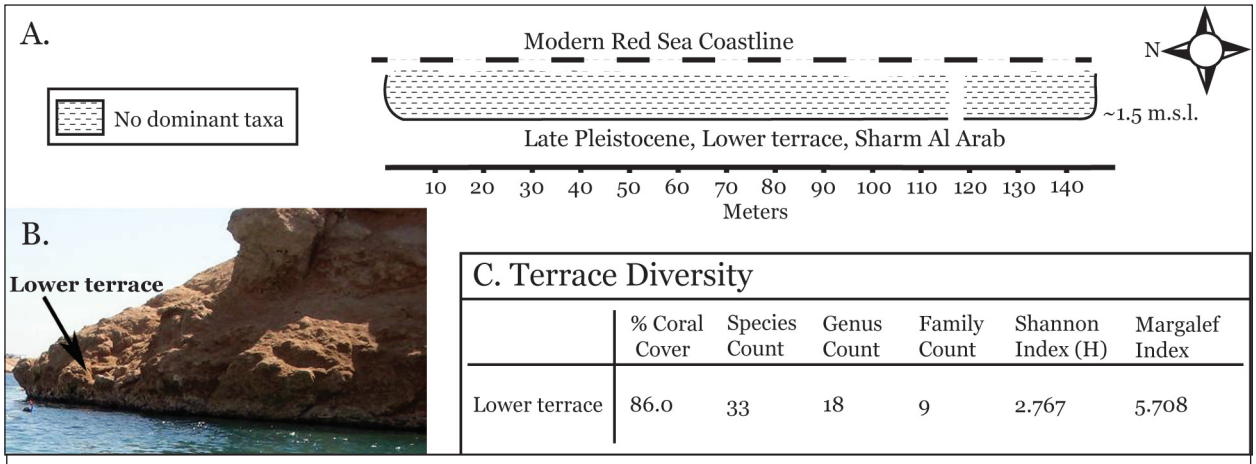

C. Terrace Diversity

	% Coral Cover	Species Count	Genus Count	Family Count	Shannon Index (H)	Margalef Index
Lower terrace	86.0	33	18	9	2.767	5.708

Figure 19. Diversity of lower Late Pleistocene terrace, Sharm Al Arab. A, dominant taxa per 10 meters of transect. Gaps in image represent real gaps in transect data due to absent, covered or inaccessible outcrop; B, image of outcrop does not share orientation with graphic in A; C, Table of diversity measures for lower Late Pleistocene terrace, Sharm Al Arab.

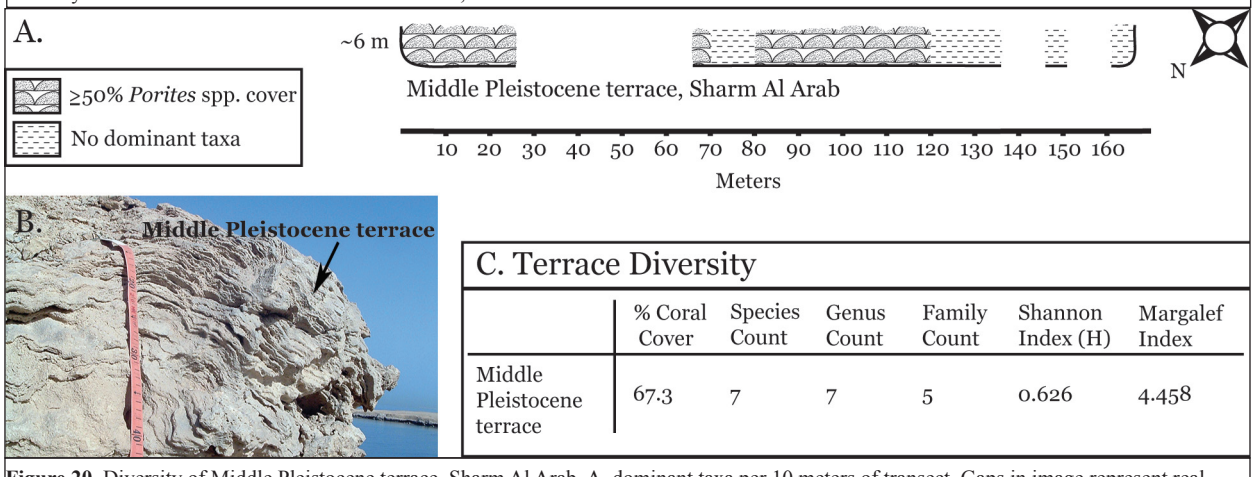

C. Terrace Diversity

	% Coral Cover	Species Count	Genus Count	Family Count	Shannon Index (H)	Margalef Index
Middle Pleistocene terrace	67.3	7	7	5	0.626	4.458

Figure 20. Diversity of Middle Pleistocene terrace, Sharm Al Arab. A, dominant taxa per 10 meters of transect. Gaps in image represent real gaps in transect data due to absent, covered or inaccessible outcrop; B, image of outcrop does not share orientation with graphic in A; C, Table of diversity measures for Middle Pleistocene terrace, Sharm Al Arab.

phenomenon of fossil preservation and give no indication of being a result of significant change across glacial events.

Late Pleistocene terraces

There is nothing to indicate the lower and upper terraces of the Late Pleistocene represent distinct episodes of reef growth as suggested by earlier workers (El Moursi et al. 1994). The complimentary reef zones seen at Wadi Gawasis and the similarity of coral assemblages at Wadi Wizr indicate these terraces belong to a single period of reef growth. This is in agreement with the findings of Plaziat et al. (2008).

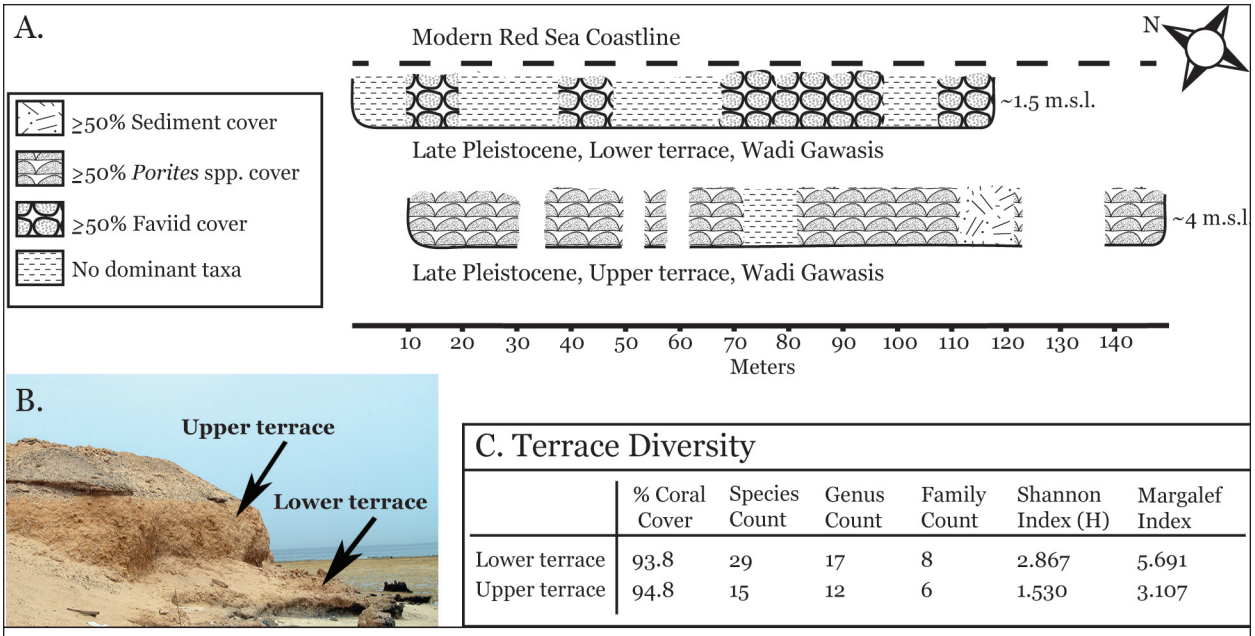

C. Terrace Diversity

	% Coral Cover	Species Count	Genus Count	Family Count	Shannon Index (H)	Margalef Index
Lower terrace	93.8	29	17	8	2.867	5.691
Upper terrace	94.8	15	12	6	1.530	3.107

Figure 21. Diversity of upper and lower Late Pleistocene terraces, Wadi Gawasis. A, dominant taxa per 10 meters of transect. Gaps in image represent real gaps in transect data due to absent, covered or inaccessible outcrop. Positions of upper and lower transect reflect actual position of outcrop transects to each other; B, image of outcrop does not share orientation with graphic in A; C, Table of diversity measures for upper and lower Late Pleistocene terraces, Wadi Gawasis.

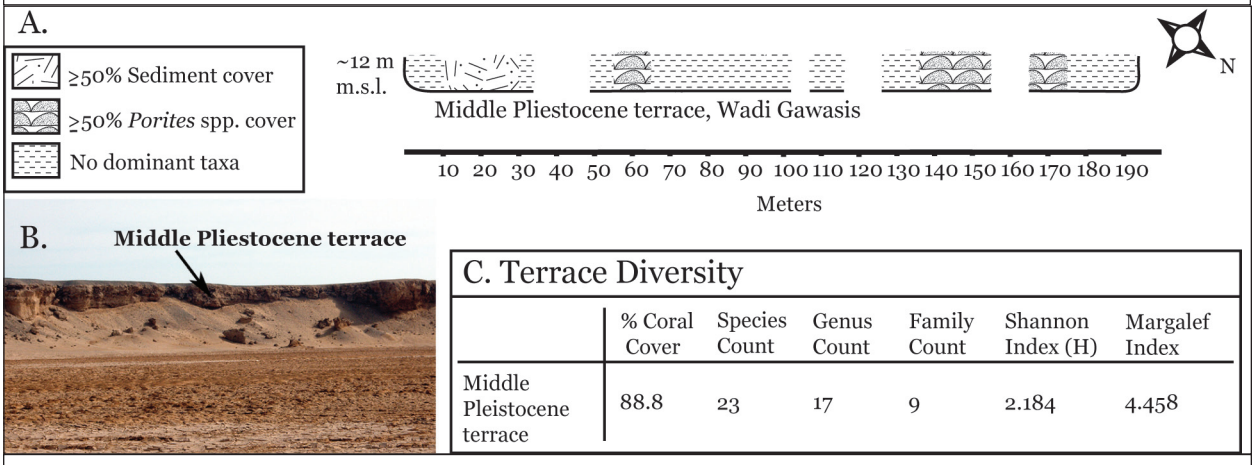

C. Terrace Diversity

	% Coral Cover	Species Count	Genus Count	Family Count	Shannon Index (H)	Margalef Index
Middle Pleistocene terrace	88.8	23	17	9	2.184	4.458

Figure 22. Diversity of Middle Pleistocene terrace, Wadi Gawasis. A, dominant taxa per 10 meters of transect. Gaps in image represent real gaps in transect data due to absent, covered or inaccessible outcrop.; B, image of outcrop does not share orientation with graphic in A; C, Table of diversity measures for Middle Pleistocene terrace, Wadi Gawasis.

Reef stability through time

The constancy of taxa and coral assemblages on 8 Egyptian reef terraces from the Middle Pleistocene to the present suggests that the coral reef communities of the Red Sea have been stable across glaciations for at least 250,000 yrs. The stability of coral reefs across Pleistocene glaciations has been documented elsewhere in the Indo-Pacific (Pandolfi 1996) and Caribbean (Jackson Jeremy B. 1992, Pandolfi and Jackson 2006), however the result is more surprising for the Red Sea than for other locations. The changes to the physical environment during sea level low stands made the Red Sea particularly hostile to life; either coral communities had to persist in extreme environments, or they went locally extinct and re-colonized the entire basin after each glaciation.

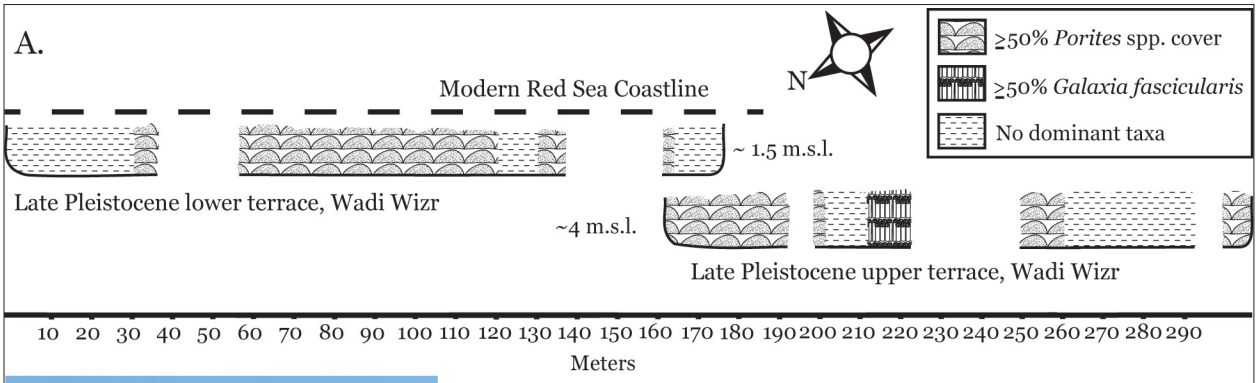

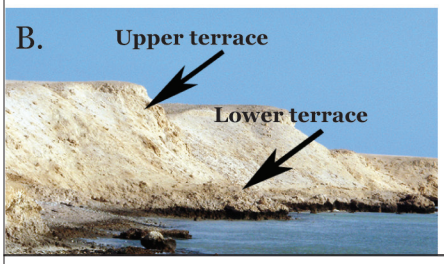

C. Terrace Diversity

	% Coral Cover	Species Count	Genus Count	Family Count	Shannon Index (H)	Margalef Index
Lower terrace	82.4	11	9	5	1.427	2.100
Upper terrace	97.7	20	13	8	1.845	3.929

Figure 23. Diversity of upper and lower Late Pleistocene terraces, Wadi Wizr. A, dominant taxa per 10 meters of transect. Gaps in image represent real gaps in transect data due to absent, covered or inaccessible outcrop. Positions of upper and lower transect reflect actual position of outcrop transects to each other; B, image of outcrop does not share orientation with graphic in A; C, Table of diversity measures for upper and lower Late Pleistocene terraces, Wadi Wizr.

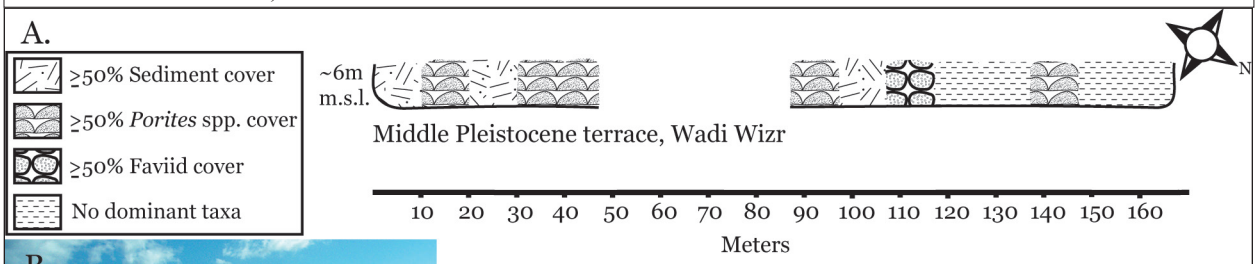

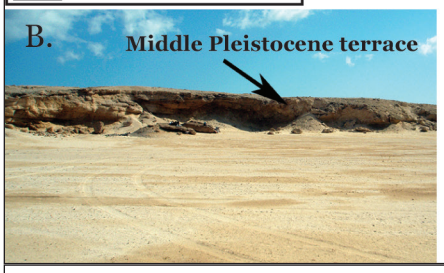

C. Terrace Diversity

	% Coral Cover	Species Count	Genus Count	Family Count	Shannon Index (H)	Margalef Index
Middle Pleistocene terrace	60.0	9	8	4	1.114	1.836

Figure 24. Diversity of Middle Pleistocene terrace, Wadi Wizr. A, dominant taxa per 10 meters of transect. Gaps in image represent real gaps in transect data due to absent, covered or inaccessible outcrop; B, image of outcrop does not share orientation with graphic in A; C, Table of diversity measures for Middle Pleistocene terrace, Wadi Wizr.

Sharm Al Arab, L. Pleistocene, lower		**Wadi Gawasis, L. Pleistocene, lower**	
Galaxea fascicularis	21.3%	*Porites* spp.	21.5%
Porites spp.	14.9	*Galaxea fascicularis*	11.1
Favites pentagona	7.1	*Favia stelligera*	6.3
Pocillopora damicornis	6.4	*Platygyra daedalea*	6.3
Echinopora gemmacea	6.4	Coralline algae	4.9
Acropora spp.	5.0	*Pocillopora damicornis*	4.9
Coralline algae	4.6	*Leptastrea bottae*	4.9
Cyphastrea microphthalma	4.3	*Favia speciosa*	4.2
Favia pallida	3.6	*Lobophyllia hemprichii*	3.5
Platygyra daedalea	3.6	*Echinopora lamellosa*	3.5

Wadi Gawasis, M. Pleistocene		**Wadi Wizr, M. Pleistocene**	
Porites spp.	40.8	*Porites* spp.	53.7
Galaxea fascicularis	8.8	Coralline algae	17.9
Echinopora lamellosa	8.2	*Favia stelligera*	16.8
Favites micropentagona	6.8	*Stylocoeniella guentheri*	5.3
Goniopora sp. A	6.8		
Coralline algae	5.4		

Sharm Al Arab, M. Pleistocene		**Wadi Gawasis, L. Pleistocene, upper**	
Porites spp.	78.3	*Porites* spp.	63.5
Coralline algae	9.6	*Pocillopora damicornis*	7.1
		Platygyra acuta	5.6
		Platygyra daedalea	4.0
		Leptoria phrygia	3.2
		Favia speciosa	3.2

Wadi Wizr, L. Pleistocene, upper		**Wadi Wizr, L. Pleistocene, lower**	
Porites spp.	49.6	*Porites* spp.	50.0
Galaxea fascicularis	18.9	*Galaxea fascicularis*	16.4
Pocillopora damicornis	5.6	Coralline algae	12.7
Favia stelligera	3.2	*Pocillopora damicornis*	6.7
Favites pentagona	3.2	*Favia stelligera*	3.7
		Favites pentagona	3.7

Table 2. Species abundances > 3%

During the Penultimate (MIS 6) and Last Glacial (MIS 2) Maximums, the Red Sea basin's already narrow and shallow connection to the wider Indian Ocean became highly restricted, with depths as shallow as 17 meters at the shallowest point, the Hanish Sill (Fernandes et al. 2006, Siddall et al. 2004). This resulted in net evaporation that caused salinities to increase dramatically, with average values over 50‰ in surface and bottom waters (Almogi-Labin 1982, Almogi-Labin et al. 1998, Badawi et al. 2005, Fenton et al. 2000, Hemleben et al. 1996, Thunnell et al. 1988). Surface waters during the Last Glacial Maximum have been reconstructed to 57‰ in the north, 53‰ in the central Red Sea and 47‰ in the south (Fenton et al. 2000, Hemleben et al. 1996), resulting in a complete disappearance of planktonic foraminifera (which have a salinity tolerance of 49‰) in the north and central Red Sea (Hemleben et al. 1996). Badawi et. al. (2005) also found higher salinities in the north than in the south during glacial periods.

Stronger winds in the north resulted in increased dust input leading to increased flux of organic matter during MIS 2, 4 and 6 (Badawi et. al. 2005). But while higher surface productivity is characteristic of glacial oceans in general, the precipitous rise in salinity is an obstacle to survival during glaciations specific to the Red Sea. Based on turn-over in reef-associated molluscan fauna between the Late Pleistocene and modern Red Sea (Taviani 1998) proposed a series of "complete biotic recolonizations" of all reef fauna from the Indian Ocean after mass extinction during glacial periods. Earlier authors had proposed a similar scenario of extreme salinities wiping out local fauna, requiring subsequent recolonizations when sea level rose again (Gvirtzman et al. 1977), and it has been suggested specifically for corals since (Coles 2003, Sheppard C. R. C. and Sheppard 1991).

Reef building corals are usually characterized as stenotopic, thriving in a narrow range of temperature, salinity and nutrient exposure with a limited ability to survive prolonged exposure to conditions outside their preferred range. While this has proven true for many coral populations, there are also instances of locally adapted corals able to tolerate temperature and salinity extremes. In the Arabian Gulf 11 species of coral have been found living in temperatures up to 36°C and salinities up to 48‰ (*Porites* in particular have been found flourishing at 48‰) (Coles 2003), and Sheppard C. R. C. and Sheppard (1991) report similar findings plus an additional 3 species living at 50‰ (*Porites nodifera, Cyphastrea microphthalma,* and *Siderastrea savignya-*

Publication	Depth (m)	Exposure	n	Average Margalef's +/- SD
Reigl & Velimirov (1994)	1-5	Exposed	5	2.81 +/- .65
	6-10	Exposed	5	3.21 +/- 1.05
	1-5	Sheltered	5	2.23+/- .70
	6-10	Sheltered	5	2.67+/- .72
	1-5	Semi-exposed	5	2.97+/- .67
	6-10	Semi-exposed	5	3.74+/- .58
Heiss et. al. (2005)	5 & 10	Exposed	16	3.16
	5 & 10	Sheltered	9	2.68
This study	shallow	Exposed	3	4.84+/- 1.50
	shallow	Sheltered	3	2.56+/- 1.66
	shallow	Semi-exposed	2	3.02+/-1.29

Table 3. Comparison of average Margalef diversity indices with modern Red Sea reefs

na). In laboratory experiments *Siderastrea sidera* was able to acclimate from 30‰ to 42‰ over 30 days with no ill effects (Muthiga and Szmant 1987), so it seems that for some species at least, adaptation to high salinity environments may be rapid.

While glacial salinities in the Red Sea averaged over 50‰, in the south it dropped to an average of 47‰ (Badawi et al. 2005, Fenton et al. 2000, Hemleben et al. 1996) with at least the possibility of even lower values closer to the Bab Al Mandeb where limited water exchange continued with the less saline Gulf of Aden. A more likely scenario than basin-wide extinction is the persistence of more tolerant coral taxa in the southern Red Sea, (particularly important frame-builders such as *Porites*) with recolonization by less tolerant taxa once sea level rose. This would still have required recolonization of at least two thirds of the Red Sea basin from small, limited communities restricted to hostile but endurable locations in the south for thousands to tens of thousands of years. Having a reduced number of the same core species available for early reef re-settlement after sea level rise may help to explain why coral assemblages do not change

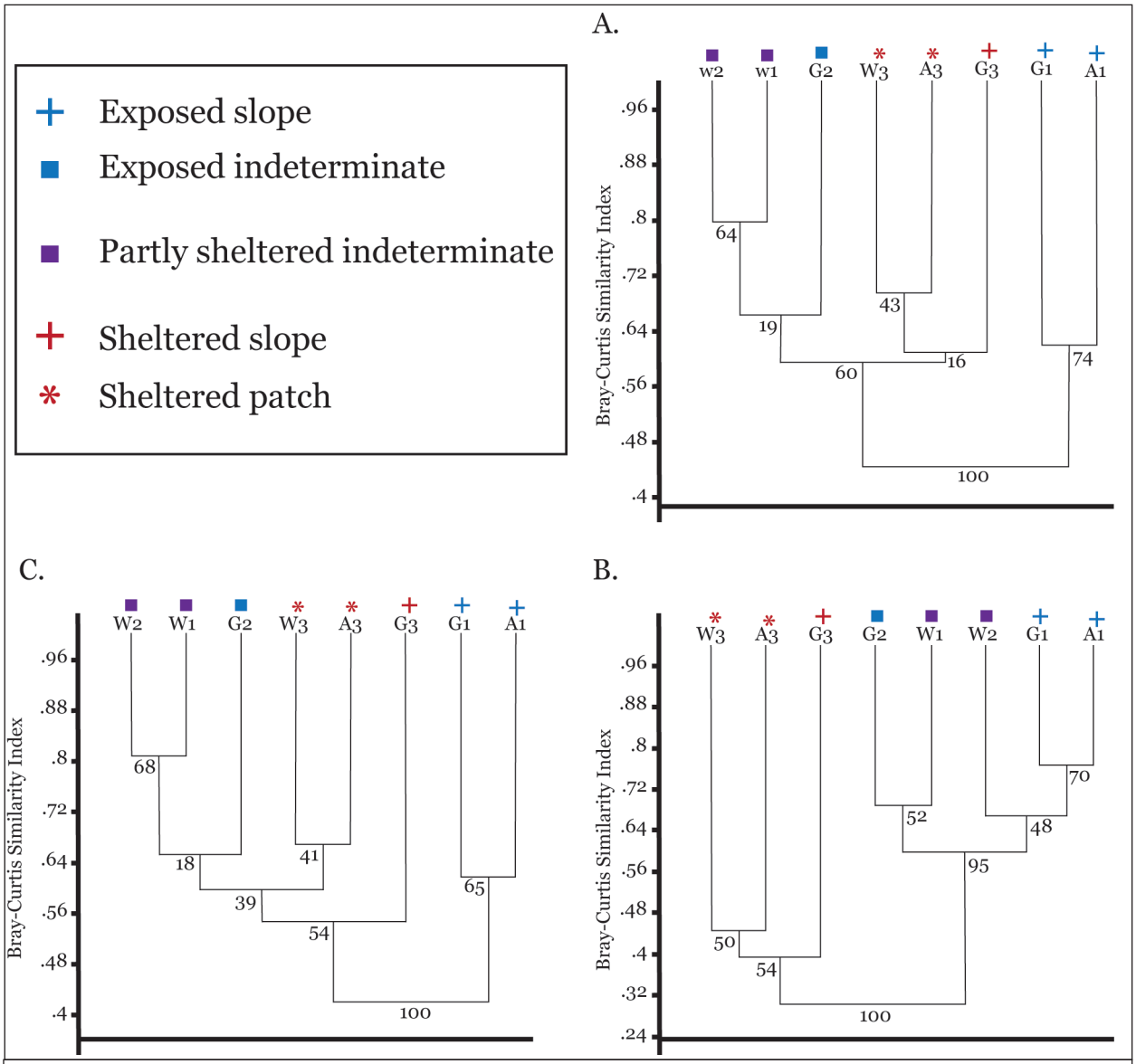

Figure 25. Cluster analyses with Bray-Curtis distances and bootstrap values (n=1000). A. Dendogram for raw abundance data; B, Dendogram for presence-absence data; C, Dendogram for abundance data as proportions of total transect counts.

dramatically from interglacial to interglacial.

Coring and dating of submerged terraces would provide the most definitive test of this hypothesis, because if coral communities persisted in significant numbers they should still be there. It might also be reasonable to expect that salinity tolerant taxa are over-represented on Red Sea reefs as compared to the average Indo-Pacific reef, because they had less distance to migrate. A genetic survey of the Red Sea's most salinity-tolerant species and their neighboring populations from the Gulf of Aden might reveal to what degree they have been isolated from one another, and for how long. This last test may be the most conclusive and feasible.

Lessons from the Red Sea

The Red Sea provides an imperfect natural laboratory for the future of coral reefs; imperfect because increasing salinity and falling sea level are not threats facing modern reefs - increasing temperature, decreasing pH, rising sea level and habitat destruction are. It does however provide a model of environmental catastrophe, survival and recovery. If populations of corals can be sustained - even in marginal and geographically limited habitat, they retain the potential to re-establish themselves with restored water quality and available substrate. And while preservation of the broadest genetic variability is ideal, the intentional cultivation of corals able to tolerate extreme environmental variability may be the best option for survival in a rapidly changing ocean environment.

Table 4. Record of reef building Scleractinia in the Red Sea from Middle Pleistocene to present. All modern Red Sea data are from the Coral Geographic of Veron (unpublished). Fossil records are from the Late Pleistocene terraces of Jordan (Al-Rifaiy and Cherif 1988), Saudi Arabia (Dullo 1990), Eritrea (Bruggemann et al. 2004) and from the Middle and Late Pleistocene terraces of the south Sinai (El-Sorogy 1997) and mainland Egypt (this study). Records marked in grey with question marks are from mainland Egypt (El-Sorogy 2008) and were reported only as "Pleistocene" in age.
(N/C) taxa are found only in the north and central Red sea; (S) taxa are found only in the southern Red Sea province.

Middle Pleistocene	Late Pleistocene	Modern Red Sea
		Acanthastrea brevis
	----------	*Acanthastrea echinata*
		Acanthastrea faviaformis
		Acanthastrea hemprichii
		Acanthastrea ishigakiensis (N/C)
		Acanthastrea lordhowensis (S)
	----------	*Acanthastrea rotundoflora*
		Acanthastrea subechinata (N/C)
		Acropora abrotanoides
		Acropora acuminata
		Acropora anthocercis
		Acropora arabensis
		Acropora austera
		Acropora cerealis
-------?---------	-------?---------	*Acropora clathrata*

Middle Pleistocene	Late Pleistocene	Modern Red Sea
-------?---------	-------?---------	*Acropora cytherea*
		Acropora digitifera
		Acropora divaricata (S)
		Acropora donei (S)
		Acropora downingi
		Acropora elseyi (S)
		Acropora formosa
	----------	*Acropora forskali*
		Acropora gemmifera
		Acropora glauca (S)
	----------	*Acropora haimei*
-------?---------	-------?---------	*Acropora hemprichii*
		Acropora horrida
	----------	*Acropora humilis*
-------?---------	-------?---------	*Acropora hyacinthus*
		Acropora lamarcki (N/C)
-------?---------	-------?---------	*Acropora latistella*
		Acropora listeri
		Acropora loripes (S)
		Acropora lutkeni
		Acropora maryae (N/C)
		Acropora massawensis (S)
		Acropora microphthalma (S)
		Acropora millepora (S)
		Acropora nasuta
		Acropora nobilis
		Acropora ocellata (N/C)
		Acropora parapharaonis (N/C)
----------	----------	*Acropora pharaonis*
		Acropora plantaginea
		Acropora polystoma
		Acropora retusa (N/C)
-------?---------	-------?---------	*Acropora robusta*
		Acropora rufus (N/C)
		Acropora samoensis
		Acropora scherzeriana
		Acropora secale
		Acropora selago

Middle Pleistocene	Late Pleistocene	Modern Red Sea
		Acropora spicifera
		Acropora squarrosa
		Acropora subulata
		Acropora tenuis
		Acropora valenciennesi
-------?---------	-------?---------	*Acropora valida*
		Acropora variabilis
		Acropora variolosa (N/C)
		Acropora vaughani
		Acropora yongei (S)
		Alveopora allingi
		Alveopora daedalea
		Alveopora fenestrate (N/C)
		Alveopora ocellata (N/C)
		Alveopora spongiosa
		Alveopora tizardi
		Alveopora viridis
		Anacropora spumosa (N/C)
		Anomastraea irregularis (S)
		Astreopora cucullata
		Astreopora expansa (S)
		Astreopora gracilis (N/C)
		Astreopora listeri (N/C)
	----------	*Astreopora myriophthalma*
		Astreopora suggesta (N/C)
		Balanophyllia europaea (N/C)
		Barabattoia amicorum (N/C)
-------?---------	-------?---------	*Blastomussa merleti*
		Cantharellus doederleini (N/C)
		Cantharellus noumeae
		Caulastrea connata
	----------	*Caulastrea tumida*
-------?---------	-------?---------	*Coscinaraea columna*
----------	----------	*Coscinaraea monile*
		Ctenactis crassa
	----------	*Ctenactis echinata*
	----------	*Cycloseris costulata*
		Cycloseris curvata (N/C)

Middle Pleistocene	Late Pleistocene	Modern Red Sea
	----------	*Cycloseris cyclolites (N/C)*
	Cycloceris marginata	Not reported from modern Red Sea
-------?---------	-------?---------	*Cycloseris patelliformis*
		Cycloseris somervillei (S)
		Cycloseris tenuis (S)
	----------	*Cycloseris vaughani*
	----------	*Cynarina lacrymalis*
		Cyphastrea chalcidicum
		Cyphastrea hexasepta
----------	----------	*Cyphastrea microphthalma*
	----------	*Cyphastrea serailia*
		Diploastrea heliopora
	----------	*Echinophyllia aspera*
		Echinophyllia echinata (S)
		Echinophyllia orpheensis (N/C)
		Echinopora forskaliana
		Echinopora fruticulosa
----------	----------	*Echinopora gemmacea*
		Echinopora hirsutissima
		Echinopora irregularis (N/C)
----------	----------	*Echinopora lamellosa*
		Echinopora mammiformis (N/C)
		Echinopora tiranensis (N/C)
	----------	*Erythrastrea flabellata (N/C)*
		Favia albidus
-------?---------	-------?---------	*Favia danae*
	----------	*Favia favus*
-------?---------	-------?---------	*Favia helianthoides (N/C)*
-------?---------	-------?---------	*Favia lacuna (N/C)*
-------?---------	-------?---------	*Favia laxa*
-------?---------	-------?---------	*Favia lizardensis*
	----------	*Favia matthaii*
		Favia maxima
----------	----------	*Favia pallida*
-------?---------	-------?---------	*Favia rotumana (N/C)*
	----------	*Favia rotundata*
----------	----------	*Favia speciosa*
----------	----------	*Favia stelligera*

Middle Pleistocene	Late Pleistocene	Modern Red Sea
-------?---------	-------?---------	*Favia veroni (N/C)*
	----------	*Favites abdita*
	Favites auticollis	Not reported from modern Red Sea
	----------	*Favites chinensis*
----------	----------	*Favites complanata*
	----------	*Favites flexuosa*
-------?---------	-------?---------	*Favites halicora*
Favites micropentagona		Not reported from modern Red Sea
	----------	*Favites paraflexuosa*
----------	----------	*Favites pentagona*
		Favites russelli (S)
		Favites spinosa
	----------	*Favites vasta*
	----------	*Galaxea astreata*
----------	----------	*Galaxea fascicularis*
		Galaxea horrescens (S)
----------	----------	*Gardineroseris planulata*
-------?---------	-------?---------	*Goniastrea aspera*
-------?---------	-------?---------	*Goniastrea australensis*
		Goniastrea columella (S)
		Goniastrea deformis (S)
		Goniastrea edwardsi
		Goniastrea favulus (S)
----------	----------	*Goniastrea pectinata*
	----------	*Goniastrea peresi*
----------	----------	*Goniastrea retiformis*
		Goniastrea thecata (N/C)
		Goniopora burgosi
		Goniopora ciliatus
	----------	*Goniopora columna*
		Goniopora djiboutiensis
		Goniopora lobata
-------?---------	-------?---------	*Goniopora minor*
		Goniopora pearsoni (N/C)
	----------	*Goniopora planulata*
	----------	*Goniopora savignyi (N/C)*
		Goniopora somaliensis
		Goniopora stokesi

Middle Pleistocene	Late Pleistocene	Modern Red Sea
		Goniopora sultani (N/C)
	----------	*Goniopora tenella*
		Goniopora tenuidens
----------	----------	*Gyrosmilia interrupta*
		Herpolitha limax
		Herpolitha weberi (N/C)
-------?---------	-------?---------	*Hydnophora exesa*
	----------	*Hydnophora microconos*
----------	----------	*Leptastrea bottae*
		Leptastrea inaequalis
	----------	*Leptastrea pruinosa*
	----------	*Leptastrea purpurea*
	----------	*Leptastrea transversa*
----------	----------	*Leptoria phrygia*
	----------	*Leptoseris explanata*
		Leptoseris foliosa
		Leptoseris gardineri (S)
		Leptoseris hawaiiensis
		Leptoseris incrustans
		Leptoseris mycetoseroides
		Leptoseris scabra
	----------	*Leptoseris yabei*
	----------	*Lobophyllia corymbosa*
		Lobophyllia hataii
	----------	*Lobophyllia hemprichii*
		Lobophyllia robusta
		Madracis kirbyi (S)
		Madracis pharensis (N/S)
		Merulina ampliata
		Merulina scheeri
		Micromussa amakusensis (S)
		Montastrea annuligera
----------		*Montastrea curta*
		Montastrea magnistellata
		Montipora aequituberculata
		Montipora aspergillus
		Montipora circumvallata
		Montipora cocosensis (N/C)

Middle Pleistocene	Late Pleistocene	Modern Red Sea
		Montipora cryptus
		Montipora danae
		Montipora echinata
		Montipora floweri
		Montipora foliosa (S)
		Montipora hemispherica (N/C)
		Montipora hispida
		Montipora informis
		Montipora meandrina
		Montipora millepora (N/C)
		Montipora mollis
		Montipora monasteriata
		Montipora niugini (N/C)
		Montipora nodosa
		Montipora pachytuberculata
		Montipora peltiformis (S)
		Montipora saudii
----------	----------	*Montipora spongiosa*
		Montipora spongodes
		Montipora spumosa
		Montipora stellata
		Montipora stilosa
		Montipora tuberculosa
		Montipora turgescens
		Montipora venosa
		Montipora verrucosa
	----------	*Mycedium elephantotus*
		Mycedium umbra (N/C)
		Oculina patagonica (N/C)
	----------	*Oulophyllia bennettae (S)*
		Oulophyllia crispa
		Oxypora convolute (N/C)
		Oxypora crassispinosa
		Oxypora egyptensis (N/C)
		Oxypora glabra (N/C)
		Oxypora lacera
		Pachyseris rugosa (N/C)
	----------	*Pachyseris speciosa*

Middle Pleistocene	Late Pleistocene	Modern Red Sea
		Parasimplastrea sheppardi (S)
	----------	*Pavona cactus*
		Pavona clavus
		Pavona danai (N/C)
----------	----------	*Pavona decussata*
		Pavona diffluens
		Pavona duerdeni
	----------	*Pavona explanulata*
	----------	*Pavona frondifera*
	----------	*Pavona maldivensis*
		Pavona varians
	----------	*Pavona venosa*
		Physogyra lichtensteini
	----------	*Platygyra acuta (N/C)*
		Platygyra carnosus (N/C)
	----------	*Platygyra crosslandi*
	----------	*Platygyra daedalea*
	----------	*Platygyra lamellina*
		Platygyra pini
----------	----------	*Platygyra sinensis*
	----------	*Plerogyra sinuosa*
--------?---------	--------?---------	*Plesiastrea versipora*
----------	----------	*Pocillopora damicornis*
		Pocillopora eydouxi (N/C)
	----------	*Pocillopora verrucosa*
		Podabacia crustacea
		Podabacia Sinai (N/C)
	----------	*Porites columnaris*
		Porites echinulata
		Porites harrisoni
		Porites lichen
		Porites lobata
----------	----------	*Porites lutea*
		Porites monticulosa
		Porites nigrescens (S)
	----------	*Porites nodifera*
		Porites rus
----------	----------	*Porites solida*

Middle Pleistocene	Late Pleistocene	Modern Red Sea
		Psammocora contigua
		Psammocora explanulata
		Psammocora haimeana
		Psammocora nierstraszi
		Psammocora profundacella
		Psammocora superficialis
		Pseudosiderastrea tayami
		Sandalolitha Africana (N/C)
	----------	*Seriatopora caliendrum*
	----------	*Seriatopora hystrix*
----------	----------	*Siderastrea savignyana*
		Stylocoeniella armata
----------		*Stylocoeniella guentheri*
-------?---------	-------?---------	*Stylophora danae (N/C)*
-------?---------	-------?---------	*Stylophora kuehlmanni (N/C)*
		Stylophora mamillata
----------	----------	*Stylophora pistillata*
-------?---------	-------?---------	*Stylophora subseriata (N/C)*
		Stylophora wellsi
		Symphyllia agaricia
	----------	*Symphyllia erythraea*
		Symphyllia radians
		Symphyllia valenciennesii
		Trachyphyllia geoffroyi (N/C)
		Turbinaria frondens
		Turbinaria irregularis (N/C)
	----------	*Turbinaria mesenterina*
	Turbinaria peltata	Not reported from modern Red Sea
		Turbinaria reniformis
		Turbinaria stellulata

References

Acevedo R, Morelock J, Olivieri RA. 1989. Modification of coral reef zonation by terrigenous sediment stress. Palaios 4: 92-100.
Al-Rifaiy IA, Cherif OH. 1988. The fossil coral reefs of Al-Aqaba, Jordan. Facies 18: 219-229.

Almogi-Labin A. 1982. Stratigraphic and Paleoceanographic significance of late Quaternary pteropods from deep-sea cores in the Gulf of Aqaba (Elat) and northernmost Red Sea. Marine Micropaleontology 7: 53-72.
Almogi-Labin A, Hemleben C, Meischner D. 1998. Carbonate preservation and climatic changes in the central Red Sea during the last 380 kyr as recorded by pteropods. Marine Micropaleontology 33: 87-107.
Badawi A, Schmiedl G, Hemleben C. 2005. Impact of late Quaternary environmental changes on deep-sea benthic foraminiferal faunas of the Red Sea. Marine Micropaleontology 58: 13-30.
Bray JR, Curtis JT. 1957. An ordination of the upland forest communities of southern Wisconsin. Ecological Monographs 27: 325-349.
Bruggemann JH, Buffler RT, Guillaume MMM, Walter RC, von Cosel R, Ghebretensae BN, Berhe SM. 2004. Stratigraphy, palaeoenvironments and model for the deposition of the Abdur Reef Limestone: context for an important archaeological site from the last interglacial on the Red Sea coast of Eritrea. Palaeogeography, Palaeoclimatology, Palaeoecology 203: 179-206.
Coles SL. 2003. Coral species diversity and environmental factors in the Arabian Fulf and the Gulf of Oman: a comparison to the Indo-Pacific region. Atoll Research Bulletin 507: 1-19.
Denny MW, Helmuth B, Leonard GH, Harley CDG, Hunt LJH, Nelson EK. 2004. Quantifying scale in ecology: lessons from a wave-swept shore. Ecological Monographs 74: 513-532.
DeVantier LM, De'Ath G, Klaus R, Al-Moghrabi S, Abdulaziz M, Reinicke GB, Cheung C. 2004. Reef-building corals and coral communities of the Socotra Archipelago, a zoogeographic 'crossroads' in the Arabian Sea. Fauna of Arabia 20: 117-168.
Ditlev H. 1980. A Field Guide to the Reef-Building Corals of the Indo-Pacific. Klampenborg: Dr. W. Backhuys Publisher, Rotterdam & Scandanavian Press Ltd.
Donner SD, Heron SF, Skirving WJ. 2009. Future Scenarios: a review of modelling efforts to predict the future of coral reefs in an era of climate change. Pages 159-173 in van Oppen MJH, Lough JM, eds. Coral Bleaching - Patterns, Processes, Causes and Consequences. Berlin, Heidelberg: Springer-Verlag.
Dullo W-C. 1990. Facies, fossil record, and age of pleistocene reefs from the Red Sea (Saudi Arabia). Facies 22: 1-45.
Edinger EN, Pandolfi JM, Kelley RA. 2001. Community structure of Quaternary coral reefs compared with recent life and death assemblages. Paleobiology 27: 669-694.
El-Asmar HM. 1997. Quaternary isotope stratigraphy and paleoclimate of coral reef terraces, Gulf of Aqaba, South Sinai, Egypt. Quaternary Science Reviews 16: 911-924.
El-Sorogy AS. 1997. Pleistocene coral reefs of sourther Sinai, Egypt: fossil record, facies analysis and diagenetic alterations. Middle East Research Center , Ain Shams University, Earth Science Series 11: 17-36.
—. 2008. Contributions to the Pleistocene coral reefs of the Red Sea coast, Egypt. Arab Gulf Journal of Scientific Research 26: 63-85.
El Moursi M, Hoang CT, El Fayoumy IF, Hegab O, Faure H. 1994. Pleistocene evolution of the Red Sea coastal plain, Egypt: evidence from uranium-series dating of emerged reef terraces. Quaternary Science Reviews 13: 345-359.
Faith DP, Minchin PR, Belbin L. 1987. Compositional dissimilarity as a robust measure of ecological distance. Vegetatio 69: 57-68.
Fenton M, Geiselhart S, Rohling EJ, Hemleben C. 2000. Aplanktonic zones in the Red Sea. Marine Micropaleontology 40: 277-294.

Fernandes CA, Rohling EJ, Siddall M. 2006. Absence of post-Miocene Red Sea land bridges: biogeographic implications. Journal of Biogeography 33: 961-966.
Gvirtzman G. 1994. Fluctuations of sea level during the past 400,000 years: the record of Sinai, Egypt (northern Red Sea). Coral Reefs 13: 203-214.
Gvirtzman G, Buchbinder B, Sneh A, Nir Y, Friedman GM. 1977. Morphology of the Red Sea fringing reefs: a result of the erosional pattern of the last glacial low stand sea-level and the following Holocene recolonization. Pages 480-491 in CNRS, ed. Second International Symposium of Corals and Fossil Coral Reefs, vol. 89. Paris: Bureau de recherches geologiques et minieres.
Hammer O, Harper DAT, Ryan PD. 2001. PAST: paleontological statistics software package for education and data analysis. Palaeontologia Electronica 4: 9.
Heiss G, Kochzius M, Alter C, Roder C. 2005. Assessment of the status of coral reefs in the El Quadim Bay, El Quseir, Egypt. Bremen, Germany: Reef Check. Report no.
Hemleben C, Meischner D, Zahn R, Almogi-Labin A, Erlenkeuser H, Hiller B. 1996. Three hundred eighty thousand year long stable isotope and faunal records from the Red Sea: influence of global sea level change on hydrography. Paleoceanography 11: 147-156.
Hoang CT, Taviani M. 1991. Stratigraphic and tectonic implications of uranium-series-dated coral reefs from uplifted Red Sea islands. Quaternary Research 35: 264-273.
Jackson JB. 1992. Pleistocene perspectives on coral reef community structure. American Zoologist 32: 719-731.
Jackson JBC, Erwin DH. 2006. What can we learn about ecology and evolution from the fossil record? Trends in Ecology & Evolution 21: 322-328.
Larcombe P, Costen A, Woolfe KJ. 2001. The hydrodynamic and sedimentary setting of nearshore coral reefs, central Great Barrier Reef shelf, Australia: Paluma shoals, a case study. Sedimentology 48: 811-835.
Loya Y. 1976. Effects of water turbidity and sedimentation on the community structure of Puerto Rican corals. Bulletin of Marine Science 26: 450-466.
Montaggioni LF. 2005. History of Indo-Pacific reef systems since the last glaciation: development patterns and controlling factors. Earth-Science Reviews 71: 1-75.
Muthiga NA, Szmant AA. 1987. The effects of salinity stress on the rates of aerobic respiration and photosynthesis in the hermatypic coral Siderastrea siderea. Biological Bulletin 173: 539-551.
Pandolfi JM. 1996. Limited Membership in Pleistocene reef coral assemblages from the Huon Peninsula, Papua New Guinea: constancy during global change. Paleobiology 22: 152-176.
—. 2011. The Paleoecology of Coral Reefs. 13-24.
Pandolfi JM, Jackson JBC. 2006. Ecological persistance interrupted in Caribbean coral reefs. Ecology Letters 9.
Perrin C, Bosence D, Rosen B. 1995. Quantitative approaches to palaeozonation and palaeobathymetry of corals and coralline algae in Cenozoic reefs. Geological Society, London, Special Publications 83: 181-229.
Plaziat J-C, Reyss J-L, Choukri A, Cazala C. 2008. Diagenetic rejuvenation of raised coral reefs and precision of dating: the contribution of the Red Sea reefs to the question of reliability of the Uranium-series datings of middle to late Pleistocene key reef-terraces of the world. Notebooks on Geology 4: 1-35.
Plaziat J-C, Baltzer F, Choukri A, Conchon O, Freytet P, Orszag-Sperber F, Raguideau A, Reyss J-L. 1998. Quaternary marine and continental sedimentation in the northern Red Sea and Gulf of Suez (Egyptian coast): influences of rift tectonics, climate changes and sea-level fluctuations.

Pages 537-573 in Purser BH, Bosence DWJ, eds. Sedimentation and Tectonics of Rift Basins: Red Sea-Gulf of Aden. London: Chapman & Hall.
Riegl B, Velimirov B. 1994. The structure of coral communities at Hurghada in the Norther Red Sea. Marine Ecology 15: 213-231.
Riegl B, Piller WE. 2000. Reefs and coral carpets in the northern Red Sea as models for organism-environment feedback in coral communities and its reflection in growth fabrics. Pages 71-88 in Insalaco E, Skelton PW, Palmer TJ, eds. Carbonate Platform Systems: Componenets and Interactions, vol. 178. London: Geological Society.
Sanders D, Baron-Szabo RC. 2005. Scleractinian assemblages under sediment input: their characteristics and relation to the nutrient input concept. Palaeogeography, Palaeoclimatology, Palaeoecology 216: 139-181.
Scheer G, Pillai CSG. 1983. Report on the stony corals from the Red Sea. Zoologica 133: 1-198.
Sheppard C, Obura D. 2005. Corals and reefs of Cosmoledo and Aldabra atolls: Extent of damage, assemblage shifts and recovery following the severe mortality of 1998. Journal of Natural History 39: 103-121.
Sheppard CRC. 1998. Biodiversity patterns in Indian Ocean corals, and effects of taxonomic error in data. Biodiversity and Conservation 7: 847-868.
Sheppard CRC, Sheppard ALS. 1991. Corals and coral communities of Arabia. Fauna of Saudi Arabia 12: 3-170.
Siddall M, Smeed DA, Hemleben C, Rohling EJ, Schmelzer I, Peltier WR. 2004. Understanding the Red Sea response to sea level. Earth and Planetary Science Letters 225: 421-434.
Stafford-Smith MG. 1993. Sediment-rejection efficiency of 22 species of Australian scleractinian corals. Marine Biology 115: 229-243.
Taviani M. 1998. Post-Miocene reef faunas of the Red Sea: glacio-eustatic controls. Pages 574-582 in Purser BH, Bosence D, eds. Sedimentation and Tectonics of Rift Basins: Red Sea-Gulf of Aden. London: Chapman & Hall.
Thunnell RC, Locke SM, Williams D. 1988. Glacio-eustatic sea-level control on Red Sea salinity. Nature 334: 601-604.
Tudhope AW, Scoffin T, P. 1994. Growth and structure of fringing reefs in a muddy environment, south Thailand. Journal of Sedimentary Research A64: 752-764.
Veron JEN. 2000. Corals of The World. Townsville, Australia: Australian Institute of Marine Sciences.
Werner F, Lange K. 1975. A bathymetric survey of the sill area between the Red Sea and the Gulf of Aden. Geologisches Jahrbuch 13: 125-130.
Wilkinson C. 2008. Satus of coral reefs of the world: 2008. Townsville, Australia: Global Coral Reef Monitoring Network, Reef and Rainforest Research Centre. Report no.